VOL.107 NO.ST6. JUNE 1981

JOURNAL OF THE STRUCTURAL DIVISION

PROCEEDINGS OF
THE AMERICAN SOCIETY
OF CIVIL ENGINEERS

VOL. 107 NO. ST6. JUNE 1981

JOURNAL OF THE STRUCTURAL DIVISION

PROCEEDINGS OF
THE AMERICAN SOCIETY
OF CIVIL ENGINEERS

Copyright© 1981 by
American Society
of Civil Engineers
All Rights Reserved
ISSN 0044-8001

John E. Bower, Editor
U.S. Steel Corporation

AMERICAN SOCIETY OF CIVIL ENGINEERS

BOARD OF DIRECTION

President
Irvan F. Mendenhall

Past President
Joseph S. Ward

President Elect
James R. Sims

Vice Presidents
Robert D. Bay
Francis J. Connell
Lyman R. Gillis
Albert A. Grant

Directors
Martin G. Abegg
Floyd A. Bishop
L. Gary Byrd
Larry J. Feeser
John A. Focht, Jr.
Sergio Gonzalez-Karg
James E. Humphrey, Jr.
Richard W. Karn
Leon D. Luck
Arthur R. McDaniel
Paul R. Munger
William R. Neuman
Leonard S. Oberman
John D. Parkhurst
Celestino R. Pennoni
Robert B. Rhode
S. Russell Stearns
William H. Taylor
Stafford E. Thornton
Robert E. Whiteside
Richard S. Woodruff

EXECUTIVE OFFICERS

Eugene Zwoyer, *Executive Director*
Julie E. Gibouleau, *Assistant to the Executive Director*
Louis L. Meier, *Washington Counsel/Assistant Secretary*
William H. Wisely, *Executive Director Emeritus*
Michael N. Salgo, *Treasurer*
Elmer B. Isaak, *Assistant Treasurer*

STAFF DIRECTORS

Donald A. Buzzell, *Managing Director for Education and Professional Affairs*
Robert A. Crist, Jr., *Managing Director for Publications and Technical Affairs*
Alexander Korwek, *Managing Director for Finance and Administrative Services*
Alexandra Bellow, *Director, Human Resources*
David Dresia, *Director, Publications Production and Marketing*
Barker D. Herr, *Director, Membership*
Richard A. Jeffers, *Controller*
Carl E. Nelson, *Director, Field Services*
Don P. Reynolds, *Director, Policy, Planning and Public Affairs*
Bruce Rickerson, *Director, Legislative Services*
James M. Shea, *Director, Public Communications*
Albert W. Turchick, *Director, Technical Services*
George K. Wadlin, *Director, Education Services*
R. Lawrence Whipple, *Director, Engineering Management Services*

COMMITTEE ON PUBLICATIONS

Stafford E. Thornton, *Chairman*
Martin G. Abegg
John A. Focht, Jr.
Richard W. Karn
Paul R. Munger
William R. Neuman

STRUCTURAL DIVISION

Executive Committee
John E. Bower, *Chairman*
Ronald G. Domer, *Vice Chairman*
Peter B. Cooper
Donald McDonald, *Secretary*
Frederick H. Sterbenz, *Management Group B Contact Member*
Joseph H. Appleton, *Management Group B Contact Member*
Roland L. Sharpe

Publications Committee
John E. Bower, ***Chairman, Editor and Exec. Comm. Contact Member***
Mihran S. Agbabian
Marvin E. Criswell
John T. DeWolf
Douglas Foutch
Ovadia E. Lev
Le-Wu Lu
Bruce E. Lyons
Walter Podolny
Emil Simiu
John F. Stolz
C. K. Wang
James T. P. Yao

PUBLICATIONS SERVICES DEPARTMENT

David Dresia, *Director, Publications Production and Marketing*

Technical and Professional Publications

Richard R. Torrens, *Manager*
Chuck Wahrhaftig, *Chief Copy Editor*
Linda Ellington, *Copy Editor*
Thea C. Feldman, *Copy Editor*
Meryl Mandle, *Copy Editor*
Joshua Spieler, *Copy Editor*
Shiela Menaker, *Production Co-ordinator*
Richard C. Scheblein, *Draftsman*

Information Services

Elan Garonzik, *Editor*

PERMISSION TO PHOTOCOPY JOURNAL PAPERS

Permission to photocopy for personal or internal reference beyond the limits in Sections 107 and 108 of the U.S. Copyright Law is granted by the American Society of Civil Engineers for libraries and other users registered with the Copyright Clearance Center, 21 Congress Street, Salem, Mass. 01970, provided the appropriate fee is paid to the CCC for all articles bearing the CCC code. Requests for special permission or bulk copying should be addressed to the Manager of Technical and Professional Publications, American Society of Civil Engineers.

CONTENTS

Undersea Suspended Cable Structures
by William J. Nordell and Dallas J. Meggitt 1025

Deterministic Fluid Forces on Structures: A Review
by John W. Leonard, G. J. Garrison, and Robert T. Hudspeth 1041

Bottom-Supported Concrete Platforms: Overview
by William J. Graff and Wai F. Chen 1059

Fixed Pile-Supported Steel Offshore Platforms
by Peter W. Marshall 1083

Delphi Methods: Theory and Design Load Applications
by Ross B. Corotis, Raymond R. Fox, and John C. Harris 1095

Predicting Torsional Response of Thin-Walled Open RC Members
by Petar Krpan and Michael P. Collins 1107

Testing Thin-Walled Open RC Structure in Torsion
by Petar Krpan and Michael P. Collins 1129

This Journal is published monthly by the American Society of Civil Engineers. Publications office is at 345 East 47th Street, New York, N.Y. 10017. Address all ASCE correspondence to the Editorial and General Offices at 345 East 47th Street, New York, N.Y. 10017. Allow six weeks for change of address to become effective. Subscription price to members is $22.50. Nonmember subscriptions available; prices obtainable on request. Second-class postage paid at New York, N.Y. and at additional mailing offices. ST.

The Society is not responsible for any statement made or opinion expressed in its publications.

DISCUSSION

Proc. Paper 16284

Aerodynamic Response of Long H-Sections,[a] by Frances J. Maher and Larry E. Wittig (Jan., 1980).
by Carl H. Gronquist 1143

INFORMATION RETRIEVAL

The key words, abstract, and reference "cards" for each article in this Journal represent part of the ASCE participation in the EJC information retrieval plan. The retrieval data are placed herein so that each can be cut out, placed on a 3 × 5 card and given an accession number for the user's file. The accession number is then entered on key word cards so that the user can subsequently match key words to choose the articles he wishes. Details of this program were given in an August, 1962 article in CIVIL ENGINEERING, reprints of which are available on request to ASCE headquarters.

[a]Discussion period closed for this paper. Any other discussion received during this discussion period will be published in subsequent Journals.

16351 UNDERSEA SUSPENDED CABLE STRUCTURES

KEY WORDS: **Cables (ropes);** Currents (water); Drag; Dynamic response; **Hydrodynamics;** Hydrostatic pressure; **Implantation; Ocean engineering;** Offshore platforms; **Suspended structures; Underwater construction; Underwater structures;** Vibration effects

ABSTRACT: The design, analysis and implantment of undersea suspended cable structures is explored. These structures have been located in water depths to 19,000 feet (5,800 m). The predominant external load imposed on the structures in-situ is current-induced drag; however, the design is often significantly influenced by the dynamic forces generated during implantment by the surface platform motions. Hydrostatic pressure may be the governing load in the design of some components. Analytical techniques are available for predicting the dynamic response of these structures subjected to implantment and in-situ forces. The influence of cable strumming on structural response can also be estimated. The design must consider the following: limitations to be imposed on the structure motion, the mean and maximum current profile, the corrosion and biofouling potential at the site, and the weather window for implantment. Implantment (or construction) techniques emphasize prefabrication to minimize on-site operations and time.

REFERENCE: Nordell, William J., and Meggitt, Dallas J., "Undersea Suspended Cable Structures," *Journal of the Structural Division,* ASCE, Vol. 107, No. ST6, **Proc. Paper 16351**, June, 1981, pp. 1025-1040

16352 DETERMINISTIC FLUID FORCES ON STRUCTURES

KEY WORDS: Currents (water); **Diffraction; Drag;** Hydrodynamic pressure; Hydrodynamics; **Inertia; Loads (forces);** Offshore structures; Underwater structures; Water waves; Wave diffraction

ABSTRACT: The deterministic wave- and current-induced hydrodynamic loadings on sea-based structures are reviewed. This state-of-the-art review does not include geotechnical, surface, or installational/operational forces. Wave-induced loadings in both the small member (Morison equation) and large member (diffraction) regimes of wave force computations are reviewed. The selection of appropriate water wave theories and hydrodynamic force coefficients is included. The effects of laboratory facilities on the evaluation of the hydrodynamic force coefficients for periodic flows are also considered.

REFERENCE: Leonard, John W., Garrison, C. J., and Hudspeth, Robert T., "Deterministic Fluid Forces on Structures: A Review," *Journal of the Structural Division,* ASCE, Vol. 107, No. ST6, **Proc. Paper 16352**, June, 1981, pp. 1041-1057

16353 BOTTOM-SUPPORTED CONCRETE PLATFORMS

KEY WORDS: Concrete (post-tensioned); Concrete (reinforced); Foundations; **Offshore drilling; Offshore platforms; Offshore structures;** Shell structures; Soil-structure interaction; Space frames; **Structural dynamics;** Underwater construction; Underwater structures

ABSTRACT: A concrete gravity platform consists of a cellular caisson made up of a collection of large concrete cylinders supporting three or four large diameter tubular columns with a steel frame deck structure on top. The huge size of the overall structure, and the variety of load conditions, make it complicated to analyze all of the problems with one structural model. The complete soil-structure-water system is divided into separate systems for analysis, and then the load cases are combined with due regard for interaction effects to determine the total response. Three general classes of analyses are involved: (1) Space frames; (2) continuum type shell problems; and (3) soil-structure interaction problems. Methods of predicting elastic-plastic-fracture behavior and implosion pressure on the outer cell walls are mentioned. Kinds of failure of gravity type foundations for offshore structures are given.

REFERENCE: Graff, William J., and Chen, Wai F., "Bottom-Supported Concrete Platforms: Overview," *Journal of the Structural Division,* ASCE, Vol. 107, No. ST6, **Proc. Paper 16353**, June, 1981, pp. 1059-1081

16354 PILE-SUPPORTED STEEL OFFSHORE PLATFORMS

KEY WORDS: **Bibliographies;** Ocean engineering; **Offshore platforms; Offshore structures; Structural design; Underwater construction;** Underwater structures

ABSTRACT: Offshore construction as we know it today began in 1947 with the installation of the first steel template-type structure in the Gulf of Mexico. Twenty years later there were over 2,000 such structures, and the technology had matured in the sense that much of the pioneering had been done, and the pattern was pretty well set for what are today's routine structures. The basic technology is outlined to provide one designer's perspective from which recent developments can be appreciated. This present state of practice is codified in API RP 2A. The outline cites 197 landmark papers from among the over 2,600 which appear in the Preprints/Proceedings of the Offshore Technology Conference, as well as 88 other key reference from other sources.

REFERENCE: Marshall, Peter W., "Fixed Pile-Supported Steel Offshore Platforms," *Journal of the Structural Division*, ASCE, Vol. 107, No. ST6, **Proc. Paper 16354**, June, 1981, pp. 1083-1094

16322 DELPHI METHOD AND DESIGN LOADS

KEY WORDS: **Buildings (codes); Communication;** Communication between engineers; Decision making; **Design;** Group dynamics; Live loads; Safety; **Standards; Structural design**

ABSTRACT: The Delphi method of highly structured group communication is described. The method is characterized by anonymity of responses from a panel of experts, controlled feedback with a statistical description of responses, and multiple iterations to reach a consensus. It is designed to extract the maximum unbiased information in reaching the most reliable results. The basic philosophy, historical development and relevance of the method to structural design loads are addressed. The Delphi method is applied to the revision of design live loads for American National Standard A58, "Building Code Requirements for Minimum Design Loads in Buildings and Other Structures." A panel of 25 outstanding structural engineers was formed and two interactions used to produce final recommended changes to the standard. A detailed discussion of the conduct of the Delphi and the implementation of the changes is included. The method offers potential for additional application in structural engineering.

REFERENCE: Corotis, Ross B., Fox, Raymond R., and Harris, John C., "Delphi Methods: Theory and Design Load Application," *Journal of the Structural Division*, ASCE, Vol. 107, No. ST6, **Proc. Paper 16322**, June, 1981, pp. 1095-1105

16333 RESPONSE OF THIN-WALLED OPEN RC MEMBERS

KEY WORDS: **Beams; Calculations; Concrete (reinforced);** Cracking; **Reinforced concretes;** Strain; **Structural dynamics; Theoretical analysis;** Torque; **Torsion;** Warpage

ABSTRACT: Procedures for calculating the torque-twist response of thin-walled open reinforced concrete members are presented. Traditional theories for predicting the warping torsion response of elastic, homogeneous beams can be modified and extended so that post-cracking and inelastic warping torsion response of reinforced concrete open thin-walled beams can be predicted. The theoretical procedures are illustrated by predicting the response of a reinforced concrete channel beam attached to rigid abutments and loaded with a torque at midspan. The predicted response includes not only the relationship between the applied torque and the resulting rotation but also estimates of the torques at which the concrete will crack, the reinforcement will yield and the member will fail.

REFERENCE: Krpan, Petar, and Collins, Michael P., "Predicting Torsional Response of Thin-Walled Open RC Members," *Journal of the Structural Division*, ASCE, Vol. 107, No. ST6, **Proc. Paper 16333**, June, 1981, pp. 1107-1127

16332 THIN-WALLED OPEN RC STRUCTURE IN TORSION

KEY WORDS: **Beams; Concrete (reinforced);** Cracking; Longitudinal stability; **Reinforced concretes;** Strain; **Structural dynamics; Tests;** Torque; **Torsion;** Warpage

ABSTRACT: A large, U-shaped, thin-walled, reinforced concrete beam, restrained at both ends with heavy diaphragms, was subjected to torsional moment at midspan and tested throughout postcracking and post yielding ranges to its ultimate capacity. Measured strains in the longitudinal steel, and stirrups, and torque-angle of twist curves, torque at yielding and cracking were compared with predictions based on the theoretical models proposed by the writers in a companion paper. Very good agreement was obtained.

REFERENCE: Krpan, Petar, and Collins, Michael P., "Testing Thin-Walled Open RC Structure in Torsion," *Journal of the Structural Division,* ASCE, Vol. 107, No. ST6, **Proc. Paper 16332,** June, 1981, pp. 1129-1140

U.S. Customary-SI Conversion Factors

In accordance with the October, 1970 action of the ASCE Board of Direction, which stated that all publications of the Society should list all measurements in both U.S. Customary and SI (International System) units, the following list contains conversion factors to enable readers to compute the SI unit values of measurements. A complete guide to the SI system and its use has been published by the American Society for Testing and Materials. Copies of this publication (ASTM E-380) can be purchased from ASCE at a price of $3.00 each; orders must be prepaid.

All authors of *Journal* papers are being asked to prepare their papers in this dual-unit format. To provide preliminary assistance to authors, the following list of conversion factors and guides are recommended by the ASCE Committee on Metrication.

To convert	To	Multiply by
inches (in.)	millimeters (mm)	25.4
feet (ft)	meters (m)	0.305
yards (yd)	meters (m)	0.914
miles (miles)	kilometers (km)	1.61
square inches (sq in.)	square millimeters (mm^2)	645
square feet (sq ft)	square meters (m^2)	0.093
square yards (sq yd)	square meters (m^2)	0.836
square miles (sq miles)	square kilometers (km^2)	2.59
acres (acre)	hectares (ha)	0.405
cubic inches (cu in.)	cubic millimeters (mm^3)	16,400
cubic feet (cu ft)	cubic meters (m^3)	0.028
cubic yards (cu yd)	cubic meters (m^3)	0.765
pounds (lb) mass	kilograms (kg)	0.453
tons (ton) mass	kilograms (kg)	907
pound force (lbf)	newtons (N)	4.45
kilogram force (kgf)	newtons (N)	9.81
pounds per square foot (psf)	pascals (Pa)	47.9
pounds per square inch (psi)	kilopascals (kPa)	6.89
U.S. gallons (gal)	liters (L)	3.79
acre-feet (acre-ft)	cubic meters (m^3)	1,233

UNDERSEA SUSPENDED CABLE STRUCTURES[a]

By William J. Nordell[1] and Dallas J. Meggitt,[2] Members, ASCE

INTRODUCTION

Cables are important structural elements in ocean engineering. Little is done in ocean construction which does not involve at one time or another a cable suspended under tension in the water column. Suspended cable structures are a common and important class of ocean structures; the ship mooring may be the earliest and most common application of this type of structure. However, cable structures are now used for a wide variety of purposes. They are used as platforms to support instrumentation (7,13,20) and as moorings for subsurface objects (15).

These structures consist of three principal subsystems: (1) The cables which serve as the principal load-carrying element; (2) the flotation which supports the system in the water column; and (3) the anchorage which secures the system to the seafloor. The assembly of these subsystems into a structure can take many forms; general classes of these forms are shown in Fig. 1. Two specific examples are shown in Figs. 2 and 3. The *Squaw* mooring (15), Fig. 2, consisted of four mooring legs (cables) with dead-weight anchors for the vertical legs and drag-type anchors for the catenary legs. The flotation was provided by the payload, the *Squaw* hull, a submarine hull which functioned as a sonar target for Navy training exercises.

A tripod mooring (20), Fig. 3, which was used to obtain measurements of internal waves, which are waves travelling along the interface between layers of different density in the ocean. The mooring consisted of three legs with flotation attached at discrete points along their lengths to reduce leg weight and thus leg catenary sag. Additional flotation was provided by a buoy at the apex. This design was aimed at minimizing the motions of the wave measurement sensors.

[a]Presented at the October 22–26, 1979, ASCE Annual Convention and Exposition, held at Atlanta, Ga.

[1]Dir., Ocean Struct. Div., Civ. Engrg. Lab., Naval Construction Battalion Center, Port Hueneme, Calif. 93043.

[2]Dir., Construction Systems Div., Civ. Engrg. Lab., Naval Construction Battalion Center, Port Hueneme, Calif. 93043.

Note.—Discussion open until November 1, 1981. Separate discussions should be submitted for the individual papers in this symposium. To extend the closing date one month, a written request must be filed with the Manager of Technical and Professional Publications, ASCE. Manuscript was submitted for review for possible publication on March 19, 1980. This paper is part of the Journal of the Structural Division, Proceedings of the American Society of Civil Engineers, ©ASCE, Vol. 107, No. ST6, June, 1981. ISSN 0044-8001/81/0006-1025/$01.00.

In recent years significant advancements have been made in the technology for the design of suspended undersea cable structures. The resulting technology base provides insight into both the techniques and the problems involved in ocean construction and, thus, provides a vehicle to acquaint engineers unfamiliar with ocean design and construction with some of the aspects involved in such an activity. This paper is directed toward this end.

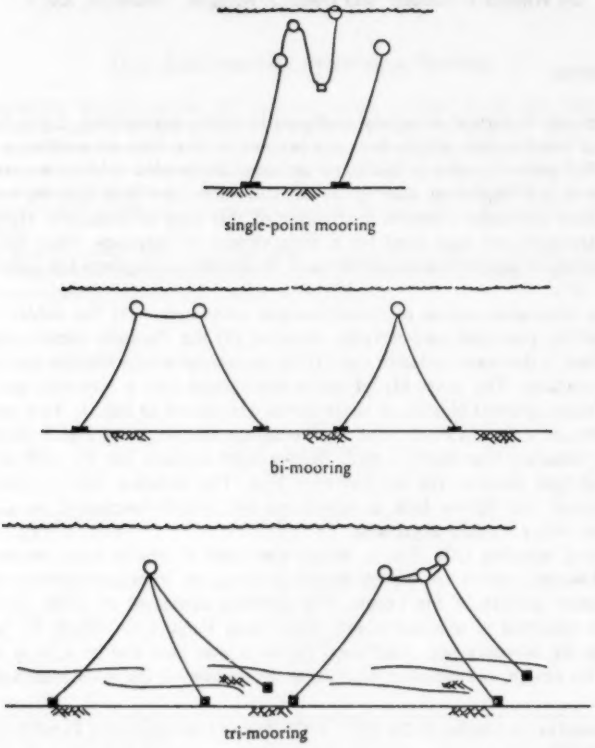

FIG. 1.—General Classes of Undersea Suspended Cable Structures

The presentation that follows is divided into three sections. The first is concerned with the structural design and analysis of the total system. The second covers design aspects of the major subsystems, and the last section describes some of the problems associated with installing such structures.

Analysis

Cables are treated normally as elements that resist only tension in the longitudinal direction. The analysis of undersea cable structures might, therefore,

appear to be a relatively simple, straightforward process. On the contrary, however, the analysis can be as complex as those associated with other classes of structures—bridges, buildings, etc. These complexities arise in part because the analysis involves the solution of an extensively nonlinear structural response problem.

The nonlinearities are caused by the following factors: (1) The large changes in configuration which undersea cable structures generally undergo in response to applied loads (geometric nonlinearity); (2) the nonlinear load-deformation behavior of cables, which also includes the lack of any significant stiffness in compression (material nonlinearity); (3) the dependency of the load on the position, shape, and orientation of the structure; (4) the drag loading which

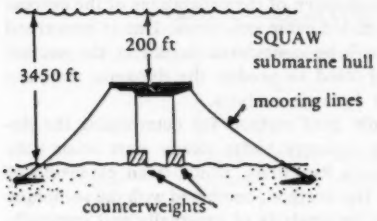

FIG. 2.—Squaw Mooring (1 ft = 0.305 m)

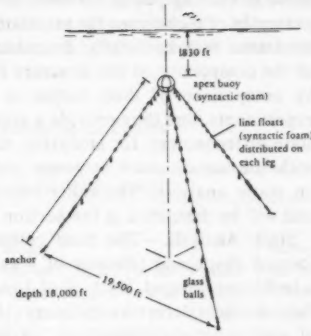

FIG. 3.—Instrumented Tri-moor (1 ft = 0.305 m)

is a function of the velocity squared; and (5) the limiting surface and seafloor constraints which are dependent on the cable response (21,22).

The analysis of an undersea cable structure can be divided into two principal problem areas. One involves the analysis of the structure as it is deployed (or retrieved) in the ocean; this is primarily a dynamic analysis because the motion of the platform can excite the cable system at one of its natural frequencies; the resulting tensions may well control the cable design. The other involves the analysis of the structure once it is implanted in the ocean; this is primarily a steady state analysis because the applied load is generated by a relatively steady current-induced drag force. However, dynamic response may be induced in this state if the cable responds to vortex shedding as the water moves past the cable.

Three major approaches have been used to describe the behavior of sea-based cable structures. Two of them subdivide the cable system into discrete elements while the other considers the cable to be, as in fact it is, a continuum. The two discrete element approaches are the lumped parameter and the finite element methods, both of which are also widely used by structural dynamicists for more conventional structures. In the continuum approach, the governing equations

are developed considering a differential element of the cable with the external and internal forces acting on it.

The lumped parameter method has great appeal because the approximation is founded to a large extent on physical intuition. A continuously distributed system is replaced by a system of discrete mass points (or lumped masses) interconnected by suitably chosen springs and dampers (dashpots). On the other hand, the finite element method represents the continuous system by a series of interconnected elements. The behavior of these elements is described by interpolation functions which are generally expressed in terms of the displacements of the end points (or nodes) of the element.

For each of these approaches, techniques have been developed for solving the governing equations. Refs. 3, 10, 21, 22 provide detailed analyses and can serve as starting points for those interested in pursuing the topic. Three specific examples of techniques for calculating the structural response of sea-based cable structures will be briefly described. These techniques are versatile in terms of the complexity of the structure that can be handled; they have been verified by comparison of their output to data obtained from laboratory and at-sea experiments, and they provide a good indication of the capabilities of the current state of technology for analyzing suspended cable structures. One is concerned with the steady state response and will be considered herein in the section on static analysis. The other two are used to predict the dynamic response and will be described in the section on dynamic analysis.

Static Analysis.—The most commonly used method for determining the deformed shape and tensions of a cable structure under steady state loads uses a technique termed Method of Imaginary Reactions, which is an extension of the consistent deformation theory (16). This method, combined with the technique of successive approximations, permits the analysis of externally and internally indeterminate cable arrays in a three-dimensional current field. This method is incorporated in the computer program DESADE (14,17) which calculates the steady state configuration and tensions given the environmental conditions, the physical and hydrodynamic characteristics of the structure's components, and the anchor locations. The environmental conditions are defined by the seawater density at the site and the current field description (horizontal and vertical distribution). The physical characteristics include the size, shape, weight (buoyancy) and location of each component, except the anchors for which only the locations need be described.

The hydrodynamic characteristics are used to define the applied force on the structural components. The applied fluid force consists of two terms, one represents the current drag loading and the other represents an inertia force, which is proportional to the mass of the displaced water, described as follows

$$F = 0.5\, C_d \rho A U\, U + C_m \rho V \dot{U} \quad \ldots\ldots\ldots\ldots\ldots\ldots\ldots\ldots\ldots\ldots (1)$$

in which C_d = drag coefficient; ρ = mass density of the fluid; A = characteristic area of the component (for a cable A per unit length of the cable = d, the cable diameter); U = current velocity = vector difference between the fluid and component velocities; C_m = mass coefficient; V = characteristic volume; for a unit length of cable, $V = (\pi d^2)/4$; and $\dot{U}$ = particle acceleration = vector difference between the fluid and component accelerations.

For the static problem the second term is zero and U equals the fluid velocity.

This force is then called the drag force and is generally expressed in terms of forces normal and tangential to the longitudinal axis of the component. It is computed based on the velocity components in and the drag coefficients for the normal and tangential directions. Because the tangential drag coefficient is in most cases orders of magnitude less than the normal drag coefficient, the tangential drag force is often neglected, since its effect on the overall steady state response is usually small.

The normal drag coefficient, C_{dn}, for the cable is generally taken to be equal to that determined from tests on a sample of the cable which is held stationary in a constant, uniform flow field. Ref. 4 provides values of C_{dn} for various types of cables. Table 1 is a summary of some of the data presented in Ref. 4. Although it provides some representative values for C_{dn}, it is recommended that, for cases where the motions or forces on the cable are an important design consideration, C_{dn} for the cable should be determined by laboratory tests. The effective drag coefficient may be increased by strumming as considered later.

TABLE 1.—Normal Drag Coefficients for Cables

Cable (1)	REYNOLDS NUMBER RANGE 10^3–10^4 Minimum (2)	Average (3)	Maximum (4)	Number of tests (5)	10^4–10^5 Minimum (6)	Average (7)	Maximum (8)	Number of tests (9)
Unjacketed stranded steel cable	0.98	1.54	2.47	65	0.30	1.29	3.60	115
Smooth jacketed steel cables	1.16	1.50	1.64	11	0.72	1.14	1.78	24
Synthetic line:								
Braided	1.11	1.14	1.15	3	1.11	1.14	1.16	5
Plaited	0.79	1.17	1.64	15	0.88	0.99	1.15	78

Dynamic Analysis.—The dynamic analysis of undersea cable structures is generally separated into two areas. One is concerned with the large displacement response where the magnitude of the displacements is much greater than the diameter of the cable. The other deals with the flow-induced small amplitude vibrations commonly referred to as cable strumming.

Large Displacement Dynamics.—Failures of cable systems occur most often during implantment or retrieval, when the deployed portion of the structure is subjected to the transient loads caused by the motions of the construction platform. Snap loads are a potential hazard during these operations; these loads occur in a cable when it becomes slack and is abruptly retensioned; snap loads six to ten times greater then the static load have been measured. The ability, therefore, to analyze the structural response during deployment or retrieval is critical to the success of the whole construction project. For the dynamic problem, the fluid force is defined by both terms of Eq. 1.

The computer program SNAPLG applies the lumped parameter approach to a large class of two-dimensional dynamic problems (8). Loadings can be from surface waves, steady ship velocity, or a nonuniform current profile. Geometric nonlinearities and velocity-squared nonlinear drag forces are included, as well as payout and reel-in operations. The material properties are assumed to be linear in the tensile region. If the cable slackens, the cable stiffness is set to zero and the computations proceed. Thus, the occurrence and location of snap loads can be defined, but the magnitude of the snap loads cannot yet be estimated reliably.

The finite element program SEADYN was developed specifically for underwater cable structure dynamic analysis (21). It is much more general than SNAPLG. The program solves 3-dimensional problems including transient and steady state behavior for complex systems which include buoys, anchors, fixed joints, different cable materials, and payout or reel-in. The combined nonlinear effects of large displacements, large strains, velocity-squared hydrodynamic loading, nonlinear materials, and constraints on the surface and bottom of the current field can be handled by SEADYN. Natural frequencies and mode shapes can be calculated. Loadings can be from point loads, nonsteady 3-dimensional current fields, surface waves or wave spectra, and wind loadings. The modelling techniques and solution options for both static and dynamic problems available in SEADYN provide a high degree of versatility in obtaining solutions of the desired accuracy at minimal cost.

Comparisons of output from these two programs have been made with data from a series of small-scale laboratory tests and indicate that both programs provide reasonable estimates of cable motion and tensions (12).

Small Amplitude Vibrations.—Relatively small-amplitude, high-frequency cable vibration due to periodic lift forces induced by vortex shedding (generally termed strumming) is a commonly observed phenomenon in the ocean. This motion frequently results in degraded sensor performance (in the case of cables serving as instrumentation platforms) and accelerated fatigue of structural elements. Furthermore, the drag of a strumming cable is significantly higher than that of a nonvibrating cable, producing higher stresses in some of the elements and a greater distortion of the structure in a given current field.

The effects of cable strumming on the steady-state response of cable arrays can be taken into account by increasing the value of the normal drag coefficient as used in the drag term of Eq. 1. A strumming predictive model is available to provide predictions of the amplitude and frequency of strumming for cables in a uniform current; using experimental data, the amplitudes and frequencies have been related to the apparent increases in the drag coefficient of strumming cables (6). Increases in C_{dn} of up to 2.5 times that of a stationary cable are possible. A strumming model was utilized with the DESADE program and the calculated response was confirmed by the SEACON II structure data (7,18). Thus, any steady state analysis must take into consideration strumming if reasonably accurate predictions are to be obtained.

Principal Components

Cables.—Two types of cables are used in undersea suspended cable structures, mechanical cables and electrical-mechanical (E-M) cables. Mechanical cables

are much like those used for terrestrial applications. The E-M cables are common in undersea structures because of the frequent need to provide both electrical conductivity and tensile strength in one cable. Electrical conductors are used to transmit power or signal, or both, while the strength member transmits the axial tensile load. Because E-M cables are generally the more unique and complex of the two types, the remainder of this section will emphasize E-M cables. Furthermore, to a large extent the discussion of the mechanical portion of an E-M cable applies equally well to mechanical cables used for undersea suspended structure applications.

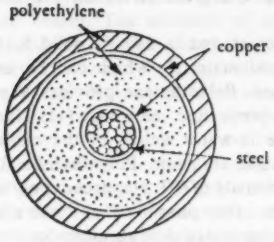

Coaxial Armorless Ocean Cable
(Polyethylene jacket diameter, 1.25 in.)

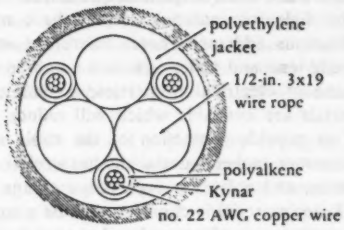

One-half-in. 3x19 cable.

(a) Internal Strength Member.

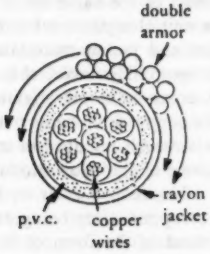

Multiconductor
Electromechanical Cable
(Rayon jacket diameter,
0.187 in.)

(b) External Strength Member.

FIG. 4.—Examples of Electrical-Mechanical Cables (1 m = 25.4 mm)

The basic elements making up an E-M cable are: (1) The conductor(s); (2) a dielectric; (3) the strength member; and (4) an outer (protective) jacket. The conductors and strength member can be configured within the cross section in various ways. The principal division depends on whether the strength member is internal or external with reference to the electrical conductors. Examples of each type are shown in Fig. 4; each has its advantages and disadvantages.

The internal strength member makes the electrical breakouts simpler and produces a more flexible cable. An external strength member provides greater protection for the electrical conductors; it is frequently referred to as armored cable.

The electrical characteristics of E-M cables will be considered only briefly here. There are two basic types of conductors, coaxial and multiconductor. The conductor material is in almost all cases copper, primarily because the E-M cables are used for signal transmission and copper provides the best combination of low cost and high conductivity—the latter being essential for maximum frequency bandwidth (11). However, the continued development of fiber optics for use in signal transmission cables will have a great effect on the design of future undersea suspended structures.

The dielectric material isolates the conductors and is usually solid for the applications addressed here. There are several materials which can be used; polyethylene and teflon are two common ones. Polyethylene provides a good balance of electrical properties, mechanical properties, and cost (11). Jacket materials are available which will reduce the in-water weight of the cable as well as provide protection of the cable against abrasion. Polyethylene foam is a common jacket material and has a relative density of 0.7. Neoprene, polyvinyl chloride, and polyether type polyurethane are other possible jacket materials. The latter material is considered to be a superior material in abrasion resistance and produces an effective bond at terminations and connectors (2).

Strength members have been made of steel, Kevlar (registered DuPont trademark; a synthetic aramid fiber), fiberglass, and polyester. However, the cable must be designed so that the strength member takes essentially all of the load. Because all the elements of the cable are effectively bonded together, they are subjected to the same unit elongation when the cable is stressed.

The stretch of the insulation and jacket materials is such that there is no problem in their being overstressed. However, this is not the case for most conductors, and the strength component material must be selected and the elements designed to prevent the copper from being overstressed. A high modulus of elasticity is desired for the strength member in order to minimize the load carried by the conductor. Because of their low modulus of elasticity compared to that of copper, synthetics other than Kevlar or fiberglass used in parallel with copper could result in the copper wires being overloaded. For many E-M cables, the copper is usually used in the form of braids and twisted multiple conductors, which greatly reduces the likelihood of the copper being overstressed.

Desirable characteristics of an E-M cable to be used in suspended cable structure are: (1) Torque-balanced or torque-free construction; (2) low unit weight; (3) small diameter; (4) high modulus of resilience; (5) ease of handling; (6) ease of termination and sensor attachment; (7) corrosion-resistant; (8) nonfouling; and (9) stable and reliable physical and electrical properties.

Unlike most terrestrial construction, ocean construction normally involves at one point a load on a free end of cable several hundred to several thousand feet long. When a load, for example a dead-weight anchor, is being lowered into the ocean the load may rotate because the tension causes the cable to unwind. When the load reaches the seafloor, the tension is reduced to zero and the stored torsional energy is released, causing loops to form in the cable. Retensioning can cause the cable to kink (a tight twist or curl of cable on itself), resulting in permanent damage to the cable (9).

A torque-balanced cable is one designed to yield zero or very small amounts of rotation under load. Therefore, a torque-balanced cable is desirable because it eliminates the problems of torque and twisting under tension. Torque-balancing can be achieved through various cable construction techniques, e.g., braided and reversed-lay cable constructions.

A lightweight cable facilitates handling and minimizes the appended buoyancy necessary to overcome the cable weight. The smaller the cable diameter, the smaller will be the drag force which is directly proportional to the diameter.

A high modulus of resilience provides a cable which is more effective in absorbing dynamic loads which may be generated as it is deployed from a surface vessel. The modulus of resilience is represented by the area under the elastic portion of the load-elongation curvé. Kevlar combines a higher stress capacity and lower E compared to steel and therefore has a higher modulus of resilience. Nylon has a greater modulus of resilience than either Kevlar or steel, but is generally undesirable for E-M cables because of its low modulus of elasticity.

Cable handling involves loading the cable aboard a platform, deploying it, and often retrieving it. The cable design should allow these manipulations without damage to the cable or excessive twisting which could lead to kinking. Generally, the more flexible a cable, the easier it is to handle. Cable flexibility is dependent on several factors: wire or fiber material and diameter, cable diameter, and type of construction.

The rationale for including the remaining characteristics is tied to the remoteness and severity of the environment into which the structure is placed. It is remote because of the difficulties in getting to and performing work on a structure whether it be in water shallow enough to be accessible by divers or in deep water so that remotely-operated vehicles or manned submersibles must be used. It is severe because corrosion and fouling (biological growth) can occur although the degree to which they are a problem is site and depth dependent. Whether the structure is maintained, repaired in-situ, or retrieved, it is not a simple or inexpensive task so the need for such activity is minimized.

Buoyancy.—In terrestrial cable-supported construction, the cables are generally suspended from fixed supports. The counterparts in undersea suspended cable structures are the buoys which support the cable and other equipment in the water column and are therefore a critical element of the system.

Buoyancy can be distributed or concentrated; however, distributed buoyancy is less efficient hydrodynamically because it increases the drag area. Cables have been designed with low density jackets which cause the cable to be positively buoyant in water. Buoys provide discrete quantities of buoyancy and are given the primary consideration in this section.

The major desirable characteristics of a buoyancy material or buoy are: (1) Low density; (2) low-water absorption or watertightness; (3) high hydrostatic pressure strength; (4) corrosion resistant; (5) antifouling; and (6) bulk modulus equal to seawater. Low density is of prime importance because of the desire to maximize buoyancy and minimize weight. There are basically two approaches: One is to displace the water by a material which has a lower density than the water. The other uses a shell which creates a cavity in the water. Buoyancy is the difference between the shell weight and the weight of displaced water.

Watertightness or low water absorption is critical to maintaining the required

buoyancy after the structure is installed. Pressure-resistant hulls should be prooftested prior to deployment to ensure watertightness. In some cases, when watertightness is absolutely critical, all the joints or mating surfaces of metallic hulls are welded.

The hydrostatic compressive strength of the buoyancy package will determine the depth to which it can be safely used. Generally, buoys to be submerged to any significant depth and constructed as a pressure hull are spherical in shape because this provides the most efficient shape based on a buoyancy-shell weight ratio.

Corrosion and fouling are two other factors which must be considered. Corrosion may be a problem with metallic pressure hulls; fouling can reduce the magnitude of buoyancy and may be a problem with any of the buoyancy alternatives. The extent of these two problems will be site dependent. Fouling will generally be a problem in warmer waters and at the shallower depths. Corrosion may reduce the structural integrity of the metallic buoyancy elements but is generally not a problem with syntactic foam and glass and acrylic hollow spheres.

A bulk modulus equal to that of seawater ensures that there is no change in the magnitude of buoyancy with depth. The bulk moduli for syntactic foams and pressure-resistant hulls are generally equal to or greater than that of seawater and, therefore, the buoyancy either remains constant or increases with depth. The loss of buoyancy with depth is generally associated with fluids and gases such as gasoline and air which are used in containers or shrouds open to the environment.

Syntactic foam, steel, glass, and acrylic are the materials most commonly used for buoys. The latter three are generally used to construct pressure-resistant hulls to act as buoys.

Syntactic foam is a plastic matrix filled with tiny hollow spheres. The microspheres which generally make up about 60% of the composition are made of glass, plastic, or ceramic. Generally, syntactic foam refers to the composite of glass spheres in an epoxy resin. Syntactic foam has many of the desirable characteristics for buoyancy materials. It has a low density, 26 pcf–42 pcf (415 kg/m^3–670 kg/m^3), a high resistance to hydrostatic pressure, 9,000 psi–21,000 psi (62,000 kPa–145,000 kPa), and is corrosion-resistant. The characteristic of most concern is the susceptibility to buoyancy loss with prolonged exposure. There is some question as to whether the buoyancy loss is due to the material absorbing water or whether the outer layers of microspheres are physically crushed, decreasing net buoyancy. Data are sparse on the long-term resistance of syntactic foam to buoyancy loss. Ref. 5 provides a summary of most of the available data. These data indicate that changes in buoyancy could be as high as 20% for a submergence period of 10 yr. The amount of buoyancy loss depends on several factors besides length of exposure, including foam density, hydrostatic pressure, and sample size and shape. Since syntactic foam is susceptible to buoyancy loss, it is critical that the amount of acceptable buoyancy change be considered in the design phase so an additional buoyancy allowance can be provided and the specification for syntactic foam can include a limit on the amount of allowable buoyancy change.

Several types of buoyancy packages are available commercially and have been used in cable structures. For operational depths above about 4,000 ft

(1,200 m), pressure hulls of plastic, steel, or aluminum are widely used, and for operational depths extending to 20,000 ft (6,100 m) syntactic foam and glass spheres are generally available. The collapse depth of steel and aluminum spherical hulls of low or intermediate strength preclude their use as efficient buoyancy

TABLE 2.—Summary of Anchor Characteristics (Ref. 19)

Anchor type (1)	Application (2)	Features (3)	Required site data (4)	Remarks (5)
Drag: (Navy Stockless)	sediment: cobbles, boulders, coral, rock	Does not bury deeply; relatively low holding-capacity-to-weight ratio; applicable to wide range of seafloors	Depth of sediment, soil type, areal variability; general characteristics of nonsediment seafloors	Easy recovery makes it good for temporary moorings; capacity decreases rapidly when uplift forces are applied
Burial: (STATO, LWT, Danforth)	sediment: adequate sediment depth required for deep burial	High holding-capacity-to weight ratio; capacity depends on deep burial in sediment; burial depth sensitive to fluke angle and soil anomalies	As above	STATO has adjustable fluke for use on sand or clay; may be difficult to recover when buried deeply; uplift decreases capacity
Dead weight: (Clump, mushroom)	sediment: minimal thickness required	Very low holding-capacity-to-weight ratio; bulky; horizontal capacity may be almost nil on fluid mud type of seafloors; does not bury deeply	As above; seafloor slopes greater than 10° have significant effect on capacity and stability	May be used to resist uplift forces (clump)
Drag anchor: (or burial) and deadweight combination	sediment	Clump resists uplift and drag anchor resists horizontal load	As above	Used to reduce mooring line scope
Propellant: actuated embedment	sediment, coral or soft rock	Resists uplift forces; high holding-capacity-to-weight ratio due to deep anchor burial	Sediment thickness, coral strength	Economical alternative to piling; special ordnance handling precautions required; not recoverable
Piling: (drilled in or driven)	sediment, coral, limestone, rock	Resists uplift forces; piling in hard coral or limestone must be drilled in and grouted	Sediment thickness and strength at anchor location; rock strength	Expensive; time-consuming, and relatively permanent; typically used where very high capacity is required

packages below about 4,000 ft (1,200 m). The pressure-resistant hulls of plastic, steel, or aluminum which are generally available commercially have buoyancies up to approximately 500 lb (230 kg). Hulls of larger buoyancy usually must be designed for the specific circumstances.

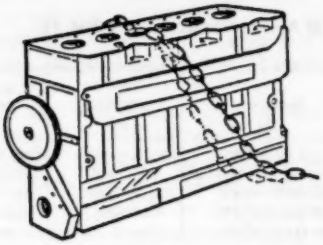

(a) Deadweight anchor.

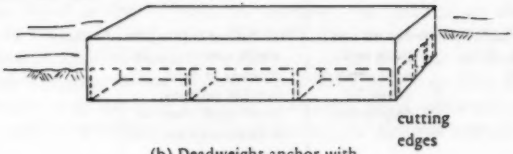

(b) Deadweight anchor with cutting edges.

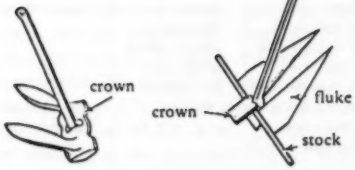

(c) Stockless drag anchor.

(d) Lightweight (burial) anchor.

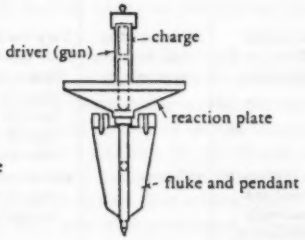

(e) Propellant-actuated direct-embedment anchor.

FIG. 5.—Anchor Types

Anchors.—As in terrestrial construction, the anchorage system resists the tensile load in the cables. This can be accomplished in one of three ways: (1) By applying adequate weight at the base to counteract the maximum force in the cable; (2) by utilizing the seafloor sediment or rock to provide the necessary resistance; or (3) by using a combination of items 1 and 2 to develop the total anchoring force. The first technique is the simple dead-weight anchor. The second includes conventional anchors, piling (drilled-in or driven), and direct-embedment anchors (propellant-actuated or vibrated). The third may be represented

by a "heavy" drag anchor or a drag anchor and deadweight combination. Fig. 5 shows examples of the different anchor types, and Table 2 provides a description of the characteristics of some commonly used anchors.

Uplift-resisting anchors have several advantages over conventional drag anchors. They reduce the scope (length) of mooring cable required; this becomes increasingly significant as the height of the structure above the seafloor increases. In addition, since these anchors do not have to be dragged to develop holding capacity, the installation can generally be accomplished in less time. This is highly desirable because it reduces the vulnerability to adverse sea and weather conditions, the nemesis of ocean construction operations. Uplift-resisting anchors also permit greater placement accuracy because they can be installed directly into the seafloor.

The holding efficiency of deadweight anchors is not near as great as other uplift-resisting anchors. Generally, they will be heavy and so may be difficult to handle. Ref. 1 summarizes the characteristics, advantages, and disadvantages or various anchor types.

Implantment

Implantment covers the on-site construction of the undersea cable structure. These construction operations are unique in two aspects: (1) The work takes place from a platform which is in motion; and (2) the structure is usually implanted in a remote location. The site is remote because it may be several hundreds of miles from land and, perhaps more importantly, because it is at a depth not easily reached by man.

It is even more true for ocean construction than terrestrial operations that planning the implantment is a necessity. For without adequate planning, failure is almost assured. This may be true of all construction projects, but it seems to be more so with ocean work because the environment seems to exploit any weaknesses in the construction scheme to the project's detriment.

When possible, the implantment is subdivided into several independent phases which can be accomplished during daylight hours. This allows convenient preplanned stopping points in case the weather should change for the worse and require the operation to cease for a time. Independent phases also permit intermediate checkouts of the system and retrieval of a portion of the system if a failure or some error is determined. For example, the SEACON II structure was implanted in eight independent steps and this multiphased approach was one of the major reasons a successful implantment was achieved (7).

All implantments have a limiting sea state beyond which the operation will have to cease. [Sea state refers to roughness of sea surface, and is expressed numerically by numbers 0–9, where zero refers to a calm sea and nine to one with exceptionally high waves, i.e., 75-ft (23-m) average.] The limiting sea state may be determined by the maximum allowable dynamic tensions which may be developed in the cable, by the capability of personnel to perform work on a deck in dynamic motion, or for some other reason. An important aspect of the implantment planning is making the equipment and operations compatible with a reasonable sea state. Sea operations, when possible, are planned for that time of year which maximizes the likelihood of good weather, i.e., the "weather window." However, a good plan provides contingencies for adverse

weather conditions. Most of these implantment operations are usually limited to sea states less than three or four.

In general, a single-vessel operation is desired to minimize the problems of communications and coordination inherent in multivessel operations. In addition, good design practice minimizes the amount of at-sea work—preassembly is emphasized. Generally, any task will take longer to complete if done at sea, and the quality will normally decrease as the weather increases. Therefore, work is generally limited to those things which absolutely *must* be done at sea.

Flexibility in the sea operations plan is a necessity. The multi-phased approach provides flexibility in response to operational problems and weather changes. Alternate courses of action are addressed in the deployment plan in order to minimize the need for improvisation at sea. "Last minute" changes should be avoided because they increase the likelihood of trouble.

Implantment testing and checkout, as well as monitoring of the system during implantment, are crucial activities if the installation is to be successful. The purpose is to uncover problems or potential problems at the earliest possible time to allow remedial actions to be taken without undoing—and then redoing—everything that has been done. Electrical and mechanical system monitoring should be done continuously during implantment, if possible, and if not, at least during the more critical stages. Monitoring the cable tensions can avoid overstressing the cable and could reveal changes in sea state which might otherwise go undetected until a more developed sea has been reached.

Training is another important aspect of the implantment process. The extent and scope of training will vary depending upon the complexity of the structure and implantment procedure, but may often include sea trials or the trial implantment of certain components.

The implantment scheme should minimize the risk of damage to the cable structure with the implantment plan providing the road map for a safe and successful operation. Development of the plan should be a team effort; engineers, riggers, and crewmen all should have an opportunity to contribute. This has proven to be a successful format.

Appendix I.—References

1. Atturio, J. M., "Modular Mooring System for Ocean Construction—User's Guide," *Technical Note N-1520*, Civil Engineering Laboratory, Naval Construction Battalion Center, Port Hueneme, Calif., Apr., 1978.
2. Bridges, R., "Structural Stresses in Undersea Cables—Their Effect on Reliability," *Journal of the Marine Technology Society*, Vol. 12, No. 5, Oct.–Nov., 1978, pp. 3–12.
3. Casarella, M. J., and Parsons, M., "A Survey of Investigations and Motions of Cable Systems Under Hydrodynamic Loading," *Journal of the Marine Technology Society*, Vol. 4, 1970.
4. Dalton, W. L., "A Survey of Available Data on the Normal Drag Coefficient of Cables Subjected to Cross-Flow," *Contract Report CR-78.001*, Civil Engineering Laboratory, NCBC, Rockville, Md., Mar, Inc. (Contract N62583-77-M-R443), Aug., 1977.
5. Davis, L. I., "Survey of Long-Term In-Site Data on Syntactic Foam and Synthetic Lines," *TR 4999-0001*, EG&G Washington Analytical Services Center, Inc., Rockville, Md., Mar., 1978.

6. Griffin, O. M., "The Vortex-Excited Strumming Vibrations of Marine Cable Systems," presented at the Oct., 1977, Fall Convention of the American Society of Civil Engineers, (Preprint 3095).
7. Kretschmer, T. R., Edgerton, G. A., and Albertsen, N. D., "Seafloor Construction Experiment, SEACON II—An Instrumented Tri-Moor for Evaluating Undersea Cable Structure Technology," *Technical Report R-848,* Civil Engineering Laboratory, NCBC, Port Hueneme, Calif., Dec., 1976.
8. Liu, F. C., "Snap Loads in Lifting and Mooring Cable Systems Induced by Surface Wave Conditions," *Technical Note N-1288,* Civil Engineering Laboratory, Naval Construction Battalion Center, Port Hueneme, Calif., Sept., 1973.
9. Liu, F. C., "Kink Formation and Rotational Response of Single and Multistrand Electromechanical Cables," *Proceedings of Civil Engineering in the Oceans III,* ASCE, Univ. of Delaware, June, 1975, pp. 546–568.
10. Nath, J. H., "State of the Art on Analysis of Cable Dynamics," *Proceedings of Civil Engineering in the Oceans III,* American Society of Civil Engineers, Univ. of Delaware, June, 1975, pp. 623–631.
11. Padilla, J. R., et al., "State of the Art of Electro-Mechanical Cables," *Technical Note N-1303,* Naval Civil Engineering Laboratory, Port Hueneme, Calif., Aug., 1973.
12. Palo, P., "Small-Scale Cable Dynamics Comparisons," *Proceedings of Civil Engineering in the Oceans IV,* ASCE, Sept., 1979.
13. Savage, G. H., and Hersey, J. B., "Project Seaspider: The Design, Assembly, Construction and Sea Trials of a Tri-Moored Buoyant Structure with Neutrally Buoyant Legs to Provide a Near-Motionless Instrument Base for Oceanographic Research," *Journal of the Marine Technology Society,* Vol. 3, No. 2, Mar., 1969, pp. 95–112.
14. Sergev, S., "DECEL1 Users Manual—A Fortran IV Program for Computing the Static Deflections of Structural Cable Arrays," *Technical Note TN-1584,* Civil Engineering Laboratory, NCBC, Port Hueneme, Calif., Aug., 1980.
15. Shipley, H. P., and Brown, D. F., "Deep-Sea Subsurface Mooring of a Model Submarine Hull," *Proceedings of the Conference on Civil Engineering in the Oceans,* American Society of Civil Engineers, 1967, pp. 305–349.
16. Skop, R. A., and O'Hara, G. J., "The Analysis of Internally Redundant Structural Cable Arrays," *Naval Research Laboratory Report 7296,* Naval Research Lab., Washington, D.C., Sept., 1971.
17. Skop, R. A., and Mark, J., "A Fortran IV Program for Computing the Static Deflections of Structural Arrays," *Naval Research Laboratory Report 7640,* Naval Research Lab., Washington, D.C., Aug., 1973.
18. Skop, R. A., Griffin, O. M., and Ramberg, S. E., "Strumming Predictions for the SEACON II Experimental Mooring," *Proceedings of the Ninth Annual Offshore Technology Conference,* May, 1977, Vol. III, pp. 61–66.
19. Taylor, R. J., Jones, D., and Beard, R. M., "Handbook for Uplift Resisting Anchors," Civil Engineering Laboratory, NCBC, Port Hueneme, Calif., Sept., 1975.
20. Walden, R. G., and Berteaux, H. D., "Design and Performance of a Deep-Sea Tri-Moor," *Proceedings of the Tenth Annual Conference of the Marine Technology Society,* 1974, pp. 81–96.
21. Webster, R. L., "Nonlinear Static and Dynamic Response of Underwater Cable Structures Using the Finite Element Method," Paper No. OTC 2322, *Proceedings of the Seventh Annual Offshore Technology Conference,* May 5–8, 1975, pp. 753–762.
22. Webster, R. L., "Finite Element Analysis of Deep Sea Moors and Cable Systems," presented at the Oct. 17–21, 1977, Fall Convention of the American Society of Civil Engineers, held at San Francisco, Calif. (Preprint 3033).

Appendix II.—Notation

The following symbols are used in this paper:

A = characteristic area of component;
C = coefficient;
d = cable diameter;

F = fluid force;
U = current velocity = vector difference between the fluid and component velocities;
$\dot{U}$ = fluid particle acceleration = vector difference between fluid and component accelerations;
V = characteristic volume; and
ρ = mass density of the fluid.

Subscripts

d = drag;
m = mass; and
n = normal.

DETERMINISTIC FLUID FORCES ON STRUCTURES: A REVIEW

By John W. Leonard,[1] A. M. ASCE, C. J. Garrison,[2] and Robert T. Hudspeth,[3] Members, ASCE

INTRODUCTION

The purpose of this paper is to provide an introductory review for structural engineers of the environmental sources and characteristics of the descriptive methods presently available for computing the deterministic loads applied to sea-based structures. Most attention is focused on the fluid transmitted loadings. Three types of loads which are *not* transmitted by fluid pressure fluctuations are the following:

1. Geotechnical forces: Loads transmitted to a bottom-fixed structure by motion of the sea floor. Large vertical or lateral structural motions beneath the mudline may be caused by actions such as seismic events, internal waves, storm waves in shallow water, slope destabilization following extensive erosion or scour, and geothermal or other types of subsidence. In the case of seismic loads, it is usually the stiffer structures in relatively shallow water with relatively higher natural frequencies (>0.5 Hz) which are more susceptible to damage. For deeper-water structures or platforms, or both, with smaller lateral motion restraints, earthquake loads are usually of secondary interest. In a seismic analysis (quasistatic or dynamic) one must include the effects of both added mass and hydrodynamic damping on the structural motions, as these two parameters significantly affect the structural mass and damping matrices such that lower natural frequencies are obtained.
2. Surface forces: Loads applied to structural components on or above the

[a]Presented at the October 22–26, 1979, ASCE Annual Convention and Exposition, held at Atlanta, Ga.

[1]Prof., Dept. of Civ. Engrg. and Ocean Engrg. Programs, Oregon State Univ., Corvallis, Oreg. 97331.

[2]Consultant in Marine Hydrodynamics, C. J. Garrison and Assoc., 3088 Hacienda Drive, Pebble Beach, Calif. 93953.

[3]Assoc. Prof., Dept. of Civ. Engrg. and Ocean Engrg. Programs, Oregon State Univ., Corvallis, Oreg. 97331.

Note.—Discussion open until November 1, 1981. Separate discussions should be submitted for the individual papers in this symposium. To extend the closing date one month, a written request must be filed with the Manager of Technical and Professional Publications, ASCE. Manuscript was submitted for review for possible publication on March 19, 1980. This paper is part of the Journal of the Structural Division, Proceedings of the American Society of Civil Engineers, ©ASCE, Vol. 107, No. ST6, June, 1981. ISSN 0044-8001/81/0006-1041/$01.00.

ocean surface by loads such as ice or wind loads. For fixed structures sized to resist hydrodynamic loads, wind loads will usually be of a secondary nature. For compliant floating platforms, the wind loading may lead to critical conditions either by wind heeling or by overstressing of the mooring lines. Loadings due to floating sea ice are severe and will usually govern a design of a surface structure if they are anticipated. In shallow water, bottom pipelines may be subjected to the ice scour if thick ice or icebergs are present.

3. Installational and operational forces: Loads applied to the structure either during implantation of the system or during normal operation of on-board components. Installational loads need to be considered carefully in that the primary designs may have been based on a certain configuration of the structure or on loads which may not be present during implantation, e.g., buoyancy loads to counteract dead weight and point loads. One operational characteristic to be considered is the effect of marine fouling over the lifetime of immersed structural components. In addition to corrosive action, marine fouling also will increase the size and roughness of structural members with regard to hydrodynamic drag and inertia forces.

In the following sections, we will consider various aspects of deterministic hydrodynamic loads on structures. These dynamic loads, or their quasistatic simulators, are due to pressure fluctuations normal to immersed surfaces which are caused by the relative motion between the fluid medium and the structure. These loads are to be added to the hydrostatic and to the buoyancy loads. The buoyancy force on a structure is a surface-directed force equal to the product of the immersed volume and the *in-situ* water density.

The deterministic hydrodynamic loads to be considered are those due to waves and currents. Current effects are important mainly as a velocity vector addition to the wave velocity vector. Current velocities are the principal source of loads for pipelines. Wave forces are due to the pressures and velocities of water particles moving in elliptical orbits. Wave forces decay exponentially with depth from the free surface. Wave theories for the prediction of water particle velocities are considered subsequently.

In the design of sea-based structures, one must consider both normal and extreme loading conditions. Predictions of sea states are made either by extrapolating tabulated site data or by using historical weather data as input to calibrated computer simulators. Normal conditions are those sea states regularly expected over the structural lifetime. Both the expected storm and normal wave conditions will lead to a large number of cycles of structural response and will require a fatigue analysis. This condition may control the design for monolithic or jacketed structures in severe wave environment locations. For normal condition cases, linear frequency domain analyses are indicated because of the broad frequency spectrum of hydrodynamic inputs expected.

Extreme load conditions are those rare events which are expected during the lifetime of the structure due to intense sea states or storm surges. A nonlinear time-domain analysis is indicated for compliant structures both to simulate the drag forces in the extreme load case and to account for greater energy absorption in the nonlinear structural response. In the selection of the extreme sea states for design purposes, the designer should examine less severe sea states for which spikes in the wave energy spectra may coincide with the fundamental

or higher normal modal frequencies of the structure.

Probabilistic analysis of the wave climate is important in the study of both the normal and the extreme wave cases. In the extreme wave case, probability analyses are used to select the "design" wave (15,44). In a spectral analysis for the normal case, random wave systems are considered and a probabilistic analysis of the resulting load is carried out (28,47).

Hydrodynamic Action on Compliant Small Structures

A semi-intuitive equation was introduced by Morison, et al. (39) to compute wave forces on immersed objects having characteristic dimensions which are small compared to the wavelength of the incident wave. This equation has been extended to 3-dimensional analyses of arbitrarily oriented members of offshore structures.

The Morison equation in vector form is

$$F = F_D + F_I \quad \ldots \quad (1)$$

in which F = hydrodynamic force per unit axial length acting normal to the axis of the member; F_D = drag force; and F_I = inertia force. The drag force term per unit length is taken (as in the case of steady unidirectional flow) as

$$F_D = \frac{1}{2}\rho d C_D |U_n - U'_n|(U_n - U'_n) \quad \ldots \quad (2)$$

in which ρ = fluid mass density; d = projected width of member in the direction of the cross-flow component of velocity; C_D = dimensionless drag coefficient; U_n = component of fluid velocity vector normal to the member axis; and U'_n = component of member velocity vector normal to the member axis. Note the nonlinear dependence on velocity. Drag forces are predominantly due to flow separations of the velocity field as it passes the member.

The linear inertia force vector per unit length is due to the pressure gradient associated with the relative acceleration of the member and fluid and is given by

$$F_I = \rho A a_n + \rho A C_m (a_n - a'_n) \quad \ldots \quad (3)$$

in which A = cross-sectional area of the member; C_m = dimensionless added mass coefficient; a_n = component of the total fluid acceleration vector normal to the member axis; and a'_n = component of the member acceleration vector normal to the member axis. Although fluid acceleration a_n denotes the total acceleration, the convective part is usually small compared to the temporal acceleration and may usually be neglected. Often inertia coefficient $C_M = 1 + C_m$ is reported rather than added mass coefficient C_m.

In wave action, the velocity and acceleration vectors are generally not collinear and, therefore, the drag, F_D, and the inertia, F_I, forces act in different directions. The 3-dimensional form given above assumes that the drag and inertia forces are independent and that the "strip theory" principle applies: viz., the forces are based on normal components of velocity and acceleration. The generally accepted limit (36) of member size for applications of the Morison equation

is $d/L \leq 0.2$, in which L = the wave length of the incident wave.

In addition to the in-line drag and inertia forces, there is also a force component normal to the incident velocity vector called the lift force. It is due to the formation of eddies which are shed alternatively on each side of the member and may be expressed by

$$F_L = \frac{1}{2} \rho d C_L (U_n - U'_n)^2 \quad \ldots \ldots \ldots

wave-induced velocity before the sum is squared.

Assuming that both the wave amplitude and the current magnitude are small, the concept of superposition as described above is valid. The two components act independently and may be simply superimposed. However, this superposition is strictly valid only for small waves and currents so that only the magnitude of the interaction process is of interest. Dalrymple (6,7) has carried out a numerical investigation of the nonlinear interaction of shear currents and waves. His numerical results indicate that the nonlinear interaction effect is rather minor for typical practical applications. The error resulting from the superposition of the wave and current magnitudes tends to be somewhat greater at the wave trough than crest, but this is not of much practical importance because the drag component is greatest at the crest. As a general conclusion, it appears that the nonlinear interaction effect of the current and wave motion is of minor importance in most practical applications; and the simple vector addition of wave-induced and current-induced velocities represents a valid assumption. Peregrine (41) reviews other more complicated alternative methods for modeling wave-current interaction.

Impact Loads in Splash Zone

Impact or wave slamming loads can occur on members of a structure located near the free surface and may result in large local stresses. Such loads are normally not used to design the complete structure but rather to check the design of critical members or parts of the structure near the free surface which are subjected to wave slamming. Typically, damage occurs because of repeated wave slamming on a given member, and, therefore, these wave slamming loads may be used in a fatigue analysis wherein a long-term counting process is used.

Recent experience in the North Sea has emphasized the need to consider the impact loading and varying buoyancy forces acting on horizontal members in the splash zone. As a horizontal member with axis parallel to the wave crest passes in and out of the water surface, the buoyant force rapidly varies between zero and its fully submerged value. At the same time, an impact load occurs due to water entry of the member. Repeated loading of this type can result in fatigue damage and eventual failure of the member.

The most complete formula for the vertical force on a member was given by Kaplan and Silbert (30) as

$$F = \rho g A_i + \rho A_i \ddot{\eta} + \frac{\partial}{\partial t}\left[m_3(\dot{\eta} - w)\right] \quad \ldots\ldots\ldots\ldots\ldots\ldots\ldots\ldots (5)$$

in which ρ = mass density of water; A_i = time-dependent immersed cross-sectional area of the member; g = acceleration of gravity; $\ddot{\eta}$ = vertical acceleration of the water surface; $\dot{\eta}$ = vertical velocity of the water surface; m_3 = the vertical added mass coefficient which is appropriate to the immersed or semi-immersed cylinder at the free surface; and w = the vertical velocity of the member.

Based on experimental results obtained in a wave tank, Dalton and Nash (8) proposed an equation for the wave slamming force, i.e.:

$$\bar{F} = \frac{1}{2}\rho A C_s \bar{U}^2 \quad \ldots\ldots\ldots\ldots\ldots\ldots\ldots\ldots\ldots\ldots\ldots\ldots (6)$$

in which A = projected area normal to plane of wave impact; $\bar{U}$ = local wave particle velocity; and C_S = dimensionless slam coefficient. Experimental values for C_S show considerable scatter with values ranging between 1 and 5.

Because of the impulsive nature of the loading and of the elastic properties of the member, the resulting stresses in the member must be computed through application of a dynamic/elastic analysis which takes into consideration the mass distribution and the end connections of the member. The integration of the equations describing this sytem results in a stress history versus time during a given impact.

Diffraction Theory for Larger Structures

The Morison equation represents a simple procedure for computing wave loads on cylindrical members of offshore platforms whose diameters are less than about $0.2L$ in which L = the wavelength. For caissons or other large displacement components of a structure, it is necessary to apply a more fundamental approach to the evaluation of the wave loading. A procedure which may be applied to bodies of arbitrary shape and which may be used to compute all components of forces and moments is often referred to as "*diffraction theory*" (22).

In the linear diffraction theory, the fluid is assumed to be incompressible and inviscid; and a linear wave is assumed to interact with the immersed surface of the structure. This interaction gives rise to a scattered wave so that the total wave potential may be represented by a linear sum of the *incident* and the *scattered* wave potentials.

The hydrodynamic wave-induced pressure acting on the immersed surface of the structure is computed by a linearized form of the Bernoulli equation. The net forces and moments are computed by integration of the pressure over the total immersed surface. Two components of the pressure (and resulting force) are sometimes identified. The first contribution to the net force results from the pressure component associated with the incident wave alone and is called the Froude-Krylov force. A second component is due to the diffraction of the incident wave which is caused by the presence of the structure. For a consideration of the application of the diffraction theory based on the distributed source method to fixed bodies (see Refs. 17, 18, 22, 27).

Yue, et al. (53) have developed a procedure based on a hybrid finite element procedure which also appears to be a promising method for practical application (see also Ref. 37).

Although the numerical diffraction theory as applied to offshore structures has been in common usage for only a few years, the recent interest in North sea gravity platforms has given considerable impetus to its development and acceptance for practical design. There are currently several examples which show excellent agreement between predictions and large-scale wave channel tests of both simple geometric shapes (27) and models of actual designs of offshore gravity structures (18,22). In the case of the calculations presented by Garrison (22), the structure was composed of a large displacement caisson with a superstructure composed of smaller diameter members. This procedure described for the first time a method in which the loads on the caisson are

computed by use of a diffraction analysis and the loads on the superstructure by use of the Morison equation.

Limitations of Linear Diffraction Theory.—While the linear diffraction theory has proved to be useful well beyond its original expectations, there are, of course, limitations which must be taken into consideration in applications. Firstly, the analysis is based on linear wave theory. Consequently, as the wave height increases, a point will eventually be reached where the theory will no longer give satisfactory results. Arctic gravity platforms and ship loader caissons (2) represent examples where nonlinear effects tend to become pronounced. In these examples, caissons are placed in rather shallow water and are acted upon by fairly large-amplitude design waves. Secondly, in shallow water, the nonlinearities in the incident wave itself tend to be pronounced, and these nonlinearities are reflected in the wave loads on the caisson. In cases where the incident wave is nonlinear, the linear diffraction analysis underpredicts the force and, therefore, is nonconservative. Thus, it is necessary to establish the limits of a linear diffraction theory.

Available data which can be used to indicate the limits of linear diffraction analysis are not extensive. However, available data (2,19,24,27) indicate that, in general, when the water depth to wave length ratio becomes less than about 0.04, nonlinear effects in the wave loads begin to become apparent. Because the nonlinear effects in waves tend to die out with increasing depth, the nonlinear effects tend to be less pronounced on deeply submerged caissons than on surface-piercing caissons. In the case of surface-piercing caissons where the nonlinear effects tend to be most pronounced, the loads can become substantially greater than predicted by the linear theory as noted by Apelt and McKnight (2) in the case of the ship loader caisson.

Presently, only linear diffraction analysis is commonly used in practice. A few attempts to develop nonlinear analyses have been made (4,20,29), but the value of such nonlinear analyses is uncertain at present. For this reason, when nonlinear effects become significant, the present state-of-the-art dictates that a properly designed model test should be conducted to evaluate the wave loads. In most model tests of large displacement caissons where drag or other viscous effects are expected to be minor, geometric and Froude scaling is appropriate.

Wave Theories

The deterministic method of wave force calculation is commonly used as a primary basis for design, particularly when nonlinear effects associated with the drag force in the Morison equation are important. Such a procedure generally involves the "*design wave*" concept wherein a periodic wave of prescribed wave height, H, and wave period, T, propagating in water of constant depth, h, is applied to the structure. The design wave will be of finite amplitude. Therefore, it is appropriate to apply some nonlinear wave theory in order to compute the wave kinematics required for subsequent use in computing the hydrodynamic force on the members of the structure.

There are a number of wave theories which could be used in design. Consequently, those theories which give the most realistic representation of the fluid kinematics for a given set of wave conditions within the limits of validity for that wave theory are of practical interest to the designer.

Wave theories may be divided into two general categories: (1) Analytical theories; and (2) numerical theories. The analytical theories result in closed-form expressions for the various physical wave parameters of interest. The numerical theories rely on some type of numerical iteration procedure in order to compute numerical values for certain coefficients required in the theory. The numerical theories usually require the use of a properly designed computer program and possibly some judgment on the part of the user to obtain valid results. However, in the case of the numerical Stream Function Wave Theory, Dean (11) has developed tables to facilitate applications.

In general, a periodic gravity wave may be specified by the design parameters of wave period, T, mean water depth, h, and wave height, H. The wave height, H, is defined as the vertical elevation difference between the wave trough and crest. For purposes of specifying the characteristics of waves, these three independent physical quantities may be arranged into two dimensionless groups: $h/(gT^2)$ and $H/(gT^2)$, in which g = the acceleration of gravity. However, it is common to disregard the gravitational constant, g, and to use the dimensional forms, h/T^2 and H/T^2, which have units of either feet per second per second or meters per second per second.

The Stokes' wave theories (48) provide valid solutions in deep water, i.e., $h/L > 0.5$. For values of h/T^2 less than about 0.5 ft/sec^2 (0.15 m/s^2), the upper limit for H/T^2 at which a valid solution may be realized decreases as h/T^2 decreases. Unfortunately, the limiting value of H/T^2 for a given value of $h/T^2 < 0.5$ ft/sec^2 (0.15 m/s^2) is not known with any degree of accuracy. However, judging from the free surface boundary condition errors plotted by Dean (10), it appears that for Stokes' fifth-order wave theory at $h/T^2 = 0.5$ ft/sec^2 (0.15 m/s^2), the limit on H/T^2 might be as low as 0.04 ft/sec^2 (0.012 m/s^2). In contrast, for $h/T^2 = 1.0$ ft/sec^2 (0.3 m/s^2), the value of H/T^2 may extend up to the breaking condition of about $H/T^2 = 0.8$ ft/sec^2 (0.24 m/s^2).

The newer cnoidal wave theories of Laitone (33) and Chappelear (5) are mathematically rigorous, being based on the perturbation expansion developed by Friedrichs (16). However, these solutions suffer the same difficulty as Stokes' wave theory. As the wave height (or H/T^2) becomes large, the series diverge. While valid results may be obtained at small values of H/T^2 (in the case of cnoidal wave theory H/h is more appropriate), the limiting value has not been established, and, therefore, the use of such theories tends to be hazardous. In the experimental data presented by LéMehauté, et al. (35), and by Tsuchiya and Yamaguchi (50), the cnoidal theories, in general, tended to overpredict the velocities under the wave crest as the wave height increased.

The solitary wave theory of McCowan (40) has shown no tendencies to diverge and predicts velocities under the wave crest of shallow water waves rather well. However, when applied to periodic waves, the crest elevation is shifted upward. On the basis of the comparisons of LéMehauté, et al. (35), it appears that McCowan's solitary wave theory tends to overpredict the velocities under the crests for h/T^2 greater than 0.06 ft/sec^2 (0.018 m/s^2) and, therefore, should be limited to applications in which h/T^2 is less than 0.06 ft/sec^2 (0.018 m/s^2).

The Dean Stream Function Wave Theory (9) has demonstrated as good or better agreement with experimental wave channel tests results when compared with other wave theories over a wide range of h/T^2; i.e., 0.043 ft/sec^2–0.436

ft/sec^2 (0.013 m/s^2–0.13 m/s^2). It, therefore, appears to represent the most appropriate wave theory for engineering applications. The other numerical wave theories of Chappelear (5) and Lambrakos and Brannon (34) are presumed to give results equivalent to the Stream Function Wave Theory, but results of extensive calculations have not been presented in the literature.

Hydrodynamic Coefficients

The correct values of the drag and inertia coefficients to use in the Morison equation for the design of offshore structures has been a topic of considerable interest and discussion for nearly three decades. Many experiments have been conducted during this period but with limited success. Test results have frequently shown rather extreme scatter leaving the designer in the unfortunate position of possibly grossly overdesigning the structure or using coefficients which are less than the general range of reported values. Thus, at the present time, the state of knowledge remains incomplete. There are, however, certain trends and conclusions which may be drawn from the results of tests conducted to date and which should be considered in arriving at appropriate design values.

Effects of Reynolds Number and Surface Roughness.—It is generally understood that the drag and inertia coefficients in wave-induced motion are dependent on both the Reynolds number and surface roughness, *inter alios*. The influence of these two parameters on drag in steady flow has been fairly well-studied (1,38,43,49). In general, the drag coefficient for *smooth* cylinders in steady flow tends to remain a constant equal to 1.2 in the Reynolds number interval from 2×10^4 to 1×10^5. The value then decreases to a minimum value of 0.2–0.3 near a Reynolds number of 6×10^5. Beyond this minimum point, the drag coefficient increases again to a new constant value of about 0.6 in the supercritical range above a Reynolds number of about 3×10^6. This variation of the drag coefficient with Reynolds number corresponding to steady flow past a *smooth* circular cylinder is not given here because it has been widely reproduced in the references previously cited.

The notion of a "*smooth cylinder*" in wave force calculations for offshore structures is essentially only academic because all members have some roughness even in the initially installed state. With the passage of time, marine growth (38) adds to this natural roughness, and in parts of the structure near the surface, the marine growth can become fairly thick. In design it is appropriate to estimate the thickness of the marine growth and to add this thickness to the radius of the member. In addition, a reasonable value for the relative roughness, e.g., $k/d = 0.2$, should be considered in selecting the hydrodynamic coefficients.

The effect of roughness on the drag coefficient in steady flow as determined from systematic tests is generally twofold: (1) The minimum value and the subsequent rise to a new constant value of the drag curve (which is referred to as supercritical flow) occurs at *lower* values of the Reynolds number; and (2) the value of the drag coefficient is generally *higher* than that corresponding to smooth cylinder conditions. Since the supercritical flow regime is reached at much smaller values of the Reynolds number in the case of rough cylinders, the dependence on Reynolds number is not very important due to the fact that most cases of practical interest lie in the supercritical flow regime. Thus, it is generally only necessary to consider the supercritical values of the drag

coefficient in practical applications in offshore design.

Effects of Displacement Ratio on Drag Coefficient.—The preceding review of the twofold effects of roughness considered only steady flow past roughened cylinders. *Oscillatory* motion as induced by waves tends to cause the wake of the previous half-cycle of the motion to become the oncoming flow for the next half-cycle of motion. This kind of wake interaction has not been systematically studied in wave-induced motions, but it is apparent from systematic tests in simple rectilinear oscillatory flow (21,42,46,52) that the effect of the wake is primarily characterized by ratio $2a/d$. This dimensionless parameter is equal to the Keulegan-Carpenter number divided by π and is referred to herein as the "*displacement ratio*" in which a = amplitude of the motion and d = the cylinder diameter.

The effect of the wake in oscillatory flow appears to manifest itself in two identifiable ways (23).

1. When $2a/d$ is large (greater than about five for the case of smooth cylinders and possibly 10 for the case of fairly rough cylinders), the primary effect appears to be that the excess turbulence created by the previous half-cycle (or cycles) results in transition to supercritical flow at reduced values of the Reynolds number as compared to steady flow. However, the value of the supercritical drag coefficient is not affected by the increased "free stream turbulence" and remains essentially the same as in steady flow.
2. When $2a/d$ is small ($2a/d < 5$ to 10, depending on the roughness) the variation of C_D with the Reynolds number is fairly large in the subcritical and transcritical regimes. Then, at supercritical Reynolds numbers, the drag coefficient becomes constant at values greater than those corresponding to steady flow at equal relative roughness. This increased drag coefficient at supercritical Reynolds numbers is apparently caused by the increased relative velocity of the water over the cylinder which results from the velocity defect in the wake produced in the previous half-cycle.

The only complete, systematic study of the effect of the wake on the hydrodynamic forces on both smooth and rough cylinders has been conducted by Sarpkaya (46), although similar tests by others using smooth cylinders have also been performed. His results suggest that the wake has very little effect in the case of smooth, supercritical conditions but has an increasing effect as the roughness is increased. The increase in the effect of the wake with increasing roughness is to be expected, however, because the magnitude of the velocity defect in the wake must increase with the drag. This may be verified from momentum considerations (23). Thus, the interaction effect between the roughness and displacement ratio indicated by the data is to be expected (viz., increasing wake effect with increasing roughness).

The surprising aspect of the oscillatory flow data obtained is not its general trends but the actual magnitudes. The oscillatory flow data of Sarpkaya (46) indicates very large values of the drag coefficient in general. What is even more disturbing is that his values for C_D do not appear to approach the steady flow curve as $2a/d$ becomes very large. These aspects of the Sarpkaya data, which appear contrary to the expectations and conclusions by others (meager though other data may be), lead to the conclusion that the Sarpkaya results

may not be directly applicable to wave force calculations. A possible explanation for the large drag coefficients obtained from these tests conducted in an oscillatory water tunnel, as compared to that expected in free surface fluids, is that the rigid water tunnel walls hindered the momentum transport mechanism which occurs in wake flows by restricting the influx of water. This allowed the wake to persist much longer than it otherwise would and, therefore, interact more intensely with the cylinder on flow reversals. This, of course, would result in an exaggerated increase in the drag force resulting from the interaction of the cylinder with its wake.

There are little data available to discount the high values of C_D obtained by Sarpkaya for the case of rough cylinders. However, the available data suggest that the drag in oscillatory flow does converge fairly rapidly to steady flow values as $2a/d$ increases. The limited oscillatory flow test results reported by others (21,42,45,52) are lower than the results reported by Sarpkaya, and they suggest rather rapid convergence to the steady flow curve as $2a/d$ increases. In addition, the data corresponding to smooth cylinder conditions are all slightly lower than the Sarpkaya data for high Reynolds numbers. It is suspected that the higher blockage ratio (tunnel width/cylinder diameter) in these other tests compared to the Sarpkaya tests means that the wake blockage effect was not nearly so critical to their results (23).

Dependence of Inertia Coefficient on Displacement Ratio, Reynolds Number, and Surface Roughness.—Except for the systematic rectilinear harmonic flow studies of Garrison, et al. (21), Yamamoto and Nath (52), and Sarpkaya (46), there are very little good quality data for the inertia coefficient ($C_M = 1 + C_m$) to use in the design of offshore structures. The state-of-the-art data (for both C_M and C_D) for use in space-frame structures are that obtained primarily from various offshore test piles, and in particular, the results from Wave Force Projects I and II (12,13,51) as well as results from more recent tests (25,26,31). These data tend to be somewhat drag dominated. For this reason, the inertia coefficient is determined in such cases with less precision than the drag coefficient. All of these data show significant scatter in both coefficients, but primarily in the inertia coefficient. However, space-frame structures tend to result in drag-dominated load so that the value of the inertia coefficient is much less important than is the value of the drag coefficient to the accuracy of the calculation.

From analysis of the Wave-Force Projects I and II, Dean and Aagaard (12) recommended a value of 1.33 for the "*in-line*" inertia coefficient except for large diameter members. Wheeler (51) analyzed these same data and recommended a design inertia coefficient of 1.5. Evans (13) found a value of 1.2 for these same data but felt that a value of 1.5 would be more appropriate for design. Evans recommended a value of 1.7 for the higher waves. In the test results reported by Kim and Hibbard (31), the inertia coefficient was found to be 1.2. All of the aforementioned results were obtained from sleeve-type force transducers with a smooth surface when initially installed.

The range of these reported value extends from 1.2–1.7, and, therefore, a design value of 1.5 appears to be a reasonable choice for noninertia-dominated wave forces. When $2a/d$ becomes small (small water particle orbital paths and large diameter members), it is well known that the inertia coefficient C_M approaches the inviscid flow value of 2.0 for circular cylinders.

The selection of a single design value for C_M disregards any effects of roughness,

Reynolds number, or displacement ratio. While it is generally impossible to account for such effects in any precise manner, a general notion of the effects of the important parameters is desirable as a guide for selecting design values of the inertia coefficient.

Here, as in the case of the drag coefficient, systematic tests have not been conducted in wave-induced motion. It is, therefore, appropriate to consider the results of systematic tests conducted in rectilinear oscillatory motion in order to gain insight into the effects of roughness and the wake. In the case of rough cylinders, constant values of C_M are reached at fairly small values of the Reynolds number so the supercritical values of C_M are generally appropriate for design. In the inertia coefficient data of Sarpkaya (46), just as in his drag coefficient data, the effect of the wake, as characterized by the parameter $2a/d$ is enhanced as the relative roughness (and, thus, the velocity defect in the wake of a previous half cycle) is increased. In general, the Sarpkaya data appear to indicate higher values of C_M than the data of other similar tests (21,52). As previously mentioned, a possible reason for these elevated values is the wake-blockage mechanism. While the direct application of these values for the inertia coefficient to wave-induced motion may be questionable, the trends are useful for judging the effects on the inertia coefficient of roughness and the wake in supercritical flow.

Vortex-Excited Cyclic Loading

When water flows past a small member of an offshore structure, discrete vortices resulting from the vorticity generated in the boundary layer tend to roll up and are alternately shed from each side of the member. The vortices shed from the two sides rotate in opposite directions and move downstream from the member forming a wake which is called a Karman vortex street. Because of the unsteadiness of this type of flow and as a result of the discrete vortex shedding (even though the oncoming flow may be steady), oscillatory forces are induced on the member. If, in addition, it occurs that the natural frequency of the member in water is near to the frequency of the exciting force and the damping is not too large, then rather severe oscillations of the member may ensue. In cases where the current speeds or typical wave-induced velocities are such as to produce sustained resonance of a given member, fatiguing of the member will tend to result.

In complex space-frame type structures, it is unlikely that such vortex excited oscillations could affect the response of the complete structure. Variations in member sizes and orientations and in the water velocities give rise to different vortex shedding frequencies. Consequently, the forcing function for all members, even all major members, would most likely never act in concert.

Vortex Shedding from Stationary Cylinder.—The frequency of vortex shedding, f_v, and the excitation force produced is characterized by the dimensionless Strouhal number defined as $\mathrm{S} = f_v\, d/V$ in which V and d = the flow velocity and cylinder diameter, respectively.

The Strouhal number, as well as the drag coefficient of the member, depends on the Reynolds number, $\mathrm{R} = Vd/\nu$, in which ν = the kinematic fluid viscosity, and on the relative roughness of the surface of the member, k/d, in which k = the surface roughness heights.

Roshko (45) and others have measured the vortex shedding from smooth cylinders. In the Reynolds number interval $1 \times 10^3 < R < 2 \times 10^5$, the shedding is regular and distinct. In this interval, the value of S is nearly constant and equal to about 0.2. In the transition Reynolds number region, the Strouhal number seems to increase as C_D decreases and to then decrease again to an asymptotic value at high Reynolds number as C_D increases to its asymptotic value. In the transition region ($5 \times 10^5 < R < 3 \times 10^6$), the vortices tend to be somewhat weaker than in the subcritical range, and it is difficult to define a definite shedding frequency.

Vortex Shedding and Response of Flexible Members.—In dealing with flexible members, as opposed to stationary ones, two parameters in addition to the Strouhal number which characterizes the dynamics of the member must be used in describing the vortex shedding phenomenon: (1) The "*reduced velocity*," defined as $V/f_n\, d$ (f_n = the natural frequency of the member) characterizes the tuning of the member; and (2) the "*stability parameter*," defined as $K_s = 2m_e\delta/\rho d^2$ (m_e = the equivalent mass/unit length; δ = the logarithmic decrement; and ρ = the mass density of the fluid). This stability parameter results from an energy balance at resonance. It is believed that the reduced amplitude of oscillatory response (Y_0/d, in which Y_0 = the response amplitude) may be defined for members of marine structures in terms of both the reduced velocity and the stability parameter (32).

If the cylinder or member of an offshore structure is flexible, interactions may occur between the vortex shedding mechanism and the dynamic response of the member. As the flow velocity is increased from zero, e.g., the frequency of vortex shedding, which is given by $f_v = V(S/d)$, also increases. If conditions are right as the vortex shedding frequency approaches the natural frequency of the member ($f_n = f_v$), the member will begin to oscillate at its natural frequency. The vortex shedding tends to "*lock-in*" to the member natural frequency at this point and remains constant at that frequency over a range of velocity which is referred to as the "*synchronization range.*" The length of the synchronization range is dependent on the damping. For highly damped systems, *lock-in* will not occur at all; but for very lightly damped systems, this *lock-in* range can be very extensive. As the flow velocity is increased still further, the frequency remains constant until a point is reached at which the large amplitude motion ceases and the vortex shedding reverts to the frequency associated with the stationary cylinder. In the synchronization region, the oscillations are classed as *self-excited.*

Vortex Shedding in Wave-Induced Motion.—The aforementioned analysis is related to *steady* flow past cylinders such as is due to currents. When the motion of the fluid is oscillatory, as induced by waves, the mechanism of the vortex formation and shedding is more complicated and the understanding of such flow is much less complete.

Bidde (3) has made a laboratory study of the lateral (or lift) force acting on a stationary, vertical test pile. The results of the rather small scale laboratory experiment indicated that the maximum lateral force can be as large as 60% of the longitudinal force and appears to be greatest at a Keulegan-Carpenter number of about 15 (or an amplitude ratio of about five). However, studies carried out in simple rectilinear oscillatory flow (42,46,52) indicate that the magnitude of the transverse force is dependent on the Reynolds number. At

values of R less than 2×10^5, the lift coefficient C_L in Eq. 4 appears to approach a constant value independent of the Reynolds number in a manner very much similar to that observed in steady flow.

The primary difference between *oscillatory* (wave-induced) motion past a cylinder and *steady* flow is the effect of the wake from the previous half cycle of the motion interacting with the cylinder (23). This, of course, tends to be most pronounced when the displacement amplitude ratio is small; when the displacement ratio becomes large, the vortices shed from the previous half cycle have time to dissipate before flow reversal. Both Bidde (3) and Sarpkaya (46) indicate that no vortices are shed when the displacement ratio, $2a/d$ (in which a = the amplitude of the water motion), is less than about unity. Sarpkaya (46) also reports that the shedding frequency is dependent on the Keulegan-Carpenter number (or $2\pi a/d$) and on the Reynolds number; but, for rough cylinders, the Strouhal number remains constant at about 0.22, which is the same as for steady flow.

Conclusions

Deterministic hydrodynamic forces on small cylindrical members should be computed by the Morison equation (Eq. 1) when the member diameter to wavelength ratio is less than approximately 0.2. Current-induced velocities should be added vectorially to the wave-induced velocities before squaring the sum to compute the drag force component. Impact loads should be computed for members subjected to wave-slamming conditions near the free surface.

For caissons or other large displacement members, deterministic hydrodynamic wave forces should be computed by a diffraction theory which accounts for the scattering of the incident wave by the structure. Either an analytical or a numerical wave theory should be selected based on realistic limits of the validity of the theory for the specified design wave conditions. Hydrodynamic force coefficients should be selected based on their dependence upon Reynolds number = Vd/ν, relative roughness = k/d, and Keulegan-Carpenter number = VT/d or relative amplitude parameter = $2a/d$.

Appendix I.—References

1. Achenbach, E., "Influence on Surface Roughness on the Cross-Flow Around a Circular Cylinder," *Journal of Fluid Mechanics*, Vol. 46, Part 2, 1971, pp. 321–335.
2. Apelt, C. J., and McKnight, A., "Wave Action on Large Off-Shore Structures," *Proceedings*, 15th Coastal Engineering Conference, 1976.
3. Bidde, D. D., "Laboratory Studies of Lift Forces on Circular Piles," *Journal of the Waterways, Harbors and Coastal Engineering Division*, ASCE, Vol. 97, No. WW4, Proc. Paper 8495, Nov., 1971, pp. 595–614.
4. Chakrabarti, S. K., "Second-Order Wave Force on Large Vertical Cylinder," *Journal of the Waterways, Harbors and Coastal Engineering Division*, ASCE, Vol. 101, No. WW3, Proc. Paper 11476, Aug., 1975, pp. 311–317.
5. Chappelear, J. E., "Direct Numerical Calculation of Wave Properties," *Journal of Geophysical Research*, Vol. 66, No. 2, Feb., 1961, pp. 501–508.
6. Dalrymple, R. A., "Water Wave Models and Wave Forces with Shear Currents," *Technical Report 20*, Univ. of Florida, Gainesville, Coastal Engineering Laboratory, 1973.
7. Dalrymple, R. A., "Models for Nonlinear Water Waves on Shear Currents," *Proceedings*, Offshore Technology Conference, Paper No. OTC 2114, Vol. II, 1974, pp. 843–856.

8. Dalton, C., and Nash, J. M., "Wave Slam on Horizontal Members of an Offshore Platform," *Proceedings*, Offshore Technology Conference, Paper No. 2500, Vol. 1, 1976, pp. 769–780.
9. Dean, R. G., "Stream Function Representation of Nonlinear Ocean Waves," *Journal of Geophysical Research*, Vol. 70, No. 18, Sept., 1965, pp. 4561–4572.
10. Dean, R. G., "Relative Validity of Water Wave Theories," *Journal of the Waterways, Harbors and Coastal Engineering Division*, ASCE, Vol. 96, No. WW1, Proc. Paper 7092, Feb., 1970, pp. 105–119.
11. Dean, R. G., *Evaluation and Development of Water Wave Theories for Engineering Application, Vols. I and II*, Special Report No. 1, United States Army Corps of Engineers, Coastal Engineering Research Center, Ft. Belvoir, Va., 1974.
12. Dean, R. G., and Aagaard, P. M., "Wave Forces: Data Analysis and Engineering Calculation Method," *Journal of Petroleum Technology*, Vol. 22, March, 1970, pp. 368–375.
13. Evans, D J., "Analysis of Wave Force Data," *Journal of Petroleum Technology*, Vol. 22, March, 1970, pp. 347–358.
14. Forristall, G. Z., "Three-Dimensional Structure of Storm-Generated Currents," *Journal of Geophysical Research*, Vol. 79, No. 18, June 20, 1974, pp. 2721–2729.
15. Forristall, G. Z., Ward, E. G., Borgman, L. E., and Cardone, V. J., "Storm Wave Kinematics," *Proceedings of the Offshore Technology Conference*, Vol. III, 1978, pp. 1503–1514.
16. Friedrichs, K. O., "On the Derivation of the Shallow Water Theory," *Communications on Pure and Applied Mathematics*, Vol. I, 1948, pp. 81–85.
17. Garrison, C. J., Seetharama, Rao V., and Snider, R. H., "Wave Interaction with Large Submerged Objects," *Proceedings gf the Offshore Technology Conference*, Paper No. OTC 1278, 1970, pp. 521–532.
18. Garrison, C. J., and Chow, P. Y., "Wave Forces on Submerged Bodies," *Journal of the Waterways, Harbors and Coastal Engineering Division*, ASCE, Vol. 98, No. WW3, Proc. Paper 9098, Aug., 1972, pp. 375–392.
19. Garrison, C. J., Gehrman, F. H., and Perkinson, B. T., "Wave Forces on Bottom-Mounted Large-Diameter Cylinder," *Journal of the Waterways, Harbors and Coastal Engineering Division*, ASCE, Vol. 101, No. WW4, Proc. Paper 11699, Nov., 1975, pp. 343–356.
20. Garrison, C. J., "Consistent Second-Order Diffraction Theory," presented at the 1976, 15th Coastal Engineering Conference, held at Honolulu, Hawaii.
21. Garrison, C. J., Fields, J. B., and May, M. D., "Drag and Inertia Forces on a Cylinder in Periodic Flow," *Journal of the Waterway, Port, Coastal and Ocean Division*, ASCE, Vol. 103, No. WW2, Proc. Paper 12913, May, 1977, pp. 193–204.
22. Garrison, C. J., "Hydrodynamic Loading of Large Offshore Structures," *Numerical Methods in Offshore Engineering*, O. C. Zienkiewicz, R. W. Lewis, and K. G. Stagg, eds., John Wiley and Sons, Inc., New York, N.Y., 1978, pp. 87–140.
23. Garrison, C. J., "A Review of Drag and Inertia Forces on Circular Cylinders," *Proceedings of the Offshore Technology Conference*, Paper No. OTC 3760, Vol. III, 1980, pp. 205–218.
24. Hafskjold, P. S., Torum, A., and Eie, J., "Submerged Offshore Concrete Tanks," International Navigation Congress, Ottawa, Canada, 1973.
25. Haring, R. E., Olsen, O. A., and Johansson, P. I., "Total Wave Force and Moment Versus Design Practice," *Proceedings*, Civil Engineering in the Oceans IV, ASCE, Vol. II, Sept. 10–12, 1979, pp. 805–819.
26. Heideman, J. C., Olsen, O. A., and Johansson, P. I., "Local Wave Force Coefficients," *Proceedings*, Civil Engineering in the Ocean IV, ASCE, Vol. II, Sept. 10–12, 1979, pp. 684–699.
27. Hogben, N., and Standing, R. G., "Experience in Computing Wave Loads on Large Bodies," *Proceedings*, Offshore Technology Conference, Paper No. OTC 2189, Vol. I, 1975, pp. 413–437.
28. Houmb, O. G., "Wave Statistics for Design," *Port Engineering*, Per Bruun, ed., Gulf Publishing Co., Houston, Tex., 1976, pp. 131–141.
29. Isaacson, M., "Shallow Wave Diffraction Around Large Cylinders," *Journal of the Waterways, Port, Coastal and Ocean Division*, ASCE, Vol. 103, No. WW1, Proc. Paper 12756, Feb., 1977, pp. 69–82.

30. Kaplan, P., and Silbert, M. N., "Impact Forces on Platform Horizontal Members in the Splash Zone," *Proceedings*, Offshore Technology Conference, Paper No. 2498, Vol. 1, 1976, pp. 751–768.
31. Kim, Y. Y., and Hibbard, H. C., "Analysis of Simultaneous Wave Force and Water Particle Velocity Measurements," *Proceedings*, Offshore Technology Conference, Paper No. OTC 2192, 1975, pp. 461–470.
32. King, R., "A Review of Vortex Shedding Research and Its Applications," *Ocean Engineering*, Vol. 4, 1977, pp. 141–172.
33. Laitone, E. V., "The Second Approximation to Cnoidal and Solitary Waves," *Journal of Fluid Mechanics*, Vol. 9, Part 3, Nov., 1960, pp. 430–444.
34. Lambrakos, K. F., and Brannon, H. R., "Wave Force Calculations for Stokes and Non-Stokes Waves," *Proceedings*, Offshore Technology Conference, Paper No. OTC 2039, Vol. II, 1974, pp. 47–60.
35. LéMehauté, B., Divoky, D., and Lin, A., "Shallow Water Waves: A Comparison of Theories and Experiments," *Proceedings*, Coastal Engineering Conference, Chapter 7, 1968, pp. 86–107.
36. MacCamy, R. C., and Fuchs, R. A., "Wave Forces on Piles: A Diffraction Theory," *Technical Memorandum 69*, United States Army Corps of Engineers Beach Erosion Board, Washington, D.C., 1954.
37. Mei, C. C., "Numerical Methods in Water-Wave Diffraction and Radiation," *Annual Reviews Fluid Mechanics*, Vol. 10, 1978, pp. 393–416.
38. Miller, B. L., "The Hydrodynamic Drag of Roughened Circular Cylinders," *Journal of the Royal Institute of Naval Architects*, Vol. 119, Mar., 1977.
39. Morison, J. R., O'Brien, M. P., Johnson, J. W., and Schaaf, S. A., "The Force Exerted by Surface Waves on Piles," *Petroleum Transactions*, Vol. 189, TP 2846, 1950, pp. 149–154.
40. Munk, W. H., "The Solitary Wave Theory and Its Application to Surf Problems," *Ocean Surface Waves, Annals of the New York Academy of Sciences*, Vol. 51, Article 3, 1949, pp. 326–424.
41. Peregrine, D. H., "Interaction of Water Waves and Currents," *Advances in Applied Mechanics*, Vol. 16, 1976, pp. 9–117.
42. Rance, P. J., "Wave Forces on Cylindrical Members of Structures," *Hydraulic Research*, Hydraulic Research Station, Wallingford, England, 1969, pp. 14–17.
43. Reid, R. O., "Modification of the Quadratic Bottom—Stress Law for Turbulent Channel Flow in the Presence of Surface Wind Stress," *United States Army Beach Erosion Board*, T.M. 93, Feb., 1957.
44. Robinson, R. J., Brannon, H. R., and Kattawar, G. W., "Storm Wave Characteristics," *Society of Petroleum Engineers Journal*, 1967, pp. 87–98.
45. Roshko, A., "Experiments on the Flow Past a Circular Cylinder at Very High Reynolds Number," *Journal of Fluid Mechanics*, Vol. 10, 1961, pp. 345–356.
46. Sarpkaya, T., "Vortex Shedding and Resistance in Harmonic Flow about Smooth and Rough Circular Cylinders at High Reynolds Number," *Technical Report NPS-59SL76021*, Naval Postgraduate School, Monterey, Calif., Feb., 1976.
47. St. Denis, M., and Pierson, W. J., "On the Motions of Ships in Confused Seas," *Transactions*, Society of Naval Architects and Marine Engineers, Vol. 61, 1953, pp. 280–357.
48. Skjelbreia, L., and Hendrickson, J. A., "Fifth Order Gravity Wave Theory," *Proceedings of the Coastal Engineering Conference*, Vol. I, Chapt. 10, 1961.
49. Szechenyi, E., "Supercritical Reynolds Number Simulation of Two-Dimensional Flow Over Circular Cylinders," *Journal of Fluid Mechanics*, Vol. 70, Part 3, 1975, pp. 529–542.
50. Tsuchiya, Y., and Yamaguchi, M., "Some Considerations on Water Particle Velocities of Finite Amplitude Wave Theories," *Coastal Engineering in Japan*, Vol. 15, 1972.
51. Wheeler, J. D., "Method of Calculating Forces Produced by Irregular Waves," *Journal of Petroleum Technology*, Mar., 1970, pp. 359–367.
52. Yamamoto, T., and Nath, J. H., "High Reynolds Number Oscillatory Flow by Cylinders," *Proceedings of the 15th Coastal Engineering Conference*, July, 1976, Chap. 36, pp. 2321–2340.
53. Yue, D. K. P., Chen, H. S., and Mei, C. C., "A Hybrid Element Method for Calculating Three-Dimensional Water Wave Scattering," *Report No. 215*, Ralph M. Parsons

Laboratory for Water Resources and Hydrodynamics, Massachussetts Institute of Technology, 1977.

Appendix II.—Notation

The following symbols are used in this paper:

A = cross-sectional area of member;
A_i = time dependent immersed cross-sectional area of member;
a = amplitude of motion;
a_n = component of total fluid acceleration vector normal to member axis;
a'_n = component of member acceleration vector normal to member axis;
C_D = dimensionless drag coefficient;
C_L = dimensionless lift coefficient;
C_M = dimensionless inertia coefficient;
C_m = dimensionless added mass coefficient;
C_S = dimensionless wave-slam coefficient;
d = projected width of member normal to flow;
F = normal hydrodynamic force per unit axial length;
F_D = drag component of force;
F_I = inertia component of force;
F_L = lift force;
f_n = natural frequency of member;
f_v = vortex shedding frequency;
g = gravitational constant;
H = wave height;
h = mean water depth;
K_s = dimensionless stability parameter;
k = surface roughness heights;
L = wavelength;
m_e = equivalent mass/unit length;
m_3 = vertical added mass wave-slamming coefficient;
$\mathrm{R}(= Vd/\nu)$ = dimensionless Reynolds number;
$\mathrm{S}(= f_v d/V)$ = dimensionless Strouhal number;
T = wave period;
$\bar{U}$ = local wave particle velocity;
U_n = component of fluid velocity vector normal to member axis;
U'_n = component of member velocity vector normal to member axis;
V = flow velocity;
w = vertical velocity component of member;
Y_0 = reduced amplitude of oscillatory response;
δ = logarithmic decrement;
$\dot{\eta}$ = vertical velocity of water surface;
$\ddot{\eta}$ = vertical acceleration of water surface;
ν = kinematic fluid viscosity; and
ρ = mass fluid density.

BOTTOM-SUPPORTED CONCRETE PLATFORMS: OVERVIEW[a]

By William J. Graff,[1] and Wai F. Chen,[2] Members, ASCE

INTRODUCTION

The 1969 discovery of the Ekofisk oil field in the North Sea marks the beginning of the development of concrete offshore oil platforms. The first such gravity platform is the Ekofisk oil storage tank. Now there are 20 offshore concrete gravity platforms in operation or under construction in different parts of the world (32). Table 1 (16) lists the 14 fixed concrete gravity platforms contracted for the North Sea, installed or under construction. Abbreviations are N for the Norwegian sector and UK for the United Kingdom. Each barrel represents 42 gal.

Concrete gravity structures, designed to remain on location by virtue of their own weight, offer an attractive alternative to piled steel template platforms in hostile waters like the North Sea. There are advantages in producing structures that can be constructed onshore or in sheltered waters, towed semisubmerged to the offshore location, and then installed in a short time by flooding. Other advantages are the elimination of steel piling, the use of traditional civil engineering labor and methods instead of highly skilled welding, less dependence upon imported building materials, a structure tolerant in regard to overloading, and the high durability of the materials used (5).

The rapid development of offshore concrete structures has led to a variety of different designs. Fig. 1 shows the four designs used thus far in the North Sea (16). The conductors through which the wells are drilled are inside one of the three concrete columns of the Condeep design. The conductor tubes in the Sea Tank design are exposed, and because of their close proximity to one another they appear in the figure as a vertical band beneath the drilling derrick. Steps in the construction of the Condeep platform are shown in Fig. 2.

[a]Presented at the October 22–26, 1979, ASCE Annual Convention and Exposition, held at Atlanta, Ga.

[1]Prof. of Civ. Engrg., Univ. of Houston, Houston, Tex. 77004.

[2]Prof. and Head of Struct. Engrg., School of Civ. Engrg., Purdue Univ., West Lafayette, Ind. 47907.

Note.—Discussion open until November 1, 1981. Separate discussions should be submitted for the individual papers in this symposium. To extend the closing date one month, a written request must be filed with the Manager of Technical and Professional Publications, ASCE. Manuscript was submitted for review for possible publication on March 19, 1980. This paper is part of the Journal of the Structural Division, Proceedings of the American Society of Civil Engineers, ©ASCE, Vol. 107, No. ST6, June, 1981. ISSN 0044-8001/81/0006-1059/$01.00.

With the discovery of oil offshore North America in areas apparently favorable to the use of concrete platforms, with the demonstrated success of concrete

TABLE 1.—Fixed Concrete Gravity Platforms Contracted for North Sea: Installed or Under Construction

Type of design location (1)	Main functions (2)	Design wave height, in meters (3)	Depth, in meters (4)	Approximate concrete volume, in cubic meters (5)	Base dimension, in meters (6)	Storage capacity, in millions of barrels (7)	Installation year (8)
Doris: Ekofisk 1 (N)	Storage	24.0	70	90,000	92	1.0	1973
Condeep: Beryl A (UK)	Drilling, production, storage	29.5	120	55,000	100	0.93	1975
Condeep: Brent B (UK)	Drilling, production, storage	30.5	142	65,000	100	1.0	1975
Doris: Frigg CDP1 (UK)	Drilling	29.0	96	60,000	101	—	1975
Sea Tank: Brent C (UK)	Drilling, production, storage	30.5	142	105,000	100	0.65	1978
Sea Tank: Frigg TP1 (UK)	Production	29.0	104	70,000	72	—	1976
Sea Tank: Cormorant A (UK)	Drilling, production, storage	30.5	152	115,000	100	1.0	1978
Condeep: Brent D (UK)	Drilling, production, storage	30.5	142	65,000	100	1.0	1976
Andoc: Dunlin A (UK)	Drilling, production, storage	30.5	152	89,000	104	0.85	1977
Condeep: Statfjord A (N)	Drilling, production, storage	30.5	149	88,000	110	1.3	1977
Condeep: Frigg TCP2 (N)	Treatment compression, production	29.0	104	50,000	100	—	1977
Doris: Frigg MP2 (UK)	Pumping station	29.0	94	60,000	101	—	1976
Doris: Ninian (UK)	Drilling and production	31.2	139	142,000	140	—	1977
Condeep: Statfjord B (N)	Drilling, production, storage	30.5	144	130,000	152	1.5	1981

platforms in the North Sea, and with the rapid expansion of knowledge and experience of the behavior of concrete and concrete structures in the sea, the

usage of large fixed bottom-supported concrete platforms in American waters is forthcoming. This paper reviews the present stand on design and analysis of fixed offshore concrete structures. Herein, outlines are given with regard to environmental loads, design principles, design and strength analysis of the most important types of shell structures and foundations involved, and highlights of the present American Concrete Institute (ACI)-recommended practice for offshore concrete structures (1).

Environmental Loads

The principal environment loads are due to waves and wind. Of importance are: distribution of breaking waves, distribution of wave heights and wave periods,

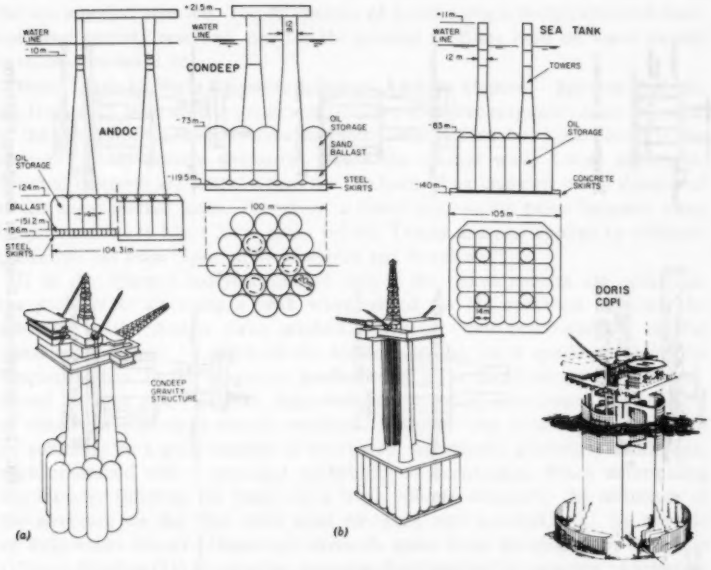

FIG. 1.—(*a*) Condeep and Andoc Gravity Structures; and (*b*) Seatank Gravity Structure and Foris CDPI Platforms

wave spectrum evaluation, duration of storms, impact loads, and ground (seismic) motions (16). The design environmental loads are normally based on environmental conditions which have a recurrence period of 100 yr; the design life time of the structure is usually 20 yr–30 yr.

Wave loads on offshore structures are generally predicted by a semi-empirical approach. The derivatives of a theoretically derived flow potential function are combined with empirical drag and inertial coefficients to predict wave forces on structural components relative to the position of the wave. There are two

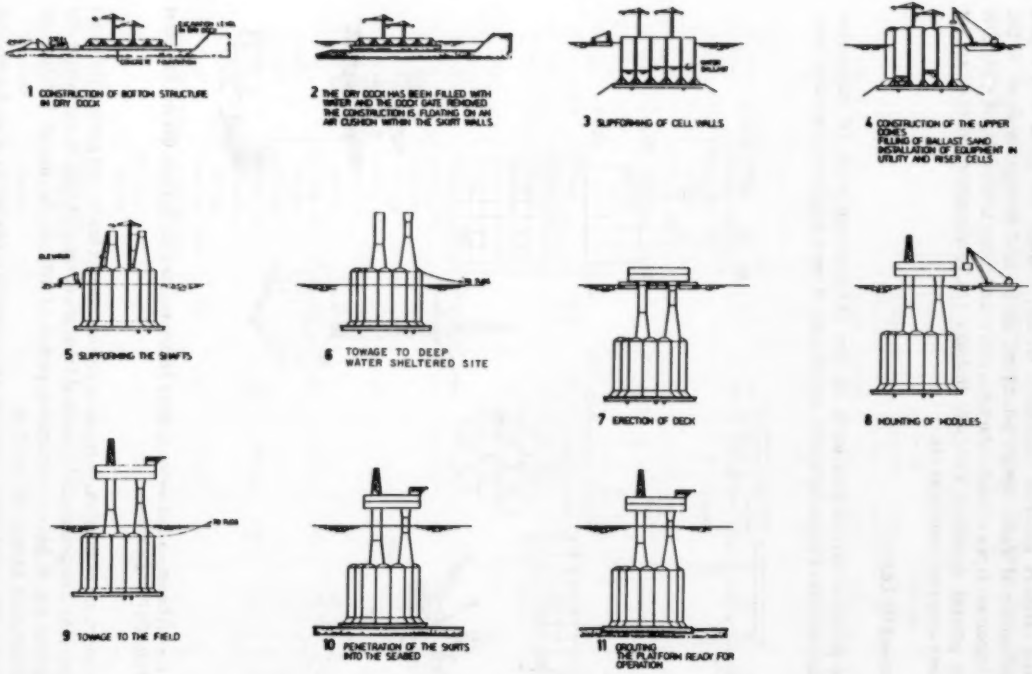
1 CONSTRUCTION OF BOTTOM STRUCTURE IN DRY DOCK
2 THE DRY DOCK HAS BEEN FILLED WITH WATER AND THE DOCK GATE REMOVED THE CONSTRUCTION IS FLOATING ON AN AIR CUSHION WITHIN THE SKIRT WALLS
3 SUPPORMING OF CELL WALLS
4 CONSTRUCTION OF THE UPPER DOMES FILLING OF BALLAST SAND INSTALLATION OF EQUIPMENT IN UTILITY AND RISER CELLS
5 SUPPORMING THE SHAFTS
6 TOWAGE TO DEEP WATER SHELTERED SITE
7 ERECTION OF DECK
8 MOUNTING OF MODULES
9 TOWAGE TO THE FIELD
10 PENETRATION OF THE SKIRTS INTO THE SEABED
11 GROUTING THE PLATFORM READY FOR OPERATION

FIG. 2.—Construction Steps for Condeep Platform

basic methods of evaluating the wave loads on a fixed offshore structure, i.e., the design wave method and the spectral analysis method.

Wave Loads by Design Wave Method.—This static method has been most often used in the past. The loads are derived from the passage of a single regular wave of given height and length past the structure. The most commonly used wave period for the North Sea is 15 sec. The period to be used should be that which causes the worst loading on the structure.

This method works fine on piled steel template structures where non-linear drag force usually dominates and generally provides adequate accuracy when designing a structure against extreme waves of 50 yr or 100 yr recurrence periods in shallow to moderate water depths. For large volume structures like those shown in Fig. 1, the force is often found to increase continuously with increasing wave period, and maximum forces on caisson structures are very sensitive to the wave period selected. The difficulties of establishing a design criterion have not been entirely resolved, but for the present a 20-sec limit on wave period is recommended (1,16).

Wave Loads by Wave Response Spectrum Analysis Method.—Spectral analysis has frequently been used to predict maximum wave force responses as an alternate to the deterministic design wave method. This method has been found to be appropriate for gravity structures where the inertial wave forces dominate. Spectral methods are useful where the nonlinear drag loads are small compared to the linear inertial loads. Therefore, a linear relationship exists between wave heights and wave force for a given period. Linear analysis applied to offshore platforms has been reported by Malhotra and Penzien (23).

If in the spectral analysis method only a few wave spectra are specified, the problem of choosing a peak wave period for the spectrum is much the same as in the design wave method. Thus for short-term analysis careful consideration must be given to the location of the wave spectrum along the frequency axis. In the long-term prediction of wave distributions and wave-induced motions and loads on ships and other floating structures, the problem of choice of periods is largely avoided. The long-term prediction is obtained by summing up a great number of short-term statistically stationary conditions, each combined with a specified probability of occurrence. When determining the transfer function for loads on a large volume structure, the influence of the structure on the flow field must be taken into account, e.g., by the use of diffraction theory. Numerical methods have been developed by Garrison (17) and Hogben (21) to calculate pressure distributions for caissons of arbitrary geometry. For circular, cylindrical structures, approximate methods by Gran (18) and McCamy (24) may be applicable.

Wind Loads.—The force of the wind on an offshore structure is a function of the wind velocity, the orientation of the structure, and the aerodynamic characteristics of the structure and its members. The wind force exerted on a structure consists of two components, one parallel to the wind and one perpendicular to the wind (3). It has the following forms:

$$F_D = C_d^{1/2} p V_z^2 A \quad \text{(force parallel to wind)} \quad \ldots \quad (1)$$

$$F_L = C_L^{1/2} p V_z^2 A \quad \text{(force perpendicular to wind)} \quad \ldots \quad (2)$$

in which C_d = drag coefficient; C_L = lift coefficient; p = density of the air;

V_z = wind velocity; and A = area perpendicular to wind velocity. Values for C_D and C_L may be found in Meyers, et al. (25). In preliminary calculations the wind force perpendicular to the wind direction is often neglected.

Due to the shear forces with the earth's surface, the wind velocity is not constant, but is zero at the surface and increases exponentially to a limiting maximum speed known as the gradient wind. Over water the wind speed at any elevation is represented by the one-seventh power law

$$V_z = V_{\text{Ref}} \left[\frac{z}{\text{Ref}} \right]^{1/7} \quad \ldots \ldots \ldots

should be designed for the fastest-mile-velocity having a period of recurrence at a given site of 100 yr. For computation of wind forces to be used in conjunction with maximum wave force, the 100-yr sustained wind velocity should be used. The American Petroleum Institute (API) (2) provides minimum design guidance for wind loading. An extensive investigation of wind forces on structures may be found in an ASCE publication (3).

Current Forces.—Two major components of the current are considered: tidal current and wind driven current. It is generally accepted that the wind driven current at the still water surface may be taken as 1% of the sustained wind speed at 30 ft (10 m) above the still water level. The current velocity should be added vectorially to the wave particle velocity before computing the drag force. Because drag depends on the square of the horizontal particle velocity, and because the current decreases slowly with depth, a comparatively small current can increase drag significantly. In design, the maximum wave height is sometimes increased by 3–4% to account for the current effects and the

TABLE 3.—Partial Load and Material Factors

Loading conditions (1)	Load Factors, h_f					Material Factor, h_m	
	Permanent loads, P (2)	Live loads, L (3)	Deformation loads, D (4)	Environmental loads, E (5)	Accidental loads, A (6)	Concrete (7)	Steel[a] (8)
ULS: ordinary[b]	1.3	1.3	1.0	0.7	—	1.5	1.15
ULS: extreme	1.0	1.0	1.0	1.3	—		
PLS, FLS, SLS	1.0	1.0	1.0	1.0	1.0[c]	1.0	1.0

[a]Value depends on mode of failure and how resistance is evaluated.
[b]For well-controlled loads, $h_f = 1.2$ may be used for the loads P and L when temporary.
[c]Only accounting for accidental loads in PLS.

current per se is neglected. Currents may be important for the design of auxiliary equipment, such as exposed risers and well conductors. Such components should also be investigated for vortex shedding. An excellent treatment of this phenomenon may be found in the Construction Industry Research and Information Association, (CIRIA) publication (6).

Design Principles

From the beginning of the development of offshore concrete structures, the design has been based on limit state (semiprobabilistic) methods. The definition of limit state is (16): A structure or structural member reaches a limit state of fitness in a condition where it just ceases to fulfil the resistance requirements or other specifications as regards structural performance for which it has been designed. The various limit states used in design are given in Table 2 (26).

The principal parameters governing the design are basically random variables. Usually full statistical information is not available, so the main uncertainties

are included as partial load and material safety factors. Characteristic load effects Q_c and characteristic resistances R_c are defined as certain percentiles of the distribution functions for load and resistance. Parameter Q_c is the mean of the characteristic load effects distribution plus one or two standard deviations. Parameter R_c is the mean of the characteristic resistance distribution minus one or two standard deviations.

In general, the design load effect, Q_d, is the most unfavorable combination of a specified set of loads and associated partial load factors, h_f, i.e.:

$$Q_d = \text{effect of } \Sigma\, h_f Q_c \quad \ldots\ldots\ldots\

precedence. The safety as well as the functional requirements must be determined with great care considering the hostile environment and the grave consequences of a possible failure.

Oil storage is usually one of the principle functional requirements. Repair of an offshore underwater concrete oil storage structure could be done at best only under extreme difficulty. The consequences of a possible oil leak could be very serious. Thus the establishment of realistic serviceability limit state (SLS) criteria is very important. Structural components containing oil should be designed completely tight with respect to oil leakage, which means only very limited cracking of the concrete may be allowed. If the internal pressure of the stored oil is always kept below the external pressure of the surrounding

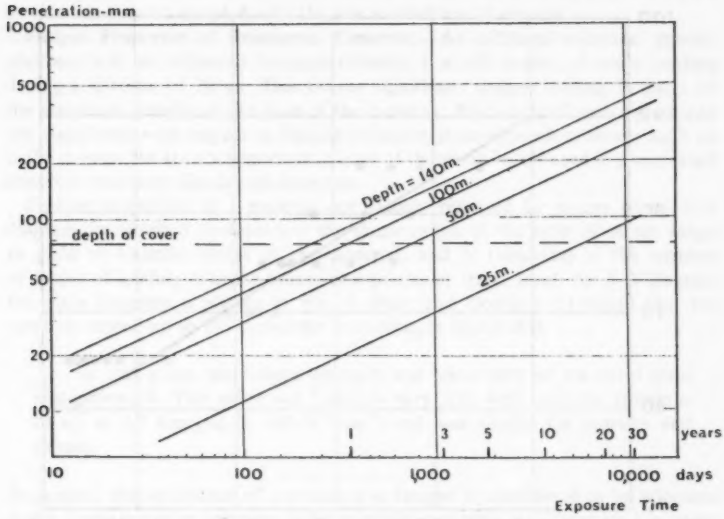

FIG. 3.—Penetration of Sea Water into Well-Compacted Concrete at Various Water Depths

water, then somewhat less severe requirements may be used. Sometimes a separate water-containing chamber is provided between the stored oil chamber and the outside ocean water.

For installation of the steel deck structure on the concrete gravity platform, the caisson and its three or four concrete columns is submerged to a very deep draft leaving column lengths of only 1 m or 2 m extending out of the water. The deck structure supported between two barges is floated over the columns, and the steel transition pieces are welded to the column ends. The caisson is deballasted enough to raise the deck structure slightly, and the barges are removed. During the deep submersion the caisson walls may have to resist a net hydrostatic pressure in excess of 9 tons/sq ft). Should failure occur, it would be from implosion of the cell walls of the caisson. Very careful attention

must be given to determining the load carrying capacity of the cellular structure. Besides the nonlinear influence of geometry on deformations, the material nonlinearities aggravate the tendency of the concrete to crack. Sufficient load carrying capacity must be present in the deformed condition to preclude any inelastic instability.

Instability modes of failure in reinforced concrete members should be interpreted as ultimate load-bearing capacity failures rather than critical stress problems as reflected by the classical theory of elastic instability. Instability failures of reinforced concrete should be analyzed on the basis of critical strains rather

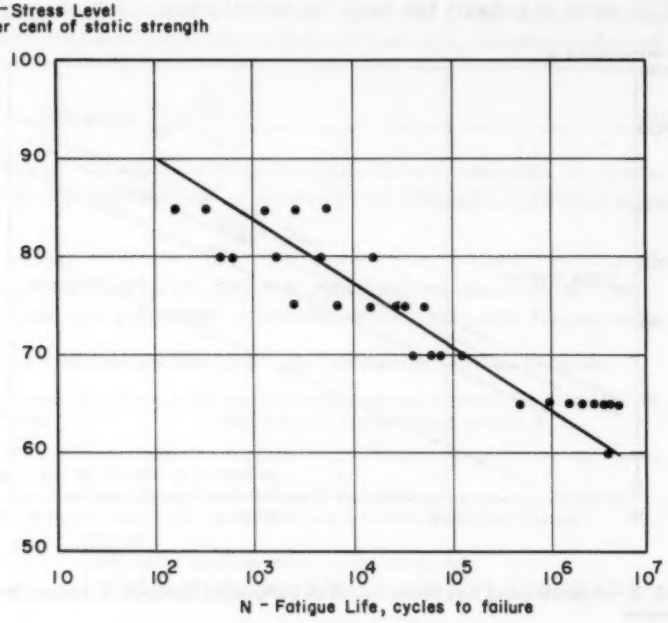

FIG. 4.—*S-N* Curve for Plain Concrete

than critical stresses. Many simplifications must be made in order to do a realistic analysis of the nonlinear behavior of a large complex concrete structure. Understanding of the nonlinear material characteristics, cracking, creep, and other rheological effects is still in the active development stage. Predicting the margin of safety of a concrete cellular shell structure may become a difficult task even when dealing with a well-defined load like hydrostatic pressure. Further discussions on the design and strength analysis of the most important types of shell structures are given in the later part of this paper.

Durability of Reinforced and Prestressed Concrete.—Marine structures made of reinforced concrete with hard, dense aggregates combined with a low

water/cement ratio have proven to be very durable. Prestressed concrete structures have shown excellent durability in marine environments also (5).

The coefficient of permeability of concrete varies widely with the water/cement ratio, cement content, and maturity of the concrete. Penetration of seawater into reinforced concrete may lead to corrosion of the reinforcement. The results of recent seawater penetration tests on well-compacted concrete are shown in Fig. 3 (5). Regardless of depth, penetration of seawater to the reinforcement is likely to occur in a few years, even in well-compacted concrete, i.e., well within the design life of the structure. A survey of existing reinforced concrete structures in marine environments has shown that no significant degradation occurs over the years in permanently immersed concrete, even when severe corrosion occurs in the splash zone. This is because of the low, uniform levels of chloride present coupled with the low availability of oxygen.

Fatigue Properties of Reinforced Concrete.—An offshore concrete gravity platform will be subjected to approximately 1×10^8 cycles of wave loading during a lifetime of 20 yr. This causes significant fatigue loading in parts of the structure, notably at the base of the columns. The levels of stress produced are significant with regard to fatigue behavior in reinforced concrete such as in the caisson but are not important in view of the stress levels used in prestressed concrete members like the tall columns.

Fatigue properties of a material are usually reported by means of an S-N diagram, in which S (ordinate) = the stress range or the ratio of stress range to yield or ultimate stress of the material; and N (abscissa) = the number of cycles of loading to cause failure at a particular stress level. An S-N diagram for plain concrete is shown in Fig. 4. Bury and Domone (5) report that for concrete tested up to 10^7 cycles the investigators found that

> . . . at that point, the fatigue strength was about 60% of the short term static strength. This value was found to vary little with concrete strengths of up to 8.7 kips/sq in. (60 N/mm^2) and was similar for mortars and pastes.

In general, the resistance of a structure to fatigue is considered to be adequate if the stress range in concrete under monthly recurring maximum load is under $0.5f'_c$ in compression and 200 psi (1.4 MPa) in flexural tension and no membrane tensile stress. Bond values, for sections under cyclic reversing loads, should not exceed 50% of those for static loads.

Fatigue tests on reinforcing bars have been carried out in uniaxial loading in air or have been done as flexural loading of reinforced concrete beams. The fatigue life of reinforcing steel depends on the range of stress applied and not on the absolute values of minimum and maximum stress, provided the maximum stress does not exceed the yield stress of the material. Bury and Domone (5) report the work of several investigators in Fig. 5 for both mild steel and a number of ribbed high tensile strength steel reinforcing bars. They also report that for reinforced members designed to be structurally economic ". . . the steel is likely to fail in fatigue before the concrete." This is not true for heavily over-reinforced sections. In general, the cyclic stresses in reinforcing or prestressing steel should limit to 20,000 psi (140 MPa) but reduce to 10,000 psi (70 MPa) for bent or welded reinforcements.

Other Important Design Problems.—Several other important aspects of the design of offshore concrete gravity structures are:

1. Cumulative fatigue damage at the column bases.
2. Temperature stresses within the ciasson caused by storage of hot oil.
3. Structural instability of the columns and the inner walls of the caisson.
4. Local earth pressures on the base raft.
5. Impact load capacity of reinforced concrete.
6. Ultimate load carrying capacity in complex regions where structural members of various geometry are connected.
7. Potential instability of the structural system during towout operation due to the topside structural weight.

Steel Decks on Concrete Platforms.—All of the concrete gravity structures constructed so far have had steel decks. The main reason for this is to minimize

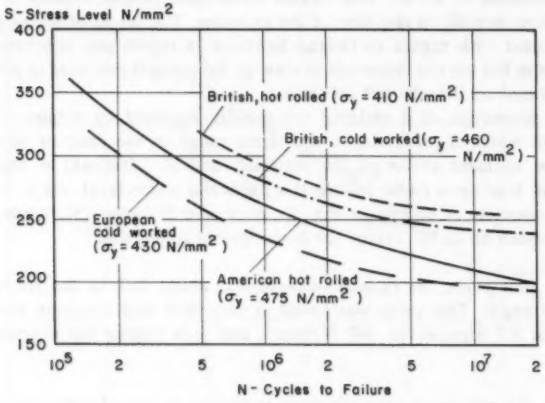

FIG. 5.—*S-N* Curve for Various Reinforcing Bars

the topside structural weight. The topside structural weight is of great significance during towout of the platform to its final offshore location.

Types of Decks.—The dimensions and weights (for oil production function) of several platform decks are listed in Table 5 (15). Generally speaking there are three common deck types, i.e., plate girders, box girders, and truss girders either using tubulars or plate sections. These types of decks have also been categorized into two groups, i.e., intergrated decks and modularized decks.

The only integrated steel deck built thus far is that on the Beryl A platform, although the deck on the Statfjord A is partially integrated. The integrated deck has the advantage of lower structural self-weight and consequently lower cost. However, it is critically dependent on timewise correct delivery of the equipment to be installed. The possibility of making modifications to the processing equipment is very limited. Constructing the deck (while simply called the deck, the structure may consist of three or four levels or elevations each

of which could be called a deck) of modules provides much more flexibility in scheduling and location of fabrication work; it also is more expensive. To minimize topside weight during towout to location, some of the uppermost modules are towedout separately on a barge and lifted into place after the basic platform has been ballasted into position on the sea floor.

Design Loads.—The mass or inertial component of the passing wave force is predominant, although the drag force is also considered in the design. Ordinarily the wave period which yields the highest loads on the entire structure is not the one which yields the highest loads on the deck structure. Several wave periods must be investigated to establish the maximum wave loading.

The wind loading is considerably less than the wave loading but is frequently the governing design load for various parts of the deck. Flare towers, telecommunication towers, drilling derrick, and heliport transmit large wind loads through their anchorage points. These points must be carefully analyzed in the design.

With integrated deck structure most of the equipment is distributed evenly throughout the decks. With modules the loads represented by the modules are transferred to the deck substructure through four to six support points. These points of concentrated load require analysis to ensure sufficient local strength.

TABLE 5.—Dimensions and Weights for Some Platform Decks

Platform (1)	Dimensions $L \times B \times H$, in meters (2)	Area, in square meters (3)	Self-weight, in tons (4)	Maximum weight, in tons (5)
Brent B	72 × 70 × 6	3,650	4,200	26,000
Beryl A	72 × 70 × 10	3,650	6,500	32,000
Statfjord A	86 × 83 × 10	5,000	7,000	42,000
Cormorant A	82 × 70 × 6	3,600	5,700	30,000

Maximum deck loads cause compressive stresses in the concrete columns of the platform. Minimum deck loads combined with wave loads may cause tensile stresses in one or more of the columns. The concrete columns are post-tensioned by a series of internal cables so as to keep the stresses in the concrete always compressive. This stress may approach zero in the worst storm condition, but it should not become tension.

The sequence of lifting and placing modules on the deck substructure must also be investigated as regards local strength problems.

Excepting the structures in water depths less than 100 m, the concrete platforms shown in Table 1 have resonance periods in the range of 2 sec–4 sec. Thus a dynamic amplification factor must be applied to the wave forces if these are found by a quasistatic analysis. This is especially important for the many smaller waves (ordinary operating waves) since they make up most of the fatigue loading on the platform. Of course, in the North Sea these ordinary waves are still quite high, estimated to be on the average 65% of the maximum storm wave height. In a 20-yr lifetime from 12,000 to 15,000 of these ordinary operating waves will pass the platform.

Special Design Considerations.—Waves and wind produce large deformations

of the deck. Accompanying the deformations are rotations of the column ends which in turn cause bending moments in the deck elements. Static loads on the deck also cause deformations and rotations in the column because of eccentricity. The dynamic stress sometimes may be as high as five times the static stress. Steel plate thicknesses are sometimes over 2.5 in. (60 mm); considering the welding of such sections, one can see why fatigue is an important part of the deck design.

Three grades of steel are usually used in deck construction. Special high strength steel is used for the transition pieces between the concrete column ends and the deck substructure and for all of the main cruciform joints. Primary structural steel is used for all other structural members except ancillary items like walkways, ladders, railing, buckling stiffeners, etc. These are made of a secondary grade of steel.

Recommended ACI Practice for Offshore Concrete Structures

Recently, the ACI Committee 357 on Offshore Structures issued a report on Recommended Practice for Fixed Offshore Concrete Structures (2). This report is prepared in the anticipation of the forthcoming usage of large fixed concrete sea structures in American waters. This recommended American design practice was developed with much guidance from the three specifications listed as Refs. (2,13,14).

Building Code Requirements for Reinforced Concrete (ACI 318-77) are to be used together with this recommended practice. Because of the nature of the marine environment, certain recommendations made in this offshore practice override the requirements of ACI 318-77.

Some important features concerning design and analysis of fixed concrete sea structures as recommended by ACI Committee 357 are here briefly described.

1. Elastic static analysis may be used to determine the distribution of forces and moments in the structure. The member stiffness to be used in the analysis should be based on the stiffness of the uncracked section. The structural members are then proportional to satisfy strength requirements.
2. If dynamic analysis is required, such an analysis should include the effects of the foundation, surrounding water, and the nonlinear behavior of the soil.
3. For shell structural elements, a strength reduction factor of 0.7 for the concrete material is recommended. For the case of instability analysis, the modulus of elasticity obtained from ACI 318-77 should be reduced 10%. The design of shell elements should be based on the assumption that compressed air will not be employed to offset external hydrostatic pressures during installation on the site. To design against liquid leakage in regions of high bending gradients, at least 25% of the wall thickness must be in compression.
4. Temperature loads due to fluid containments and concrete hydration may lead to severe cracking in regions of structural restraints. The effect of such cracking upon future performance of the structure under service and extreme environmental conditions should be investigated.
5. A survival strength analysis is needed in order to prevent the structure from catastrophic collapse in the event of rare natural or man-made events such as ductility level earthquake, adverse ice condition, collisions, or explosion.

Analysis and Design of Shell Structures

As can be seen from Fig. 1, concrete gravity platforms consist mainly of various cylindrical shells of large dimensions. These shells are capped with spherical or conical domes at bottom and top. Further, all these platforms are equipped with concrete or steel skirts in the form of short cylindrical shells, or both, as a means of scour protection and of assuring sufficient resistance against horizontal sliding. Shell structural elements are most effective in resisting high water pressures and at the same time offer considerable economical advantages. The complexity of the various shell components connected together coupled with the complex actions of the environmental loads and other load combinations renders the analysis and design of such structures difficult. Herein, a brief outline is given with regard to the basic concept of the design and strength analysis of spherical and cylindrical shell structures.

The walls of concrete shell must be properly proportioned to prevent catastrophic collapse against various periods of large hydrostatic pressure exposure. Potential failure modes to be considered are material failure and structural stability. A rational analysis of the behavior and failure of the shell structure must consider the nonlinear material behavior, creep, cracking, and the effects of possible geometrical imperfections. In the case of stability analysis, the second-order effects produced by deformation must also be considered. In the following, three typical approaches to the problem from quasi-empirical to analytically complex are briefly described.

Quasi-Empirical Methods.—In this approach, strength and buckling equations are first derived on the basis of simple elastic analysis and then modified so as to obtain a best possible fit to the experimental data at hand. Tests on cylindrical and spherical concrete shells subject to hydrostatic pressure have been conducted in the Civil Engineering Laboratory at Port Hueneme since 1966. Based on these test results, design guides for designing spherical and cylindrical concrete structures to resist hydrostatic loads and, thus, to predict the implosion failure pressure have been published (19). Both thin-walled and thick-walled structures are considered. These semi-empirical design equations are generally conservative and should serve as a useful guidance for a preliminary design calculation or quick check. These equations are summarized in Table 6.

Tangent Modulus Methods.—Research has shown that the tangent modulus buckling concept is proper for the prediction of the maximum strength of many types of columns, i.e., centrally load columns (11). This concept is not adequate for cylindrical shells, because the tangent modulus approach pertains to idealized perfect structural members while actual structural members contain significant geometric imperfections and/or lateral loads. Nevertheless, tangent modulus approach is a powerful simplified model to an actual structure in that:

1. It takes account of the nonlinear stress-strain behavior of material.
2. It uses linear elastic buckling analysis.

This approach is found to give reasonable predictions for the structures whose in-plane forces are dominating. The design method proposed by Furnes (15) is briefly described in the following paragraphs.

The first step in this method is to obtain the linear elastic buckling stress

for an idealized perfect structural member with constant elastic modulus E_c. Critical stress σ_{cr} can be written in the general form as

$$\sigma_{cr} = \rho E_c \quad \ldots \ldots \ldots

The nonlinear stress-strain behavior for concrete may now be taken into account in Eq. 7 by simply replacing the Young modulus E_c by the tangent modulus E_{cr}, which is a function of concrete stress σ. Assuming a second-order parabola for the concrete stress-strain relation, E_{cr} can be expressed in term of concrete stress σ. Substitution of E_{cr} and E_c in Eq. 7 yields

$$\frac{\sigma_{cr}}{f'_c} = \alpha = \frac{2}{1 + \sqrt{1 + \left(\frac{\epsilon_{ult}}{\rho}\right)^2}} \quad \ldots\ldots\ldots\ldots\ldots\ldots\ldots\ldots\ldots\ldots\ldots\ldots (10)$$

For short term loading, ϵ_{ult} = strain at f'_c is normally chosen to be 0.002. For long-term loading ϵ_{ult} may be modified by creep factor ψ, i.e.

$$\epsilon'_{ult} = \epsilon_{ult}(1 + \psi) \quad \ldots\ldots\ldots\ldots\ldots\ldots\ldots\ldots\ldots\ldots\ldots\ldots\ldots\ldots (11)$$

to allow for the effect of creep. Normally, range $0.5 \leq \psi \leq 1.0$ is found appropriate. The effect of reinforcement may be considered by changing α to

$$\alpha' = \alpha\left(1 + \frac{f_s A_s}{f'_c A_c}\right) \quad \ldots\ldots\ldots\ldots\ldots\ldots\ldots\ldots\ldots\ldots\ldots\ldots\ldots (12)$$

in which α is defined in Eq. 10; f_s = the steel strength; and A_s and A_c = the steel and concrete sectional areas, respectively.

Magnification factor $(1 - \sigma/\alpha_{cr})$ may be used to obtain design moment M_d by simply multiplying this factor to first-order moment M_{d0}. The design moment is then obtained, i.e.

$$M_d = \frac{M_{d0}}{1 - \frac{1}{e_t}\frac{\sigma}{\sigma_{cr}}} \quad \ldots\ldots\ldots\ldots\ldots\ldots\ldots\ldots\ldots\ldots\ldots\ldots\ldots\ldots (13)$$

in which factor e_t = the correction on stiffness which depends on the stress level and slenderness ratio.

Computer Methods.—Analyses of reinforced concrete structures are complicated, mainly due to the nonlinear geometrical and material behavior as the result of cracking, creep, and nonlinear stress-strain relationship of concrete. For the most part, analytical studies of the response of reinforced concrete structures have in the past been focused, by necessity, on the behavior of isolated simple structural elements such as beams and columns, etc. As quantitative information on the load-deformation behavior of concrete developed and computing capability expanded, the scope of analysis capability has been broadened to include the triaxially-loaded concrete structures such as concrete offshore platforms. With the present state of development of computer programs, inadequate material models are often one of the major factors in limiting the capability of computerized structural analysis. The formulation of such general constitutive equations for reinforced concrete material is of prime importance. Considerable research is currently underway in many countries. The current trend in research in concrete constitutive modeling is moving toward the development of three-dimensional stress-strain relations based on the principles

of plasticity as well as elasticity. A comprehensive review on this development is given in a recent paper by Chen (9).

Various nonlinear computer programs for reinforced concrete are now available and suitable for investigating strength and stability of structural shell elements (15).

In the following, some highlights of the recent test results and a comparison of those results to computational predictions for 15 unreinforced concrete cylindrical shells subjected to external hydrostatic loading are here briefly described. Details are presented elsewhere (20).

The analyses use a finite element program called NONSAP-A with an advanced constitutive relation subroutine for the concrete. The analysis is found to predict the behavior of the specimens with good accuracy.

The concrete stress-strain relationships under general stress states were developed in three parts: elasticity, plasticity, and fracture. For elastic concrete, it is assumed that the material was initially isotropic, homogeneous linearly elastic. For plastic concrete, a strain-hardening plasticity model was used to describe the nonlinear irreversible behavior. The plastic incremental stress-strain relations based on the normality flow rule in the theory of plasticity are developed in detail in the book by Chen (8).

When the state of stress reached a certain critical value, concrete failed by fracturing. Two different types of fracture mode are defined, i.e., "cracking" type and "crushing" type. When concrete cracks, the material is assumed to lose only its tensile strength normal to the crack direction but retains its strength parallel to the crack direction. On the other hand, when concrete crushes, the material element loses its strength completely. A dual representation of fracture criterion expressed in terms of both stresses and strains was adopted; details are given elsewhere (9).

Two computer codes have been developed to implement the advanced material model described herein. The first computer program is called EPFFEP (Elastic-Plastic-Fracture-Finite-Element-Program). The details of this program are given in the report by Suzuki and Chen (29). In order to make the results readily available in analysis for structural engineers in general, a second computer program in the form of a subroutine has also been developed. This subroutine is readily adaptable for use in any existing or postulated large finite element analysis computer program. In particular, the subroutine has been incorporated in the nonlinear structural analysis program called NONSAP-A, which is a modified version of the NONSAP program originally developed by Bathe, et al. (4) of the University of California at Berkeley. Nonlinearities considered in the program include nonlinear materials, large displacement, and large strains. The details of the development of the present subroutine are given in the report by Chang and Chen (7).

As an example, consider the two cases shown in Fig. 6, which were performed using isoparametric shell elements. Case 1 was modeled as axisymmetrical problem with simply supported end condition, and Case 2 was treated as a three-dimensional problem with large displacement. Out-of-roundness in the form of cos 3θ was included in the analysis.

It can be seen that the introduction of out-of-round imperfection causes a significant reduction in implosion pressure (about 44%). The effect of out-of-roundness depends on cylinder thickness to diameter ratio t/D_0. Cases 1 and

2 shown in Fig. 6 were thinner specimens than all others. For example, the thinner specimens ($t/D_0 = 0.024$) show a 44% reduction due to out-of-roundness (about 0.15% of D_0) whereas the thicker specimens ($t/D_0 = 0.037$) show a 16% reduction.

The effect of cylinder length can also be studied. For example, for the out-of-round cylinders, the shorter cylinder ($L/D_0 = 2.35$) has a predicted increase in implosion strength of 53% over that of the infinitely long cylinders. Experimentally, the increase in strength is 41%.

Deflected cross-sectional shapes for cylinders with initial out-of-round imperfection can also be accurately predicted. The analytical radial displacement behavior of the interior wall at cylinder midlength as a function of pressure loading is compared in Fig. 6 with the experimental data. A good agreement is observed. The membrane radial displacement w_m are also shown in Fig. 6 for an experimentally perfect cylinder. The w_m curve can only extend to pressure

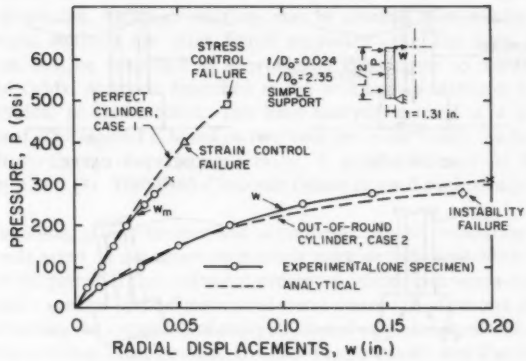

FIG. 6.—Radial Displacement at Midlength of Cylinder

equal to pressures equal to P_{im} for the out-of-round specimens, so termination of the curve does not mean implosion for an experimentally perfect cylinder.

The difference in stiffness of the cylinder wall between perfect and out-of-round specimens is dramatic. For example, an out-of-round, freely supported cylinder of $t/D_0 = 0.037$ had an ultimate radial displacement that is 6.4 times the displacement of a similar but perfect cylinder. The importance of out-of-roundness and the need to model the out-of-roundness to obtain accurate analytical predictions is apparent from the results of this study.

Foundations Design

The concrete platform foundation design depends entirely on soil parameters determined through site investigations. The site investigations may include a survey of sea bottom topography, site geology, geophysical investigations, in-situ determination of soil parameters by means of soundings, vane shear and cone

penetration tests, and sampling in bore holes with laboratory investigations of the samples. The investigation must allow identification, classification, and description of all significant soil strata, and for each stratum the geotechnical parameters necessary for the design have to be determined (22,33). The bearing capacity of a mat foundation is largely determined by the strength of soils close to the sea floor. Consequently, particular attention should be given to the developing complete information on these soils.

The stability of the foundations is the most important problem encountered in foundation design. Several possible modes of failure for a typical gravity structure is shown in Fig. 7 (22). The simplest mode of failure is sliding between the base of the structure and the sea floor as shown in Fig. 7(*a*). This is critical if the shear resistance at the interface is smaller than that in the soil mass. The risk of sliding is reduced by adding steel skirts to the bottoms of the concrete cells of the caisson and by adding several steel tubular dowels that

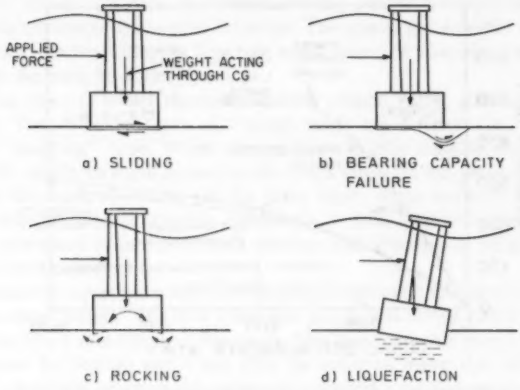

FIG. 7.—Possible Failure Modes for Foundation of Typical Gravity Platform

extend below the skirts. During deballasting for placement the dowels contact the soil first. Both dowels and steel skirts penetrate the soil and preclude sliding.

If the shear strength of the soil is exceeded, a deep-seated bearing capacity failure as shown in Fig. 7(*b*) may occur. This failure mode is typical for foundations of clay. The analysis should consider the possible reduction in shear strength due to repeated loadings.

For large foundations on sand the possibility for a bearing capacity failure for transient wave loadings depends on the undrained shear strength of the soil. In this case a bearing capacity failure like that in clay soil is not likely. However, a high shear stress level may lead to large deformations with high hydraulic gradients along the rim of the foundation and repeated loading may lead to softening of the soil and rocking failure [see Fig. 7(*c*)]. Another problem with the foundation of concrete platforms is that the currents around the perimeter of the caisson can cause scour and undermining. Generally, rock is dumped

around this area to prevent the scouring failure.

Liquefaction is another mode of failure for gravity structures on sandy soil. This mode of failure would most likely occur during a storm wherein repeated shear stress applications lead to a gradual increase in pore water pressure which causes a reduction or possibly a complete loss of shear strength of the sand so that it behaves like a heavy liquid. The structure sinks into the fluidized soil, tilting at the same time if there is eccentric loading on the deck [Fig. 7(*d*)]. Such effects can be accounted for in the design only on the basis of tests on the actual soil or relevant experience with similar soils. In general, the effects of repeated loading should be included in the evaluation of stability by using stress analysis, or by using increased pore pressures in effective stress analysis, as indicated by data from tests with repeated cyclic loads.

At the present time, there are three methods generally associated with the stability analysis of foundations. These are: (1) Slip line method; (2) limit equilibrium method; and (3) limit analysis method. The slip line method involves a construction of a family of shear or slip lines in the vicinity of the soil structure interfaces. Although solutions may be obtained analytically, numerical and graphical methods are often found necessary (28). The limit equilibrium method can best be described as approximate approaches to the construction of slip line fields. Methods described in the well-known textbook by Terzaghi (31) are typical of this method. The limit analysis method is a more recent development. The method is based on two limit theorems which can be rigorously derived from theory of perfect plasticity. A good treatment of this subject is given by Chen (8). The Mohr-Coulomb failure is used exclusively in all these analyses.

The evaluation of movements and settlements of the foundation caused by various loads acted on the structure is much more complicated. With the present state of development of finite element programs, inadequate stress-strain models for soil under general three-dimensional stress states are often one of the major factors in limiting the capability of analysis for soil structure interaction problems. Some analyses using Tresca model, Drucker-Prager model, and Cambridge strain hardening models are summarized in the book by Chen (8), and many more studies including strain softening behavior of soils can be found in the current literature.

Appendix.—References

1. "Guide for the Design and Construction of Fixed Offshore Concrete Structures," American Concrete Institute Committee 357 on Offshore Concrete Structures, *Journal of the American Concrete Institute*, Vol. 75, No. 12, Dec., 1978, pp. 684–709.
2. "API Recommended Practice for Planning, Designing and Construction Fixed Offshore Platforms," *API RP2A*, American Petroleum Institute, 7th ed., Jan., 1976.
3. "Wind Forces on Structures," Task Committee on Wind Forces, *Transactions*, ASCE, Vol. 126, Part II, Paper No. 3269, 1961, p. 1,124.
4. Bathe, K. J., Wilson, E. L., and Iding, R. H., "NONSAP—A Structural Analysis Program for Static and Dynamic response of Nonlinear System," *SESM Report No. 73-3*, Dept. of Civ. Engrg., Univ. of California, Berkeley, Calif., 1974.
5. Bury, M. R., and Domone, P. L., "The Role of Research in the Design of Concrete Offshore Structures," *Proceedings*, 1974 Offshore Technology Conference, *Paper No. 1949*, 1974.
6. "Oscillation of Piles in Marine Structures," *Technical Note 40*, Construction Industry

Research and Information Association, London, England, 1972.
7. Chang, T. Y., and Chen, W. F., "Extended NONSAP Program for OTEC Structural Systems," *Report No. C00-2682-7*, Environmental Resources Development Agency, Washington, D.C., 1976 (NTIS Publication).
8. Chen, W. F., *Limit Analysis and Soil Plasticity*, Elsevier Publishing Co., Amsterdam, The Netherlands, 1975.
9. Chen, W. F., "Nonlinear Analysis of Pressure-Resistant Concrete Cylinder Structures," *Proceedings of the International Conference on Engineering Application of the Finite Element Method*, May 9–11, 1979.
10. Chen, W. F., "Constitutive Equations for Concrete," *Introductory Report*, Colloquium on Plasticity in Reinforced Concrete, *International Association for Bridge and Structural Engineering*, Copenhagen, Denmark, May, 1979, pp. 11–34.
11. Chen, W. F., and Atsuta, T., *Theory of Beam-Columns: Vol. 1, In-Plane Behavior and Design, Vol. 2, Space Behavior and Design*, McGraw-Hill Book Co., Inc., New York, N.Y., 1976, 1977.
12. *Hydrodynamic Forces on Gravity-Type Platforms*, Delft Hydraulics Laboratory, Delft, Netherlands, Mar., 1974.
13. "Rules for the Design, Construction and Inspection of Fixed Offshore Structures," Det Norske Veritas, 1974.
14. "Recommendations for the Design and Construction of Concrete Sea Structures," Federation Internationale de la Precontraint, 2nd ed., Nov., 1974.
15. Furnes, O., "Instability of Plane and Curved Concrete Walls in the Design of Gravity Offshore Platform," *Proceedings of the European Offshore Petroleum Conference and Exhibition*, Oct., 1978.
16. Furnes, O., "Overview of Offshore Oil Industry with Emphasis on the North Sea," Lectures on Offshore Engineering, Combined Proceedings of a One-Day Conference Plus Eight Weekly Seminars, Aalborg University Center, Aalborg, Denmark, 1978.
17. Garrison, C. J., et al., "Wave Forces on Large Volume Structures—A Comparison between Theory and Model Tests," *Paper 2137, Proceedings*, 1974 Offshore Technology Conference, May, 1974.
18. Gran, S., "Wave Forces on Submerged Cylinders," *Paper 1817, Proceedings*, 1974 Offshore Technology Conference, May, 1973.
19. Haynes, H. H., "Handbook for Design of Undersea, Pressure-Resistant Concrete Structures," Civ. Engrg. Lab., Naval Construction Battalion Center, Port Hueneme, Calif., Sept., 1976.
20. Haynes, H. H., Chen, W. F., Chang, T. Y., and Suzuki, H., "External Hydrostatic Pressure Loading of Concrete Cylinder Shells," *Proceedings of the 1979 ASME Pressure Vessels and Piping Congress*, American Society of Mechanical Engineers, June, 1979 (79-pvp-125).
21. Hogben, N., and Standing, R. G., "Wave Load on Large Bodies," *International Symposium on the Dynamics of Marine Vehicles and Structures in Waves*, University College, London, England, Apr., 1974.
22. Hove, K., and Foss, I., "Quality Assurance for Offshore Concrete Gravity Structures," *Paper 2113, Proceedings*, 1974 Offshore Technology Conference, 1974.
23. Malhotra, A., and Penzien, J., "Nondeterministic Analysis of Offshore Structures," *Journal of the Engineering Mechanics Division*, ASCE, Vol. 96, No. EM6, Proc. Paper 7777, Dec., 1970, p. 985.
24. McCamy, R. C., and Fuchs, R. A., "Wave Forces on Piles: A Diffraction Theory," *Technical Memo No. 69*, Beach Erosion Board, Corps of Engr., Dec., 1954.
25. Meyers, J. J., Holm, C. H. and McAllister, R. F., *The Handbook of Ocean and Underwater Engineering*, Section 12, McGraw-Hill Book Co., Inc., New York, N.Y., 1969.
26. Moan, T., and Graff, W. J., "Structural Analysis and Design of Steel and Concrete Fixed Offshore Structures," Lectures on Offshore Engineering: Combined Proceedings of a One-Day Conference Plus Eight Weekly Seminars, Aalborg University Centre, Aalborg, Denmark, 1978.
27. Moksnes, Jan, "Condeep Platforms for the North Sea: Some Aspects of Concrete Technology," Paper No. 2369, *Proceedings*, 1975 Offshore Technology Conference, 1975.

28. Sokolovskii, V. V., *Statics of Granular Media*, Pergamon Press, London, England, 1965.
29. Suzuki, H., and Chen, W. F., "EPFFEP Program for OTEC Structural Systems," *Report No. C00-2682-8*, Energy Resources Development Agency, Washington, D.C., 1976 (NTIS Publication).
30. Suzuki, H., Chen, W. F., and Chang, T. Y., "Implosion Analysis of Concrete Cylindrical Vessels," *Journal of Pressure Vessel Technology*, American Society of Mechanical Engineers, Vol. 101, No. 1, Feb., 1979, pp. 98–102.
31. Terzaghi, K., *Theoretical Soil Mechanics*, John Wiley and Sons, Inc., New York, N.Y., 1943.
32. Waagaard, K., "Fatigue of Offshore Concrete Structures: Design and Experimental Investigations," *OTC Paper No. 3009, Proceedings*, 1977 Offshore Technology Conference, Tex., 1977.
33. Young, A. G., Kraft, L. M., and Focht, J. A., "Geotechnical Considerations in Foundation Design of Offshore Gravity Structures," *OTC Paper No. 2371, Proceedings*, 1975 Offshore Technology Conference, 1975.

FIXED PILE-SUPPORTED STEEL OFFSHORE PLATFORMS[a]

By Peter W. Marshall,[1] M. ASCE

INTRODUCTION

Prior to the Civil War, tubular wrought iron structures were built several miles offshore to support lighthouses along the Florida Keys. However, offshore construction as we know it today began in 1947 with the installation of the first steel template-type structure in the Gulf of Mexico, for drilling off Louisiana in 20 ft (6 m) of water (1). Twenty years later there were over 2,000 such structures in the Gulf of Mexico, in water depths up to 340 ft (102 m). Offshore drilling platforms had also been built off Southern California, in Alaska, in the North Sea, in the Persian Gulf, and in Southeast Asia. The technology had matured in the sense that much of the pioneering had been done, and the pattern was pretty well set for what are today's routine structures.

These structures consist of three major elements:

1. A welded tubular steel jacket that extends from the sea floor to slightly above the waterline. Hollow legs provide a guide for driving piles; these are braced by a space frame that resists lateral loads imposed by nature. The typical jacket is prefabricated onshore in one piece, carried offshore by barge, launched at sea, and set on bottom by ballasting, assisted by a seagoing crane or derrick barge.
2. The platform foundation is established by driving tubular steel piling through the jacket legs and 100 ft–400 ft (30 m–120 m) into the sea floor. Pilings are attached to the jacket by welding above water or grouting, or both, to the annular space between pile and jacket. Vertical and overturning loads on the structure are resisted by axial capacity of the piling. Lateral and torsional loads at the base of the jacket are carried into the soil via shear and bending in the piles.

[a]Presented at the October 22–26, 1979, ASCE Annual Convention and Exposition, held at Atlanta, Ga.

[1]Civ. Engrg. Advisor, Shell Oil Company, two Shell Plaza, P.O. Box 2099, Houston, Tex. 77001.

Note.—Discussion open until November 1, 1981. Separate discussions should be submitted for the individual papers in this symposium. To extend the closing date one month, a written request must be filed with the Manager of Technical and Professional Publications, ASCE. Manuscript was submitted for review for possible publication on March 19, 1980. This paper is part of the Journal of the Structural Division, Proceedings of the American Society of Civil Engineers, ©ASCE, Vol. 107, No. ST6, June, 1981. ISSN 0044-8001/81/0006-1083/$01.00.

3. A superstructure, or deck section, is set on top to complete the structure. It carries the functional loads for which the structure was built, keeping men and equipment out of reach of wave action.

In addition to drilling structures, fixed offshore platforms have been built for light stations, oceanographic research, undersea testing, electronic surveillance, powerplants, sulphur mining, pipeline pump and compressor stations, supertanker terminals, human accommodation, and even pirate broadcasting.

In recent years, the technology has been refined and extended to include problems of dynamic amplification, fatigue, and sea floor instability, as well as earthquake and oceanographic loadings of unprecedented severity. One-, two-, and three-piece fixed platforms having 59,000 ton (54,000,000 kg) of steel have been built in up to 1,020 ft (306 m) of water. Construction equipment has kept pace with launch barges capable of handling 30,000-ton (27,000,000-kg) jackets, semisubmersible crane barges of 2,500-t (2,300,000-kg) lifting capacity, and pile-driving hammers rated at 600,000 ft-lb (800,000 J)—all roughly 10 times larger than what was available in the mid-1960s.

However, this paper will simply outline the basic technology, to provide one designer's perspective from which these recent developments can be appreciated. This present state of practice is codified in API RP 2A (2). The outline cites 197 landmark papers from among the over 2,600 that appear in the *Preprints/Proceedings of the Offshore Technology Conference*, which has been held annually since 1969. For brevity, these papers will be referenced herein by OTC number. Other good "starting point" references are Chryssostomidis (3) and McClelland, et al. (4).

Loading

I. Criteria Selection
  A. Operational Loads
    1. Drilling equipment (API, Ref. 5)
    2. Production modules (Koehler, OTC 2445)
    3. Supplies, fluids, people
    4. Crane and derrick hoisting loads
  B. Environmental Loads (Wiegel, Ref. 6)
    1. Data gathering (Aagard, OTC 1829)
      a. Operating conditions (Glenn, Ref. 7)
      b. Extreme conditions (e.g., Glenn, Ref. 8; Patterson, OTC 2109)
      c. Coastal data (Thompson, OTC 1963)
      d. Gulf of Mexico Deepwater Ocean Data Gathering Program—ODGP (Ward, OTC 2108 A and B)
      e. Other areas (Jonswop, OTC 1516; Draper, Ref. 9)
    2. Wind speeds
      a. Extreme winds from Weather Bureau statistics (Thom, Ref. 10)
      b. Windfield models for specified hurricanes (Collins, OTC 1346)
    3. Wave heights
      a. Standard Project Hurricane, 100-yr storm, and other recurrence intervals (Glenn, Ref. 11; Refs. 12 and 13; Bretschneider, Refs. 14 and 15)

b. Numerical storm hindcasts, calibrated on observations (Wilson, Ref. 16; Patterson, OTC 1345; Evans, OTC 1692; Cardone, OTC 2332)
c. Statistical summaries based on hindcasts (Besse and Leblanc, Ref. 17; Bea, OTC 2110; Ward, Borgman, and Cardone, OTC 3229; Ward, OTC 2846)
d. Statistical extrapolations (Thom, Ref. 18; Quayle and Fullbright, Ref. 19)
e. Wave spectra (Michel, Ref. 20; Robinson, Brannon, and Kattawar, Ref. 21; Borgman, OTC 1069; St. Denis, OTC 1819)

4. Tides and currents (Bretschneider, Ref. 22; Hall, OTC 1518; Forristall, OTC 3227; also Refs. 6 and 16)
5. Ice (Peyton, Ref. 23; Goepfert, OTC 1048; Blenkarn, OTC 1265)
6. Earthquakes (Weigel, Ref. 24; Page, OTC 2355; Wiggins, OTC 2669 and 3113; Bea, OTC 2675)
7. Marine fouling
8. Submarine mudslides (Sterling, OTC 1898; Bea, OTC 1899 & 2110; Arnold, OTC 1900; Doyle, OTC 1901; also OTC 2188, 2425, 2426, 2427, 2733, 3257, etc.)

C. Cost/Risk Optimization (Borgman, Ref. 25; Marshall, Ref. 26; Freudenthal and Gaither, OTC 1058; Bea, OTC 1839; Cornell, OTC 2350; Fjeld, OTC 3027; Moses, OTC 3046)

II. Force Computation and Application

A. Hydrodynamic Forces (Reid and Bretschneider, Ref. 27)
1. Nonlinear deterministic wave and current
a. Wave theories and water particle kinematics (Airy and Stokes, see Ref. 6; Chapellear, see Ref. 28; Dean, OTC 1613)
b. Direct measurement of kinematics (Forristall, OTC 3227; Ohmart, OTC 3276)
c. C_D and C_M coefficients in Morison's equation (Morison, et al., Ref. 29; Weigel, Beebe, and Moon, Ref. 30)
d. Flume measurements of C_D (Blumberg and Rigg, Ref. 31; Sarpkaya, OTC 2533)
e. Joint calibration of wave theory and coefficients from full scale measurements (Bretschneider, Ref. 32; Kobus, Refs. 33–35; Evans, OTC 1005; Wheeler, OTC 1006; Aagard, OTC 1007 and 1008)

2. Linearized spectral treatment of waves (Borgman, Ref. 36; Nath and Harleman, Ref. 37)
3. Vortices and flutter (King, OTC 1948; Sarpkaya, OTC 3647)
4. Slamming (OTC 2498, 2500, 2741, 3065)

B. Wind (ASCE, Ref. 38; Nath, OTC 1068)

C. Earthquake
1. Code-type force approach (Clough, see Ref. 39; Sharpe, OTC 2747)
2. Hydrodynamic added mass
3. Elastic dynamic analysis for strength level response spectrum (Clough, see Ref. 24; Bea, et al., Ref. 40)
4. Ductility level for survival under large displacements (see subsequent section on inelastic analysis)

5. Survivability of equipment and facilities (Sharpe, OTC 2750)

III. Installation Forces
- A. Loadout
- B. Transport
  1. Acceleration forces due to barge motion
  2. Tiedowns
- C. Launch
  1. Launchway and rocker beam reactions
  2. Hydrodynamic forces
- D. Upending
- E. Lifting

Analysis

I. Global Space Frame Analysis
- A. Integrated Computer Systems (Bea, Ref. 41; Meith and Gooch, Ref. 42; Keith and Feibusch, OTC 1054; Synercom, OTC 1662; Bainbridge, OTC 2410)
- B. Size Considerations for Over 14,000 Degrees of Freedom; substructuring
- C. Integration with Nonlinear Foundation (Matlock, OTC 1699 and 2955; Boston, OTC 2262)
  1. Spring-intercept method
  2. Substructure iteration
  3. Combined modelling
  4. Approximations

II. Quasistatic Analysis For Design Load Cases
- A. Operational Loads
- B. Peak Environmental Loads
  1. Wave position and direction
  2. Inclusion of wind and current
- C. Combinations

III. Dynamic Analysis (Clough, Ref. 43)
- A. Quasistatic Plus First-Order Inertial Effects (Maddox, OTC 2051)
- B. Reduced Degrees of Freedom
  1. Modal reduction (Clough, Ref. 43)
  2. Guyan reduction
  3. Stick models and lumped property models (Brannon, OTC 2120)
  4. Limitations and potential errors (Vugts, et al., Ref. 44)
- C. Response to Irregular Seas
  1. Linearized spectral (Penzein, OTC 2050; Marshall, OTC 2537; also Nath and Harleman, Ref. 37)
  2. Hydrodynamic nonlinearities retained (Burke OTC 1403)
- D. Nonlinear Analysis for Earthquake Overload of Soil-Pile-Structure Systems (Arnold, et al., OTC 2749; Gates, OTC 2751 and 2908; Berger and Pyke, OTC 2954; Penzein, OTC 2352; Hasselman, OTC 2353; Kallaby, OTC 2357 and 2748)

IV. Local Scale Analysis of Tubular Connections
- A. Finite Element Method

1. Thin shell (Greste, Ref. 45; Greimann, OTC 1823; Maison, OTC 2102; Visser, OTC 2117)
2. Isoparametric modelling of actual weld geometry (Reimer, OTC 2642)

B. Shell Theory (Dundrova, Ref. 46)
C. Experimental (Bouwkamp, Ref. 47; Toprac, Refs. 48 and 49; Grigory, Ref. 50; Holliday, OTC 1441; Graff, OTC 1669; Wordsworth and Smedley, Ref. 51)
D. Empirical (Marshall, Ref. 52; Kuang, OTC 2205)

V. Fatigue Analysis (Maddox, OTC 2261; Hansford, OTC 2606; Kinra, OTC 2608 and 3378; also OTC 2410 and 2537)
A. Wave Climate
B. Levels of Analysis
1. Global (nominal stress)
2. Local (hot spot stress)
3. Microscopic (built into S-N curve)
C. Cycle count bookkeeping
1. Deterministic
2. Spectral
D. Cumulative Damage Rule

Design

I. Conventional Steel Shapes (AISC, Ref. 53)
II. Tubular Members (AISI, Ref. 54, CRC, Ref. 55)
A. Local Buckling (Ostapenko, OTC 3086)
B. Biaxial Bending (Resultant Moment)
C. Axially Loaded Columns (Galambos, OTC 2203; Chen, OTC 2683)
D. Beam-Columns (Erzurumlu, OTC 1668 and 2684; Sherman and Erzurumlu, Ref. 56; Matlock, OTC 2953; Knapp, OTC 1663)
E. Hydrostatic Collapse (Johns, OTC 2209; Kinra, OTC 2689)
F. Inelastic Behavior (Bouwkamp, OTC 2204; Sherman, OTC 2119; Marshall, Ref. 57)
III. Tubular Joints—Static Strength
A. Simple Joints
1. Punching shear (Marshall, Refs. 58 and 59)
2. Limit load format (Reber, OTC 1664; Pan, OTC 2644)
B. Complex Joints (Marshall and Graff, Ref. 60)
IV. Fatigue of Tubular Connections
A. Classification of Details (AWS, Ref. 61; Gurney, OTC 1907; Munse, OTC 3300)
B. Experimental Results (Toprac, OTC 1062; Holliday, OTC 2208; Bouwkamp, OTC 2605; Martin, OTC 2856; UKOSRP, Ref. 62)
C. Hot Spot Stress Range, Basis for *S-N* Curve X (Marshall, Ref. 63; Rodabaugh, Ref. 64)
D. Allowable Stress for Use with Design Load Case (Derived from Prior Generic Analyses)
V. Failure Modes and Risk Evaluation
A. Reserve Strength for Wave Loads (Marshall and Bea, Ref. 65, Stahl, Ref. 66)

B. Dynamic Loads (Marshall, Ref. 67)
   1. Inelastic deformation in earthquakes
   2. Progressive deterioration in fatigue
C. Role of Redundancy (Marshall, Ref. 68)

Materials Technology

I. General Selection Strategies—Yield Strength Levels in Relation to Fracture Control and Design Criteria (Marshall, OTC 1043; Peterson, OTC 1075)
II. Fracture Toughness (Rolfe and Barsom, OTC 1044; Harrison, OTC 1909; von Rosenberg, OTC 1953; also Ref. 62)
III. Fatigue of Welded Components in Sea Water
   A. *S-N* Behavior (Havens, OTC 1045; Casad, OTC 1254; Kochera, OTC 2604; Hartt, OTC 2380 and 3511; also Refs. 47 and 62)
   B. Crack Propagation (Bristoll, in Ref. 62; Jaske, Refs. 69 & 70; Becker, OTC 1228, Plummer, OTC 2465; Dover, OTC 2853; Bardal, OTC 2855)
IV. Corrosion Protection (OTC 1038, 1042, 1049, 1047)
   A. Paint (OTC 1582)
   B. Other Coatings, e.g., Metallic Wrap (OTC 1960)
   C. Cathodic Protection (OTC 1039, 1040, 1271, 1273, 1957, 2700, 2702, etc.)
V. Lamellar Tearing (Arita, OTC 1619; Wold, OTC 1915)
VI. Weldability (Bennett, OTC 1230; Dolby, OTC 1908; also Ref. 61)

Foundation Design

I. Overview (Focht and Kraft, Ref. 71)
II. Site Exploration (Fugro, OTC 2246)
   A. Geological Setting (Bernard and LeBlanc, Ref. 72; McClelland, Ref. 73)
   B. Geophysical (King, OTC 1802)
   C. Borehole and Wireline Sampler (Perkins, Ref. 74)
   D. In-situ Vane and Cone Tests (OTC 2626 and 2787)
   E. Laboratory Tests and Interpretation (Focht, Ref. 75)
III. Loading on Piles
   A. Axial Loads and Lateral Loads (shears) from Base Reaction of Structure
   B. Deformation-induced Loads Due to Mudslides and Earthquakes
IV. Analysis
   A. Laterally Loaded Piles
      1. Discrete element model (Focht and McClelland, Ref. 76; Matlock and Reese, Ref. 77)
      2. Nonlinear soil support algorithms (*P-Y* curves)
         a. Soft clay—static and cyclic (Matlock, OTC 1204)
         b. Stiff clay (Reese and Cox, OTC 2312)
         c. Sand (Reese and Cox, OTC 2079 and 2080)
      3. Pile groups (Matlock, Ref. 78; Poulos, Ref. 79)
   B. Axially Loaded Piles (Matlock, OTC 2186)

V. Design of Piling
  A. Steel Stress (0.8 F_y)
    1. Axial from above
    2. Bending from laterally loaded pile analysis
    3. P-Δ effect
    4. Effect of overloads
  B. Ultimate Bearing and Pullout Capacity
    1. Traditional approach (McClelland, Refs. 80 and 81; Focht, Ref. 82)
      a. Soft clay (Seed and Reese, Ref. 83)
      b. Stiff clay and sand (Reese and Cox, OTC 2472 and 2473; McClelland, Ref. 84)
    2. Alpha and lambda methods (Fox, OTC 1200; Vijayvergiya, OTC 1718)
    3. Effective stress method, critical state soil mechanics (Bea and Doyle, OTC 2037; Vijayvergiya, OTC 2939; Esrig, OTC 2943 and 3406; Kraft, OTC 3307)
    4. Grouted piles
      a. In soil (Krafft, OTC 2081)
      b. Connection to structure (Billington, OTC 3083; Halliburton, OTC 3671)
    5. Pile groups (McClelland, Ref. 85)
  C. Driveability (Lowry, OTC 1055 and 1202; McClelland, OTC 1600; Audibert, OTC 3273)
VI. Other Considerations
  A. Dynamic and Cyclic Effects (Idriss, OTC 2355 and 2671; Sangrey, OTC 2944)
  B. Mud Mats
  C. Skirt Plates
  D. Scour
  E. Debris

Construction Techniques

I. Fabrication and Welding
  A. Shop Drawings and Mold Loft
  B. Pipe Mill
  C. Brace and Piling Racks
  D. Prefabrication
    1. Nodes
    2. Bents
  E. Jacket Assembly
  F. Deck Fabrication
II. Loadout
III. Transport
  A. Barge
  B. Self-Floating
IV. Launch at Sea
V. Upending and Setting on Bottom

A. Analysis (Metcalf, OTC 2035)
B. Model Tests (Tam, OTC 1406)
VI. Derrick Barges (OTC 1283, 2399, 2635)
VII. Pile Driving
A. Conventional Hammers
B. Underwater Hammer (OTC 2477, 2478)
VIII. Deck Installation
IX. Modules
A. Lifting
B. Hook-up
X. Rehabilitation and Repairs
A. Grouting (Halliburton, OTC 1137)
B. Bolting (Hull, OTC 2165)
C. Underwater Welding (Grubbs, OTC 1620; Masbouchi, OTC 1621; Ekofisk, OTC 2707; Delaune, OTC 3348)
XI. Salvage and Removal (McDonald, OTC 1135; Brown, OTC 1623; Gulf, Ref. 86)

Testing

I. Testing for Design Verification
A. Strength and Fatigue Tests of Tubular Joints
B. Tank Tests of Installation Procedures
C. Pile Tests for Special Situations
II. Quality Control during Construction (Ref. 61)
A. Duties of Inspector
B. Welder and Procedure Qualification
C. Visual Inspection
D. Nondestructive Testing
1. Radiographic
2. Ultrasonic (API, Ref. 87)
III. Monitoring and Inspection of Completed Structure (Ref. 68)
A. Timing
1. Baseline
2. Periodic or event-related
B. Methods
1. In-situ (Hughes, OTC 1565 and 2378; Fjeld, OTC 2980; Ekofisk, OTC 2982; Edwards, OTC 3385)
a. Divers, RCV's
b. Visual, photo, video
c. Cleaning
2. Dynamic signature (Vanmarke, OTC 1407; Mandery, OTC 1840; Vandiver, OTC 2267; Dodds, OTC 2549 and 2551; Ruhl, OTC 2553 and 3514; Hong, OTC 2555; Wojnarowski, OTC 2909)
3. Other methods under development
a. Acoustic emissions (OTC 2851, 2866)
b. Acoustical holography (Battelle, OTC 1096; Holosonics, OTC 3332)
c. Ultrasonics (Magnaflux, see Ref. 88; Sylvestor, OTC 3467)

C. Results—Types of Damage Found
   1. Major
      a. Parted, buckled and missing members
      b. Large cracks at tubular joints
      c. Severe general corrosion
      d. Accelerated corrosion of weld or heat-affected zones
   2. Minor
      a. Dents, punctures, abrasions
      b. Lesser cracks and corrosion
   3. False alarms
      a. Built-in discontinuities
      b. Nonfailure changes, e.g., marine growth

D. Consequences
   1. Cost/risk evaluation of repair or abandonment
   2. Role of redundancy and alternative safety measures

E. Feedback to Design Process

Appendix.—References

1. Lee, G. C., "Twenty Years of Platform Development," *Offshore*, June 5, 1968.
2. *Recommended Practice for Planning, Designing, and Constructing Fixed Offshore Platforms, API RP 2A*, American Petroleum Institute, 1st ed., 1969, 10th ed., 1979.
3. Chryssostomidis, M., *Offshore Petroleum Engineering*, A Bibliographic Guide to Publications and Information Sources, *Massachusetts Institute of Technology Sea Grant Report MIT-5G-78-5*, 1978.
4. *Fixed Offshore Structures*, B. McClelland, ed., Van Nostrand—Reinhold Co., New York, N.Y., (textbook in preparation).
5. *Drilling Rig Packaging for Minimum Self-Contained Platforms, API Spec. 2E*, American Petroleum Institute, 1973.
6. Weigel, R. L., *Oceanographic Engineering*, Prentice-Hall, Inc., Englewood Cliffs, N.J., 1964.
7. Glenn, A. H., "Oceanographic Factors Affecting Offshore Petroleum Operations," 1960.
8. Glenn, A. H., "Meteorological and Oceanographic Conditions During Hurricane Audrey," 1957.
9. Draper, L., *A Catalogue of Wave Data From the North Sea, NIO Report A57*, National Institute of Oceanography, 1971.
10. Thom, H. C. S., "New Distribution of Extreme Winds in the United States," *Journal of the Structural Division*, ASCE, Vol. 94, No. ST7, Proc. Paper 6038, July, 1968, p. 1787.
11. Glenn, A. H., "Wave Characteristics and Frequencies on the Texas-Louisiana Coast," 1958.
12. "Shore Protection, Planning, and Design," *Technical Report No. 4*, 3rd ed., U.S. Army Coastal Engineering Research Center, 1956.
13. Graham, H. E., and Nunn, D. E., "Meterological Considerations Pertinent to Standard Project Hurricane, Atlantic and Gulf Coast of the U.S.," *U.S. National Hurricane Research Project Report No. 33*, Weather Bureau, Washington, D.C., 1959.
14. Bretschneider, C. L., "Hurricane Design Wave Practices," *Journal of the Waterways and Harbors Division*, ASCE, Vol. 83, No. WW2, Proc. Paper 1238, May, 1957, pp. 1238-1–1238-33.
15. Bretschneider, C. L., "Selection of Design Wave for Offshore Structures," *Journal of the Waterways and Harbors Division*, ASCE, Vol. 84, No. WW2, Proc. Paper 1568, Mar., 1958, pp. 1568-1–1568-37.
16. Wilson, B. W., "Design Sea and Wind Conditions for Offshore Structures," presented

at the 1966, Offshore Exploration Conference OECON I.
17. Besse, C. P., and leBlanc, N. F., "An Application of Oceanographic Data in Offshore Structural Design," *Journal of Petroleum Technology*, Sept., 1967.
18. Thom, H. C. S., "Extreme Wave Height Distributions Over Oceans," *Journal of the Waterways and Harbors Division*, ASCE, Vol. 99, No. WW3, Proc. Paper 9939, Aug., 1973, pp. 355–374.
19. Quayle, R. G., and Fullbright, D. L., "Extreme Wind and Wave Periods for the U.S. Coast," *Mariners Weather Log*, Mar., 1975.
20. Michel, W. H., "Sea Spectra Simplified," presented to SNAME Gulf Section, Apr., 1967.
21. Robinson, R. G., Brannon, H. R., and Kattawar, G. W., "Storm Wave Characteristics," *SPE Journal*, Mar., 1967.
22. Bretschneider, C. L., "Estimating Wind-Driven Currents Over the Continental Shelf," *Ocean Industry*, June, 1967.
23. Peyton, H. R., "Ice and Marine Structures," *Ocean Industry*, Mar., Sept., Dec., 1968.
24. *Earthquake Engineering*, R. L. Wiegel, ed., Prentice-Hall, Inc., Englewood Cliffs, N.J., 1970.
25. Borgman, L. E., "Risk Criteria," *Journal of the Waterways and Harbors Division*, ASCE, Vol. 89, No. WW3, Proc. Paper 3607, Aug., 1963, p. 1.
26. Marshall, P. W., "Risk Factors for Offshore Structures," *Civil Engineering in the Oceans*, ASCE, Sept., 1967.
27. Reid, R. O., and Bretschneider, C. L., "Surface Waves and Offshore Structures: The Design Wave in Deep or Shallow Water, Storm Tide, and Forces on Vertical Piles and Large Submerged Objects," Texas A&M Research Foundation, College Station, Tex., Oct., 1953.
28. Borgman, L. E., and Kobus, L. C. S., "Fluid Flow Properties of Ocean Waves," *Shell EPR Report 554*, Dec., 1959–Jul., 1960 (4 vols.).
29. Morison, J. R., O'Brien, M. D., Johnson, J. W., and Schaaf, S. A., "The Force Exerted by Surface Waves on Piles," *Petroleum Transactions*, American Institute of Mechanical Engineers, 1950.
30. Weigel, R. L., Beebe, K. E., and Moon, J., "Ocean Wave Forces on Circular Cylindrical Piles," *Journal of the Hydraulics Division*, ASCE, Vol. 83, No. HY2, Proc. Paper 1199, Apr., 1957, pp. 1199-1–1199-36.
31. Blumberg, R., and Rigg, A. M., Hydrodynamic Drag at Supercritical Reynolds Numbers," ASME, June, 1961.
32. Bretschneider, C. L., "Evaluation of Drag and Inertial Coefficients From Maximum Total Range of Wave Force," *Texas A&M Report 55-5*, Texas A&M Univ., College Station, Tex., May, 1957.
33. Kobus, L. C. S., "Summary Review of Wave Force Project I, Bay Marchand, Louisiana, 1954–58," *Shell EPR Memo Report 100*.
34. Kobus, L. C. S., "Analysis of Ocean Wave Properties, 30-Foot Water Depth Test," *Shell EPR Report 657*, Feb., 1962 (summarized in OTC 1005).
35. Kobus, L. C. S., "Analysis of Ocean Wave Properties, 100-Foot Water Depth Test," *Shell EPR Report 837*, Dec., 1964 (summarized in OTC 1005).
36. Borgman, L. E., "The Spectral Density of Ocean Wave Forces," *Coastal Engineering*, ASCE, Oct., 1965.
37. Nath, J. H., and Harleman, D. R. F., "The Dynamic Response of Fixed Offshore Structures to Periodic and Random Waves," *MIT Hydro Lab Report 102*, Massachusetts Institute of Technology, Cambridge, Mass.
38. "Wind Forces on Structures," Final Report of the Task Committee, ASCE *Transactions Paper No. 3269*, American Society of Civil Engineers, 1961.
39. "Seismic Design Wrong, But Right," *Engineering News-Record*, May 6, 1965, p. 22.
40. Bea, R. G., et al., "Earthquake Response of Offshore Platforms," *Journal of the Structural Division*, ASCE, Vol. 105, No. ST2, Proc. Paper 14386, Feb., 1979, p. 377.
41. Bea, R. G., "The Use of Digital Computers in Offshore Structure Analysis and Design," *Paper No. SPE 1413*, AIME Symposium on Offshore Technology and Operations, May, 1966.
42. Meith, R. M., and Gooch, A. B., "Computer-Analysis of Offshore Drilling Platforms,"

Paper No. SPE 1414, AIME Symposium on Offshore Technology and Operations, May, 1966.
43. Clough, R. W., "Deterministic Dynamic Structural Analysis," state-of-the-art paper presented at the Structural Engineering Conference, Aug., 1976.
44. Vugts, J. H., et al., "Modal Superposition versus Direct Solution Techniques in Dynamic Analysis," *Proceedings*, BOSS'79, London, Aug., 1979.
45. Greste, O., "Finite Element Analysis of Tubular K-Joints," *Report UC-SESM-70-11*, Univ. of California, Berkeley, Calif., June, 1970.
46. Dundrova, *Stresses at Intersection of Tubes: Cross and Tee Joints, SFRL Report P550-3*, Univ. of Texas, Austin, Tex., 1966.
47. Bouwkamp, J. G., "Tubular Joints Under Static and Alternating Loads," *University of California Structures and Materials Research Reports 66-15, 67-29, and 70-4*, Univ. of California, Berkeley, Calif., 1966–1970.
48. Toprac A. A., and Johnston, L. P., "Welded Tubular Connections: An Investigation of Stresses in T-Joints," *Welding Journal*, Jan., 1966.
49. Toprac, A. A., et al., "Analysis of In-Plane *T*, *Y*, and *K* Welded Tubular Connections," *WRC Bulletin 125*, 1968.
50. Grigory, S. G., "A Study to Develop a Design Procedure for the Analysis of Plastic Fatigue Life of Tubular Joints on Offshore Structures," Southwest Research Institute, 1970.
51. Wordsworth, A. C., and Smedley, G. P., "Stress Concentrations at Unstiffened Tubular Joints," Nov., 1978 (in Ref. 62).
52. Marshall, P. W., "A Review of Stress Concentration Factors in Tubular Connections," *Shell CE-32 Report*, Apr., 1978.
53. *Manual of Steel Construction*, AISC, 1970.
54. D. R. Sherman, "Tentative Criteria for Structural Applications of Steel Tubing and Pipe," AISI Committee of Steel Pipe Producers, Aug., 1976.
55. "Circular Tubes and Shells," *Guide to Stability Design Criteria for Metal Structures, CRC TG 18*, Structural Stability Research Council (formerly CRC), 1976.
56. Sherman, D. R., and Erzurumlu, H., "Ultimate Capacity of Tubular Beam Columns," presented at the Aug., 1976, ASCE National Structural Engineering Conference.
57. "Inelastic Behavior of Tubular Members and Structures," P. W. Marshall, ed., *ASCE Combined Preprint 3302*, American Society of Civil Engineers, Oct., 1978.
58. Marshall, P. W., and Toprac, A. A., "Basis for Tubular Joint Design," *Welding Journal*, May, 1974.
59. Marshall, P. W., "A Review of American Criteria for Tubular Structures—And Proposed Revisions," *IIW Doc. XV-405-77*.
60. Marshall, P. W., and Graff, W. J., "Limit State Design of Tubular Connections," *Proceedings*, BOSS '76, Trondheim, Aug., 1976.
61. AWS *Structural Welding Code* D1.1.
62. UKOSRP, *European Offshore Steels Research*, Preprints of the Select Seminar, Cambridge, England, Nov., 1978.
63. Marshall, P. W., "Basic Considerations for Tubular Joint Design in Offshore Construction," *WRC Bulletin 193*, Apr., 1974.
64. Rodabaugh, E. C., "Review of Data Relevant to the Design of Tubular Joints for Use in Fixed Offshore Structures," *Battelle Draft Report for WRC*, Jan., 1978.
65. Marshall, P. W., and Bea, R. G., "Failure Modes for Offshore Platforms," *Probabilistic Methods in Engineering*, American Society of Civil Engineers, Stanford, Calif., June, 1974 (also *Proceedings*, BOSS '76, Vol. II).
66. Stahl, B., "Probabilistic Methods for Offshore Platforms," *API Paper No. 364-J*, Dallas, Tex., Apr., 1975.
67. Marshall, P. W., "Failure Modes for Offshore Platforms—Part II—Dynamic Loads," *Methods of Structural Analysis*, ASCE, Madison, Wisc., Aug., 1976 (also *Proceedings*, BOSS '76, Vol. II).
68. Marshall, P. W., "Strategy for Monitoring, Inspection and Repair for Fixed Offshore Structures," *Proceedings*, BOSS '79, London, England, Aug., 1979.
69. Jaske, C. E., et al., "Interpretive Report on Corrosion Fatigue of Welded Carbon Steel for Application to Offshore Structures," Battelle report to API, Feb., 1977 (see also paper presented to ASTM Symposium on Corrosion Fatigue, Denver, Colo., Nov., 1976).

70. Jaske, C. E., et al., "Final Report on Corrosion Fatigue of Cathodically Protected, Welded Carbon Steel in Cold Seawater," Battelle report to API, Feb., 1977.
71. Focht, J. A., and Kraft, L. M., "Progress With Marine Geotechnical Engineering Problems," presented at the 1976, ASCE Bicentennial Convention, held at Philadelphia, Pa.
72. Bernard, M. A., and LeBlanc, R. J., "Resumé of Quarternary Geology of the Northwestern Gulf of Mexico Province," *Shell EPR Publication 400*, Mar., 1965.
73. McClelland, B., "The Progress of Consolidation in Delta Front and Prodelta Clays of the Mississippi River," presented at Research Conference on Marine Geotechnique, Univ. of Illinois, Urbana, Ill., May, 1966.
74. Perkins, R. L., "Soil Boring Equipment and Techniques," *Ocean Engineering*, Vol. II, Shell Development Co. Technical Training Series, 1967.
75. Focht, J. A., "Interpretation of Boring and Test Results," *Ocean Engineering*, Vol. II, Shell Development Co. Technical Training Series, 1967.
76. Focht, J. A., and McClelland, B., "Analysis of Laterally Loaded Piles by Difference Equation Solution," *Texas Engineer*, Sept.-Oct.-Nov., 1955.
77. Matlock, H., and Reese, L. C., "Generalized Solutions for Laterally Loaded Piles," *Transactions*, ASCE, Paper 3370, 1962.
78. Matlock, H., "Lateral Load Behavior of a Pile Group in Clay Soil," report to Shell, 1965.
79. Poulos, H. G., "Behavior of Laterally Loaded Piles—II—Pile Groups," *Journal of the Surveying and Mapping Division*, ASCE, Vol. 97, No. SM5, Proc. Paper 8093, May, 1971, p. 733.
80. McClelland Engineers, "Appendix C," found in their Soil and Foundation Reports since 1963, revised 1967.
81. McClelland, B., Focht, J. A., and Emrich, W. J., "Problems in Design and Installation of Heavily Loaded Pipe Piles," *Civil Engineering in the Oceans*, ASCE, San Francisco, Calif., Sept., 1967.
82. Focht, J. A., "Analysis of Axial Loads on Piles," *Civil Engineering*, Vol. I, Shell Development Co. Technical Training Series, 1969.
83. Seed, H. B., and Reese, L. C., "The Action of Soft Clay Along Friction Piles," *Transactions*, ASCE, Paper No. 2882, 1956.
84. McClelland Engineers, "Pull-Out Tests of Piles Driven into Sand, Padre Island, Tex.," report to Shell, 1958.
85. McClelland Engineers, "Pile Loading Tests, Single Piles and Circular Groups, Venice and Harvey, Louisiana," report to Shell, 1966.
86. Jeffus, D. M., and Stoner, O. E., "Abandonment and Salvage of Deep Water Wells and Structures," SPE 1569, Dallas, Tex., Oct., 1966.
87. "Recommended Practice for Ultrasonic Examination of Offshore Structural Fabrication and Guidelines for Qualification of Ultrasonic Technicians," *API RP 2X*, American Petroleum Institute, June, 1978, revised June, 1979.
88. Turner, R. P., "Weld Testing—Offshore Structures," *ASME Preprint 66-PET-30*, New Orleans, La., Sept., 1966, with discussions by R. C. Anderson and C. A. Tannehill.

DELPHI METHODS: THEORY AND DESIGN LOAD APPLICATION

By Ross B. Corotis,[1] M. ASCE, Raymond R. Fox,[2] F. ASCE, and John C. Harris[3]

INTRODUCTION

The selection of design loads for codes and standards involves data collection and reduction, fitting of physical and empirical models, and a high degree of engineering judgement. The Delphi method is a formalized procedure for combining responses from professional sources. It differs from a Bayesian approach in that subjective opinion and objective data are incorporated by individuals outside of the formal Delphi. The characteristics, basic philosophy, and historical development of the Delphi method are presented in this paper, along with general guidelines for applications in structural engineering. This is followed by a description of the actual use of the Delphi method for updating the (unreduced) uniformly distributed live loads specified in the American National Standard A58 "Building Code Requirements for Minimum Design Loads in Buildings and Other Structures" (2).

DELPHI METHOD

Characteristics.—The Delphi Method is a highly structured form of communication that can be used by a panel of experts to enable a consensus to be reached. The actual procedure of applying the steps of the Delphi method is commonly termed as Delphi.

The Delphi method has four major characteristics. These characteristics have been varied in their execution, but they remain essentially basic to all applications. The first of these is anonymity of response: the experts taking part in a Delphi are not informed of the source of individual responses and often are not told the identity of the other experts taking part in the Delphi. A controlled feedback

[1]Prof. of Civ. Engrg., The Technological Inst., Northwestern Univ., Evanston, Ill. 60201.

[2]Prof. of Civ. Engrg., George Washington Univ., Washington, D.C.; also Assoc., Dames and Moore, Washington, D.C.

[3]Structural Analyst, United Computing Systems, Inc., Chicago, Ill.

Note.—Discussion open until November 1, 1981. To extend the closing date one month, a written request must be filed with the Manager of Technical and Professional Publications, ASCE. Manuscript was submitted for review for possible publication on August 27, 1980. This paper is part of the Journal of the Structural Division, Proceedings of the American Society of Civil Engineers, ©ASCE, Vol. 107, No. ST6, June, 1981. ISSN 0044-8001/81/0006-1095/$01.00.

of these responses is the second characteristic of the Delphi method. This feedback may include individual responses or questions, depending on the design of the Delphi, but it almost always includes the third characteristic, which is a statistical description of the group response. This is usually the mean response plus some indication of the range of responses. The fourth characteristic is the use of multiple iterations of questions and feedback to reach a consensus. This consensus does not necessarily imply total agreement among the experts on the actual answer or answers, but rather an agreement on the uncertainty of the answer (1).

Basic Philosophy.—A scientific investigation is termed Lockean if its basic premise is that the empirical content of data completely determines the validity of the system (15). Research into the statistical nature of loads is basically Lockean, with the greatest importance assigned to the data itself and the concept that any model can only be justified by data. This Lockean philosophy that the data are separate and prior to any formal theory is true of empirical science in general, and is especially true of fields that employ a statistical treatment of data.

A philosophy in basic contrast to Lockean is Leibnizian, in which the formal analytic theory is of first importance. Such systems are often expressed in mathematical or symbolic form, and it is assumed that general theories cannot be derived from finite data sources. Probabilistic load models have a strong Leibnizian subcurrent because of the theoretical development of probability models. Although the models are represented in formal mathematical terms, the actual choice of a model is dependent on the data. Many times models are hypothesized before the collection of the data in order to help plan the experiment, but they are often based on prior data or an intuitive knowledge of what the data will be, and the model itself ultimately depends on the data collected.

The Delphi method is a procedure for collecting data that is almost a pure example of a method based on the Lockean philosophy. As stated previously, basic to the Lockean philosophy is the lack of any formal analytical truths or theory. The truth in a Lockean model is based entirely on the empirical data. Since only a finite amount of data can ever be collected, there is an implicit uncertainty in what is said to be the truth. Because of this uncertainty, a researcher must exercise a degree of subjective judgement in transforming basic data into a final statement. This judgement in a Lockean system is based entirely on the data, and the uncertainty in this result can be expressed as a function of the data. In the Leibnizian philosophy any result must arise from formal elementary truths, and there can be no uncertainty in the results.

Studies of structural loads are typical of most Lockean systems in that they have formalized methods of data collection and less formal methods of reaching conclusions. The Delphi method reverses the role of structuring for these two activities. In conducting a Delphi, a set of questions are posed to the panel of experts.

One of the most important areas in the design of the Delphi is the selection of the panel of experts. An expert is defined for this process as a person with a high degree of knowledge in the particular area, which may be attained through organized research, field experience, or other means. Care must be exercised in the selection of the panel to avoid bias caused by inbreeding and

to gain access to as large a volume of information as possible. If the panel is too diverse it may be necessary to place experts into subgroups and weight the response of each subgroup according to its expertise on the particular question. The wording of the actual questions is an area that also can have a great effect on the outcome of the Delphi. In addition to wording a question to not suggest an answer, ambiguity must be avoided. It has been found that respondents regularly answer ambiguous questions with a high degree of confidence according to their own interpretation (19). The concept of using a statistical measure of the group response to produce more reliable answers has obvious advantages (4). Fig. 1 shows two cases. Fig. 1(*a*) might be considered a worst possible type of situation, in which the true answer is at the extreme of the distribution of the responses. The median response then is at least as close to the true answer as half of the responses. A more realistic case is shown in Fig. 1(*b*), in which the true answer is not an extreme, and the median is closer to the true answer than a majority of the individual responses.

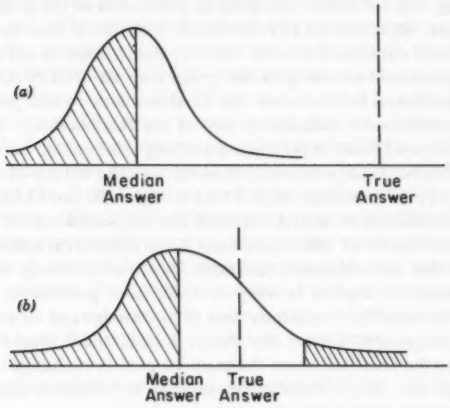

FIG. 1.—Examples of Delphi Responses: (*a*) Worst Possible Case; (*b*) Realistic Case

Anonymity of response is included in the basic characteristics of the Delphi method to try to reduce the negative psychological aspects of traditional decision making groups such as committees, panels, juries, etc. Some of these negative factors are: Specious persuasion; unwillingness to abandon a publicly expressed opinion; bandwagon effect of majority opinion; unwillingness to contradict a respected peer; and hastily formed opinions. By keeping the source of individual responses confidential, many of these undesirable factors are eliminated. If each respondent is safe within his own anonymity, pressures to protect a reputation or a position within the profession are reduced or even eliminated.

The field of social psychology supports the idea of anonymity of response, which basically reduces affective conflict (conflict of personalities) while still maintaining substantive conflict (conflict among ideas) (12). The result of this anonymity is that normative needs, which are related to the desire to reach

a group goal or to support personal feelings, are de-emphasized. This leaves cognitive needs, which relate to the desire to validate opinions or find correct information, in a dominant position.

The sequential questioning with controlled feedback between rounds is consistent with the Lockean philosophy of achieving convergence to a group consensus. While groups in affective conflict do converge, they do this by withdrawing from areas of high conflict, which does not necessarily improve the accuracy of the result. Since the Delphi method has been designed to reduce affective conflict and increase substantive conflict, the goal of the group should be convergence toward the true answer. A number of experiments have supported this hypothesis. Gordon and Helmer (10) reported that the interquartile range (range between the medians of the lower and upper quartiles) decreased on subsequent rounds of questions in most cases. They also noticed that after a few rounds a point of diminishing returns was reached. Dalkey (4), in an extensive series of experiments, found much the same results while exploring the consequences of various types of feedback. In other tests, Martino (14) found no strong bias for either optimism or pessimism in the group responses.

Feedback is an important area of the Delphi procedure. Dalkey's experiments (4) did not produce conclusive results, but they did indicate an effect of feedback on the convergence and accuracy of the group answer. Dalkey could not detect, however, a significant influence on the final estimate when justifications for numerical responses were included as part of the feedback. On the other hand, Scheibe, Skutsch, and Schofer (17) found a strong relationship between feedback and final responses. Dalkey (4) also investigated the effect of asking related questions along with the primary one. It was thought that the additional questions would stimulate additional related research and consideration of other relevant information. The results of this experiment were indecisive, although there was some evidence that the additional questions improved accuracy somewhat.

When the panel of experts is very diverse, it is possible to first conduct a Policy Delphi to establish a common base of knowledge and uniform definitions to be used subsequently. During the Policy Delphi there would be little need for restriction on the feedback since the main purpose is exchange of information. Convergence of the Policy Delphi should lead to common understanding of concepts and mutual agreement on terminology.

Historical Development.—The Delphi method was originally developed by the Rand Corporation in the early 1950s for the Air Force, but because it was primarily intended to be used in military planning it was kept secret for about 10 yr. The method is intended to improve the validity of decisions reached by a group consensus. In any group there is more information and misinformation than in any one individual, and the process by which opinion is extracted determines which has more of an effect on the answer. The characteristics of the Delphi method have been developed to extract as much information as possible and to use it to reach the most reliable conclusion.

Some of the first Delphis were conducted to decide the size of a Soviet nuclear attack necessary to eliminate the defense industry in the United States (5). Following its initial use for strategic planning, the Delphi method was applied by both industry and government in forecasting technological changes and developing policies for future resources and services (16).

The Delphi method has been used in the field of higher education for campus

and curriculum planning (11), in industry to predict new markets and future trends in products (6,9), in government to evaluate civil defense policy (20), and in the medical profession (7). Within the field of civil engineering there have been a few documented uses of the Delphi method. For the Michigan Sea Grant Program, a Delphi was employed to study problems in short-term and long-term resource management in the Great Lakes (13). Because of the complexity of the problems, three different panels of technologists, (engineers and scientists), behaviorists, and decision-makers (business and civic leaders) were used to study sources of pollution, wastewater treatment methods, and regional planning strategies. The Delphi was considered experimental and no formal proposals resulted. A Delphi was also employed for estimation of electrical generation failure rates of nuclear power plants (8). General failure modes were considered in the initial round and more detailed categories in subsequent rounds.

Relevance to Structural Design Loads.—Applications of the Delphi method in the field of civil engineering have been rather limited. The use of the method in the areas of planning, environmental engineering, and traffic engineering (17,18) are clear, and it may only be the conservative nature of the profession that has limited its use. While the applications within structural engineering may not be as obvious, potential does exist. One such area is the determination of minimum specified design loads. Traditionally this has been approached with a Lockean philosophy, and a Policy Delphi can be used to address appropriate levels of safety, standard design practices and uniform definitions of terms, which are usually dealt with by committees of various professional organizations. The determinations of the design loads themselves, however, offers the most interesting use of the Delphi method and philosophically can be compared to field data collection. The major difference is that in the Delphi method the opinion formation segment of the process is highly structured, while the data gathering, which is implied by the use of experts, is very unstructured. The Delphi cannot supplant the collection of data or development of supporting research. However, it is designed to extract a maximum amount of available information in a form that is useful in reaching a consensus.

Live Load Application for American National Standard A58

Purpose and Scope.—Legally mandated minimum design loads for buildings are usually specified directly by local building codes or by reference to one of the national model codes. The loads contained in these codes are, in turn, often adopted in whole or in part from American National Standard "Building Code Requirements for Minimum Design Loads in Buildings and Other Structures" (2), commonly referred to as the ANSI A58 Standard. This is especially true for live loads, which are defined as those loads produced by the use and occupancy of the building, and do not include environmental loadings.

In 1977 work was begun on updating the current (1972) edition of the ANSI A58 Standard. Such periodic revision is required by the American National Standards Institute. The first two writers of this paper are chairman and member, respectively, of the Live Load Subcommittee of the ANSI A58 Standard Committee. Within the live loads provisions is the very important basic table of minimum uniformly distributed live loads. While the values in this table ideally should be based on statistical analysis of field data in concert with

structural reliability theory, neither the data nor the theory is yet sufficient for such a determination. It was decided, therefore, to employ the Delphi method in the updating of this table.

Material on uniformly distributed live loads was prepared in tabular form for the Delphi panel. The table consisted of each building occupancy type (e.g., offices in office buildings, lobbies in office buildings, guest rooms in hotels), the load as specified in the 1972 edition of the ANSI A58 Standard (2), a column for the suggested load and space for supporting reasons for both revised and reaffirmed values. Instructions explained briefly about the Delphi, emphasized the need for responses for reaffirmed loads as well as suggested changes and requested return of the forms within a specified time.

Selection of Panel.—The selection of an appropriate panel of experts was clearly the most important step in assuring the success of the Delphi. It was decided that the panel should consist of practicing engineers with extensive design experience. In order to obtain the most valuable opinions and avoid having to weight the responses, only engineers who were held in high esteem by their peers were selected. In order to accomplish the selection, inquiries were made of engineers in several major cities. In each case the engineers were asked to name those structural engineers in their area of the country who were professionally regarded with highest respect. From the composite list, 25 names were chosen. It was hoped that this would produce at least 20 responses (which was somewhat arbitrarily selected as a viable minimum).

The 25 members of the panel represent a wide geographical distribution; with nine from the east coast, eight from the west coast, four from the midwest and four from the Southeast. Fourteen of the firms represented may be classified as structural engineering, six as architecture-engineering, two as civil and structural engineering, two as material supplier associations, and one as construction. All 25 panel members are structural engineers, and more than half are principals in their firms. A list of the panel members and their firms is shown in the following:

Name	Company affiliation (at time of Delphi)
Horatio Allison	Allison, McCormac and Nickolaus
Stephen B. Barnes	S. B. Barnes and Associates
Christian J. Birkeland	ABAM Engineers, Inc.
George E. Brandow	Brandow and Johnston Associates
James R. Cagley	Martin and Cagley
Edward Cohen	Ammann and Whitney
Henry J. Degenkalb	H. J. Degenkalb and Associates
David Doar	Weems/Doar Engineers, Inc.
William Dripps	Portland Cement Association
William E. Edwards	William E. Edwards, Inc.
Morton H. Eligator	Weiskopf and Pickworth
Jack D. Gillum	Jack D. Gillum and Associates
Andrew J. Gravino	Prybylowski and Gravino, Inc.
Donald Griff	Lev Zetlin Associates
S. Hal Iyengar	Skidmore, Owings and Merrill

Jack R. Janney	Wiss, Janney, Elstner, and Associates
Stephen E. Johnston	Skidmore, Owings and Merrill
Walter T. Norris	Riverside Steel Construction Company
Lester E. Poole	John Graham and Company
Leslie E. Robertson	Skilling, Helle, Christiansen, Robertson
William F. Ropp	Daniel, Mann, Johnson and Mendenhall
Robert P. Schuh	Post, Buckley, Schuh and Jernigan, Inc.
Richard H. Tatlow III	Abbott, Merkt International, Inc.
Christopher G. Tyson	American Iron and Steel Institute
Richard Weingardt	Richard Weingardt Consultants

It was felt that since the panel members have many demands on their time they might be reluctant to agree to participate in the Delphi. Therefore, a letter was sent informing them of their selection and presuming acceptance unless they responded within two weeks. This put the burden of action on the individual if he wished to refuse. It was recognized that this would probably decrease refusal, but at the expense of decreased likelihood of response to the Delphi itself. It was hoped that the panel members would be reluctant to ignore the questionnaire when it arrived. In order to encourage participation the importance of the task was emphasized. In addition, each member was sent a complete list of the tentative panel so that he could see the stature of the individuals contacted. None of the 25 panel members declined to participate.

Responses to First Round.—The first round of Delphi material was sent to the panel in August 1978. A response was requested within 10 days. Two reminder letters were sent to nonrespondents, one after approximately one month and another a month after that. By the middle of October responses had been obtained from 22 of the 25 panel members. This was considered sufficient (and somewhat miraculous) and no further attempt was made to obtain the three remaining responses.

Of the 56 occupancy types defined by the ANSI A58 Standard (2), 50 had more respondents reaffirm the current load value than all revised values combined. In 48 of these cases, there were more than twice as many votes for the current value than for any single alternative value, the exceptions being marquees and first floors in retail stores. For marquees, respondents favored the current 75 psf (3.6 kPa), but about two thirds as many selected 60 psf (2.9 kPa). For first floors in retail stores, the current 100 psf (4.8 kPa) was favored, with about two thirds as many votes for 75 psf (3.6 kPa).

For the six occupancy types without a majority of responses reaffirming the current values, suggestions were quite varied. Table 1 indicates responses for these six occupancy types as well as the two previously mentioned. For the first round not all 22 respondents replied to each occupancy type. For assembly halls with fixed seats a majority of respondents favored lowering the load to 50 psf (2.4 kPa) from the current value of 60 psf (2.9 kPa). For corridors above the first floor in libraries a plurality favored the current 80 psf (3.8 kPa), but responses varied from 50 psf (2.4 kPa)–100 psf (4.8 kPa). For corridors above the first floor in office buildings about half the votes favored 50 psf (2.4 kPa) rather than the current 80 psf (3.8 kPa). This lower value also received more than twice as many votes as any other single suggestion. Three different residential occupancies failed to obtain a majority for reaffirma-

tion. For both corridors in multifamily buildings and corridors not serving public rooms in hotels a value of 40 psf (1.9 kPa) received approximately half the votes and about twice as many as the current 80 psf (3.8 kPa). Finally, for floors above the first in dwellings the vote was split between the current load

TABLE 1.—Delphi Results for Occupancy Types with Significant Variation of Response

Occupancy type (1)	Minimum Uniformly Distributed Live Loads, in pounds per square foot			
	ANSI 1972 (2) (2)	Delphi round one (3)	Delphi round two (4)	ANSI 1980 (3) (5)
Assembly halls with fixed seats	60	10 at 50 6 at 60 1 at 100	12 at 50 5 at 60 2 at 100	60
Library corridors above first floor	80	2 at 50 2 at 60 1 at 75 7 at 80 4 at 100	3 at 50 8 at 60 3 at 80 5 at 100	80
Marquees	75	1 at 50 5 at 60 8 at 75 2 delete	10 at 60 8 at 75 1 delete	75
Office corridors above first floor	80	9 at 50 1 at 75 4 at 80 3 at 100	11 at 50 1 at 60 2 at 80 5 at 100	50
Residential floors above first in dwellings	30	7 at 30 8 at 40	1 at 30 18 at 40	30–40 (varies by use)
Residential corridors in hotels not serving public rooms	80	9 at 40 1 at 75 4 at 80 1 at 100	13 at 40 3 at 60 2 at 80 1 at 100	40
Residential corridors in multifamily buildings	80	8 at 40 1 at 75 4 at 80 3 at 100	12 at 40 2 at 60 2 at 80 3 at 100	40
Retail stores—first floors	100	6 at 75 1 at 80 9 at 100	7 at 75 12 at 100	100

Note: 1 psf = 47.9 Pa.

of 30 psf (1.4 kPa) and a value of 40 psf (1.9 kPa). This latter is the current value for first floors.

Although most supporting comments received with the responses were of a general nature, in a few cases actual computations were included to show that a given load (generally lower than the current design load) could not reasonably be exceeded.

Final Round.—Based on the response to the first round of the Delphi it was decided to conduct a second round. A new table was constructed again containing all 56 occupancy types. Alongside each occupancy, histogram type information was presented in tabular form accounting for each vote on round one. Comments received in round one for all loads other than the current ones were summarized next to each occupancy type. Space was provided for the round two response and for optional comments. A specific request was made for a response to all occupancy types. The round two material was distributed in early November 1978 with a two week requested response time. One reminder letter was sent to nonrespondents about six weeks later. By the middle of January 1979, 19 responses had been received, indicating a loss of three round one participants. The decision was made to close round two at that time.

All 48 occupancies that had been reaffirmed on round one were again reaffirmed, generally more strongly so. For marquees and first floors in retail stores there was not a major shift from round one to round two.

For the six occupancies for which a majority had not reaffirmed the current values in round one, the results for round two generally provided an even stronger mandate for change, as shown in Table 1. For assembly halls with fixed seats there was little alteration in responses. For library corridors above the first floor a slight plurality now favored 60 psf (2.9 kPa). For office corridors above the first floor the value of 50 psf (2.4 kPa) received slightly stronger support than it had in the first round. Both corridors in multifamily residences and corridors not serving public rooms in hotels received increased votes for a reduced load of 40 psf (1.9 kPa). This value was a majority for both occupancies and received at least four times as many votes as any other load value. Finally, for floors above the first in dwellings a load value of 40 psf (1.9 kPa) received almost unanimous round two support.

Based on the general convergence in load values found in the round two responses and on the likelihood of decreased response to further rounds, it was decided to terminate the Delphi after the two rounds.

Implementation.—The Delphi responses were reviewed and it was decided that there was not sufficient consensus to warrant changes for marquees, first floors in retail stores, and library corridors above the first floor. Possible changes in the remaining five categories under consideration were presented to a meeting of the ANSI A58 Standard Committee in April 1979 and then circulated to the Live Load Subcommittee of the A58 Standard Committee.

Because of similar usage characteristics, it was decided to combine the assembly hall occupancy category with theaters. The Delphi responses for assembly halls with fixed seats favored a reduction from the current 60 psf (2.9 kPa) to 50 psf (2.4 kPa) by about two to one. However, the responses for theaters favored retaining 60 psf (2.9 kPa) by 80%. On this basis it was decided that the new occupancy, assembly areas and theaters, would retain a design load of 60 psf (2.9 kPa) for fixed seating.

For office corridors above the first floor the Delphi recommendation to reduce the design load from 80 psf (3.8 kPa) to 50 psf (2.4 kPa) was followed. The new load was judged to be adequate for crowding situations and more accurately reflects modern design practice with open floor plans. Stairs and exitways were left at 100 psf (4.8 kPa) to account for possible very high crowding loads in those areas.

Corridors in multifamily residences and corridors serving private rooms in hotels were reduced from 80 psf (3.8 kPa) to 40 psf (1.9 kPa) as strongly recommended in the Delphi.

Floors above the first in dwellings presented a most interesting dilemma. Delphi responses were strongly in favor of making all habitable floors 40 psf (1.9 kPa). Supporting comments in the Delphi could be grouped into three categories. One was that waterbeds require the higher design load. The second was the 30 psf (1.4 kPa) results in too flexible a floor system. The third was that depending on the floor plan of the dwelling, heavy loads usually associated with first floors could readily be found on upper floors in bilevel or high rise dwellings. On the other hand, no reports of inadequate performance in existing dwellings could be traced to the design live loads. A request for comments from the office of Architecture and Engineering Standards of the Department of Housing and Urban Development elicited concern over an unnecessary increase in housing costs that could result from requiring 40 psf. It was finally decided to clarify that dwelling refers only to one-family and two-family houses and to redefine the design loads to be based on room usage. Habitable attics and sleeping areas were given a design load of 30 psf (1.4 kPa), while all other habitable areas were set at 40 psf (1.9 kPa). The waterbed risk was left to the indulger.

The above recommendations were included in an April 1980 comprehensive proposed revision to the ANSI A58 Standard (3), and most of them were in an earlier November 1979 draft. Of those members of the ANSI A58 Standard Committee voting on the live load provisions, 84% voted for approval. The remaining votes were abstentions except for one negative, which was not related to the changes previously described.

Conclusions

The Delphi method is a highly formalized method of communication that is designed to extract the maximum amount of unbiased information from a panel of experts. By this method the most reliable conclusions should be obtained from a panel consisting of members of approximately equal expertise. Although the method has been used for nearly 30 yr in strategic planning, applications in civil engineering have come only much more recently. No documented use in structural engineering could be found.

The Delphi method is especially well suited for such structural engineering applications as setting design loads, developing uniform terminology, and selecting appropriate levels of safety. Its success depends principally on the careful selection of the panel and formulation of the questions. Its use in updating the design live loads for the ANSI A58 Standard (2,3) was judged to be appropriate and fruitful. The principal difficulties were in maintaining the high level of response and in reaching and implementing a consensus.

Acknowledgment

In addition to the members of the Delphi panel, the writers would like to specifically acknowledge the encouragement and cooperation of Bruce Ellingwood.

Appendix.—References

1. Amara, R. C., "Some Views on the Use of Expert Judgement," *Technological Forecasting and Social Change*, Vol. 3, No. 3, 1972, pp. 279–289.
2. "Building Code Requirements for Minimum Design Loads in Buildings and Other Structures," ANSI A58.1-1972, American National Standards Institute, New York, N.Y., 1972.
3. "Building Code Requirements for Minimum Design Loads in Buildings and Other Structures," ANSI A58.1-1980/Draft, American National Standards Institute, New York, N.Y., 1980.
4. Dalkey, N. C., "The Delphi Method: An Experimental Study of Group Opinion," *Memorandum RM-5888-PR*, The Rand Corporation, Santa Monica, Calif., June, 1969.
5. Dalkey, N. C., and Helmer, O., "An Experimental Application of the Delphi Method to the Use of Experts," *Management Science*, Vol. 9, No. 3, Apr., 1963, pp. 458–467.
6. Enzer, S., "Plastics and Competing Materials by 1985: A Delphi Forecasting Study," *The Delphi Method, Techniques and Applications*, H. A. Linstone, and M. Turoff, eds., Addison-Wesley, Reading, Mass., 1975, pp. 195–209.
7. Flaherty, K. R., "Delphi Methodology Applied to Development of a Patient Follow-Up Care Systems," thesis presented to Northwestern University at Evanston, Ill., in 1975, in partial fulfillment of the requirements for the degree of Master of Science.
8. Gangloff, W. C., "What Ifs? For Nuclear Power Plants," *IEEE Spectrum*, June, 1977, pp. 53–58.
9. Goldstein, N., "A Delphi on the Future of the Steel and Ferroalloy Industries," *The Delphi Method, Techniques and Applications*, H. A. Linstone, and M. Turoff, eds., Addison-Wesley, Reading, Mass., 1975, pp. 210–226.
10. Gordon, T. J., and Helmer, O., "Report on a Long-Range Forecasting Study," *Document Number P-2982*, The Rand Corporation, Santa Monica, Calif., Sept., 1964.
11. Judd, R. C., "Use of Delphi Methods in Higher Education," *Technological Forecasting and Social Change*, Vol. 4, No. 2, 1972, pp. 173–186.
12. Large, R. D., "An Investigation of Delphi Methodology," thesis presented to Northwestern University at Evanston, Ill., in 1975, in partial fulfillment of the requirements for the degree of Master of Science.
13. Ludlow, J., "Delphi Inquiries and Knowledge Utilization," *The Delphi Method, Techniques and Applications*, H. A. Linstone, and M. Turoff, eds., Addison-Wesley, Reading, Mass., 1975, pp. 102–123.
14. Martino, J. P., "The Optimism/Pessimism Consistency of Delphi Panelists," *Technological Forecasting and Social Change*, Vol. 2, No. 2, 1970, pp. 1–224.
15. Mitroff, I. I., and Turoff, M., "Philosophical and Methodological Foundation of Delphi," *The Delphi Method, Techniques and Applications*, H. A. Linstone, and M. Turoff, eds., Addison-Wesley, Reading, Mass., 1975, pp. 17–36.
16. Podlesnik, R. A., "Delphi: An Organization Development Intervention," thesis presented to Northwestern University at Evanston, Ill., in 1977, in partial fulfillment of the requirements for the degree of Doctor of Philosophy.
17. Scheibe, M., Skutsch, M., and Schofer, J., "Experiments in Delphi Methodology," *The Delphi Method, Techniques and Applications*, H. A. Linstone, and M. Turoff, eds., Addison-Wesley, Reading, Mass., 1975, pp. 262–287.
18. Schneider, J. B., "Policy Delphi: A Regional Planning Application," presented at the July, 1971, Joint ASCE-ASME Transportation Engineering Meeting, held at Seattle, Wash. (Preprint 1454).
19. Speak, M., "Communication Failure in Questioning: Errors, Misinterpretation and Personal Frames of Reference," *Occupational Psychology*, Vol. 41, No. 4, Oct., 1967, pp. 169–181.
20. Turoff, M., "The Design of a Policy Delphi," *Technological Forecasting and Social Change*, Vol. 2, No. 2, 1970, pp. 149–171.

PREDICTING TORSIONAL RESPONSE OF THIN-WALLED OPEN RC MEMBERS

By Petar Krpan[1] and Michael P. Collins,[2] M. ASCE

INTRODUCTION

When studying the torsional response of members it is convenient to identify two different modes of torsional resistance: (1) Circulatory torsion; and (2) warping torsion.

The box beam shown in Fig. 1(*a*) primarily resists the applied torsion by shear stresses that *circulate* around the cross section. Because the shear stress (or, to be more general, the shear flow) remains constant in magnitude from point to point around the cross section, equilibrium does not require a change in magnitude of the longitudinal stresses. Apart from the local effects in the immediate vicinity of the fixed support, the stresses will remain uniform along the length of the beam and thus, the torsional strength of the beam will be independent of the beam's length.

The thin-walled channel beam shown in Fig. 1(*b*) primarily resists the applied torsion by shear stresses that are not uniform and that do not circulate in one consistent direction around the cross section. At the two bottom free edges of this open section the vertical shear stresses must be zero. If the shear stresses are to have some finite values at a distance from the free edges then there must be changes in magnitude of the longitudinal stresses [see Fig. 1(*b*)]. One of the bottom edges will be subjected to tensile stresses which increase with distance from the loaded end while the other bottom edge will be subjected to increasing compressive stresses. (For the simple section shown an estimate of the actual stress distribution can be obtained if the section is approximated by the two vertical walls acting as two independent cantilevers, one resisting an upwards load and the other a downwards load.) One vertical wall will have its top edge stretched and its bottom edge compressed while the other vertical wall will have its top edge compressed and its bottom edge stretched. Thus, the cross section of the beam will become *warped*, i.e., the points which prior to deformation lay on a plane will after deformation no longer lie on a single

[1]Asst. Prof., Ecole d'Architecture, Univ. Laval, Québec, Canada.
[2]Prof., Dept. of Civ. Engrg., Univ., of Toronto, Toronto, M5S1A4 Canada.

Note.—Discussion open until November 1, 1981. Separate discussions should be submitted for the individual papers in this symposium. To extend the closing date one month, a written request must be filed with the Manager of Technical and Professional Publications, ASCE. Manuscript was submitted for review for possible publication on July 17, 1979. This paper is part of the Journal of the Structural Division, Proceedings of the American Society of Civil Engineers, ©ASCE, Vol. 107, No. ST6, June, 1981. ISSN 0044-8001/81/0006-1107/$01.00.

plane. For this beam the torsional strength will be a function of the beam's length.

When torsion is applied to a member it will be resisted by both circulatory torsion and warping torsion with the contributions of each type being determined by their respective stiffnesses.

Theories capable of predicting the response in both circulatory torsion and warping torsion of beams made from linearly elastic homogeneous materials have been described extensively in the literature (e.g., 6, 12, 13). However, for reinforcement concrete members these theories are only directly applicable prior to cracking of the concrete. The post-cracking torsional response of reinforced concrete beams with closed sections or with squat solid sections has also been extensively treated in the literature (e.g., Ref. 2 lists about 400

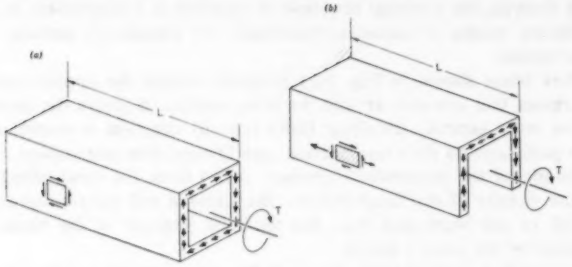

FIG. 1.—(*a*) Circulatory Torsion; (*b*) Warping Torsion

papers on the subject) so that it is possible to predict the post-cracking circulatory torsional response of such members (11). However, the post-cracking torsional response of open thin-walled reinforced concrete members such as those shown in Fig. 2 has not received anywhere near the same attention. The few available papers (5,10,14) on the subject typically either restrict their attention to the determination of ultimate load (5) or are concerned with only certain specific cross sections (10).

The objective of this paper is to present procedures capable of predicting the post-cracking response of restrained reinforced concrete thin-walled members having open and rigid cross sections loaded in pure torsion. The cross sections may be arbitrarily shaped and may have variable wall thicknesses. It is assumed, however, that the members are prismatic.

While the procedure presented is general it will be illustrated by predicting the response of a channel beam. For this beam the influence of warping torsion, circulatory torsion, and shear strains due to warping torsion will be described. A companion paper (9) describes an experimental study in which a large reinforced concrete channel beam was loaded in pure torsion to investigate the validity of the predictions made in this paper.

Outline of Problem

To show the procedures by which the torsional response of thin-walled open reinforced concrete members can be predicted the structure described in Fig.

3 will be investigated. This structure consists of a reinforced concrete channel beam 21 ft 0 in. (6.4 m) long attached to rigid abutments and loaded with a torque at midspan. The questions that need to be answered include: What is the relationship between the applied torque and the resulting rotation? At what torque will the concrete crack? When will the reinforcement yield? What will be the maximum torque that the structure can resist? What will be the relative contributions of circulatory torsion and warping torsion and how will cracking affect these contributions? Will the usually neglected shear strains significantly contribute to the flexibility of the structure?

Three rather distinct stages in the life of the beam can be identified. At very low loads the concrete will be uncracked and the response of the beam can be predicted by traditional elastic theories. At intermediate loads the concrete will be cracked but the stress levels in the concrete and the steel will be low

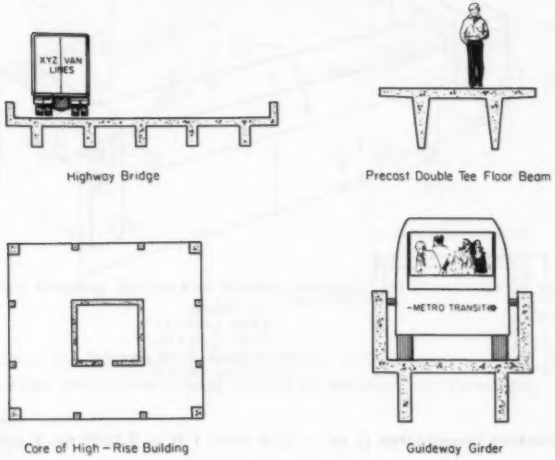

FIG. 2.—Open Thin-Walled Reinforced Concrete Members

enough (steel stress less than f_y, concrete stress less than $0.5\,f'_c$) to assume these materials are still linearly elastic. Thus, the response of the beam can be predicted by a cracked linearly elastic model. Finally, at high load levels both the steel and the concrete will become inelastic.

Uncracked Elastic Response

The beam will resist the applied torque by both circulatory torsion and warping torsion. However, to make the influence of each mode of resistance more clear it will first be assumed that all of the torque is resisted by circulatory torsion, then it will be assumed that all of the torque is resisted by warping torsion, finally the true situation of mixed torsion will be examined. In the uncracked state the presence of the reinforcement will be ignored.

Circulatory Torsion.—The response of elastic members in circulatory torsion can be predicted by using the classical theory of St. Venant. When the cross section consists of a number of long, narrow rectangles, Bach's approximation, which divides the section into its component rectangles, can be used. Thus, the relationship between the circulatory torsion, T_c, and the resulting twist, θ', can be written as

$$\theta' = \frac{d\theta}{dz} = \frac{T_c}{GK} = \frac{3T_c}{G\Sigma x_i^3 y_i} \quad \ldots\ldots\ldots\ldots\ldots\ldots\ldots\ldots\ldots\ldots (1)$$

in which G = the shear modulus of the material; and x_i and y_i = the smaller and larger dimensions of the component rectangles.

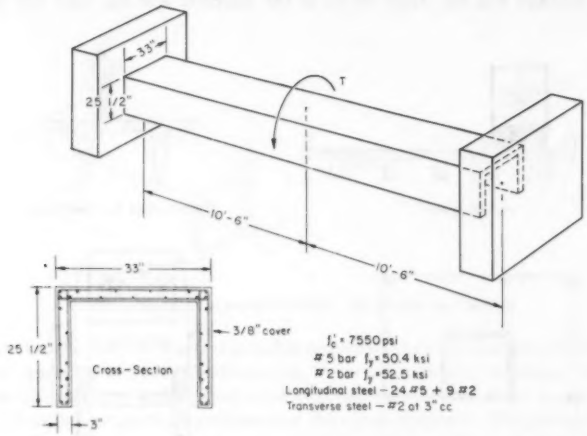

FIG. 3.—Structure Investigated (1 in. = 25.4 mm; 1 ft = 0.3048 m; 1 psi = 6.89 kPa)

If G is taken as $0.4E$ and the ACI (American Concrete Institute) (1) expression for E is used, then for the beam shown in Fig. 3 the St. Venant torsional stiffness GK will be 1.39×10^6 kip-in.^{2} (3,990 kN·m^2). Therefore, if the applied torque T is entirely resisted by circulatory torsion the midspan rotation, $\theta(L/2)$, will be 45.3×10^{-6} T rad where T is, in kip-inches (401×10^{-6} T if T is, in kilonewton-meters).

The maximum shear stress due to the circulatory torsion will be $T_c x/K$. Thus, if diagonal cracking is assumed to occur when the shear stress reaches $4\sqrt{f'_c}$ psi [$0.33\sqrt{f'_c}$ MPa] and if all the applied torque was resisted by circulatory torsion the value of the applied torque required to cause cracking would be 163 kip-in. (18.4 kN·m).

Warping Torsion.—The response of elastic members in warping torsion can be predicted by using the theory developed by Vlasov (13).

For the structure considered the distribution of warping torsion, T_ω, along

the length of the beam will be as shown in Fig. 4(*a*). This distribution is analogous to the distribution of vertical shear force, V_y, that would occur if the beam was loaded with a vertical force at midspan, Fig. 4(*b*). As already mentioned, warping torsion will cause the longitudinal stresses to change along the length of the beam. This is analogous to the way in which the presence of shear will cause longitudinal stresses to change along the length of the beam. In the case of vertical shear, V_y, the need for the longitudinal stresses to change

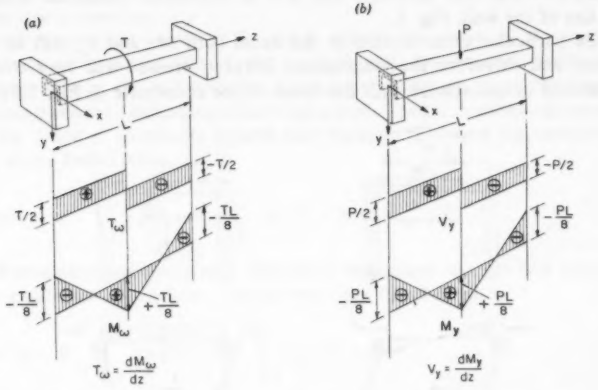

FIG. 4.—(*a*) Warping Torsion and Warping Moment; (*b*) Vertical Shear and Vertical Moment

is expressed by the changing value of the vertical moment, M_y, Fig. 4(*b*), with the shear and moment being related by well-known expression

$$V_y = \frac{dM_y}{dz} \quad \ldots\ldots\ldots\

$$I_{yy} = \int_A y^2 dA \quad \ldots \ldots \ldots

$$\epsilon = -\theta'' \omega \quad \ldots \ldots \ldots

$$Q_y = \int_0^s y.t.ds \quad \ldots \quad (15)$$

The coordinate s starts at one end of the section and follows the center line of the section around to the other end. The positive direction of s can be arbitrarily chosen. The positive direction of q will coincide with the positive direction of s.

The shear flow which results from the warping torsion described in Fig. 4(a) can be found from

$$q = -\frac{T_\omega Q_\omega}{I_{\omega\omega}} \quad \ldots \quad (16)$$

in which the sectorial static moment of the cut-off portion for a particular point s on the cross section is given by

$$Q_\omega = \int_0^s \omega.t.ds \quad \ldots \quad (17)$$

The analogy that exists between the equations for warping torsion and those for flexural shear is not merely mathematical. It follows directly from the fact that the basic geometric assumption for warping torsion (i.e., orthogonal lines remain orthogonal) is a generalization of the plane sections remain plane assumption (7).

For the section being considered here the values of ω and Q_ω are shown in Fig. 5 along with the values of y and Q_y which are given so that comparisons can be made. From the ω values the sectorial moment of inertia, $I_{\omega\omega}$, can be found to be 2.36×10^6 in.^{6} (634×10^{-6} m^6).

From Eqs. 9 and 12 it can be seen that

$$\frac{d^2\theta}{dz^2} = -\frac{M_\omega}{EI_{\omega\omega}} \quad \ldots \quad (18)$$

This relationship along with the distribution of M_ω shown in Fig. 4(a) can be used to find the midspan rotation θ ($L/2$) assuming all the applied torque T is resisted by warping torsion

$$\theta\frac{L}{2} = \frac{TL^3}{192EI_{\omega\omega}} = 7.13 \times 10^{-6}\, T \text{ rad} \quad \ldots \quad (19)$$

in which T is, in kip-inches ($63 \times 10^{-6}\, T$ if T is, in kilonewton-meters).

By comparing this rotation with that predicted for circulatory torsion, it can be seen that the warping torsional stiffness of this member is more than 6 times greater than the circulatory torsional stiffness.

Under warping torsion cracking may initiate because the longitudinal warping tensile stresses exceed the modulus of rupture of the concrete—resulting in transverse cracks or because the warping shear stresses exceed the shear stresses required to cause diagonal cracking. If the modulus of rupture is assumed to be $7.5\sqrt{f'_c}$ psi ($0.63\sqrt{f'_c}$ MPa) the value of applied torque required to cause transverse "flexural type" cracks will be 230 kip-in. (25.9 kilonewton-meters). If it is assumed that the shear stress required to cause diagonal cracking is

$4\sqrt{f'_c(\text{psi})}$ [$0.33\sqrt{f'_c(\text{MPa})}$] then the value of the applied torque required to cause "web shear type" cracks will be 1,100 kip-in. (124 kN·m).

Mixed Torsion.—At each cross section of a beam the total internal torque, $T(z)$, is the sum of the circulatory torsion at that section, $T_c(z)$, and the warping torsion at that section, $T_\omega(z)$. Thus

$$T(z) = T_c(z) + T_\omega(z) \quad \ldots\ldots\ldots\

This ratio is sometimes expressed in terms of a characteristic length, a, in which

$$a = \sqrt{\frac{EI_{\omega\omega}}{GK}} \quad \ldots\ldots\ldots\

Once again the circulatory torsional response and the warping torsional response will be studied separately.

Circulatory Torsion.—Cracked reinforced concrete members resist circulatory torsion by means of diagonal concrete compressive stresses which spiral around the beam at an angle of α to the longitudinal axis (11). As well as resisting the torsion these diagonal compressive stresses produce tensile stresses in the longitudinal and transverse reinforcement. Based on these concepts a convenient, approximate (the concrete's compressive deformation is ignored) expression for the cracked circulatory torsional stiffness, GK_{cr}, can be obtained (3), as

$$GK_{cr} = \frac{E_s}{2} \frac{4A_0^2}{p_0} \sqrt{\frac{A_l}{p_0} \cdot \frac{A_h}{s}} \quad \ldots \ldots \ldots \ldots \ldots \ldots \ldots \ldots \ldots \ldots \quad (26)$$

in which E_s = the Young's modulus of the steel; A_0 = the area enclosed by the shear flow; p_0 = the perimeter of the shear flow path; A_l = the cross-sectional area of the longitudinal steel; A_h = the cross-sectional area of one leg of the closed hoops; and s = the spacing of the hoops.

The shear flow path lies some small distance inside the outside surface of the concrete. The actual position is made difficult to determine by the fact that at higher loads the concrete cover over the hoops will spall off (10). To determine the stiffness of the beam in the cracked elastic state it will here be assumed that the shear flow path coincides with the centerline of the hoop.

For the cross section being considered in this paper (Fig. 3) application of Eq. 26 will result in an estimate of GK_{cr} of 0.25×10^6 kip-in.^{2} (720 kN·m^2). If this value is compared to the previously calculated uncracked circulatory torsional stiffness, GK, it will be seen that cracking has caused this torsional stiffness to drop to about one sixth of its previous value. If the applied midspan torque, T, was all resisted by circulatory torsion the midspan rotation $\theta(L/2)$ in the cracked state would $252 \times 10^{-6}\ T$ rad, in which T is, in kip-inches ($2{,}230 \times 10^{-6}\ T$ rad if T is in kilonewton-meters).

The tensile stress in the hoop steel, f_h, that will be caused by the circulatory torsion, T_c, can be found as

$$f_h = \frac{T_c s \tan \alpha}{2A_0 A_h} \quad \ldots \ldots \ldots \ldots \ldots \ldots \ldots \ldots \ldots \ldots \ldots \ldots \quad (27)$$

The angle of diagonal compression α can be found from

$$\tan^4 \alpha = \frac{1 + \dfrac{E_c t_d p_0}{E_s A_l}}{1 + \dfrac{E_c t_d s}{E_s A_h}} \quad \ldots \ldots \ldots \ldots \ldots \ldots \ldots \ldots \ldots \ldots \quad (28)$$

in which t_d = the effective wall thickness given by $0.75A_0/p_0$. For the cross section under analysis, Eq. 28 predicts a value of 38° for α. Knowing α the circulatory torsion required to yield the hoops can be found from Eq. 27. Thus, if the applied midspan torque T was all resisted by circulatory torsion the value of the applied torque required to cause yielding of the hoops would be 654 kip-in. (74 kN·m).

Warping Torsion.—As has already been described warping torsion, T_ω, causes longitudinal stresses which change along the length of the beam with the magnitude of these stresses being related to a term called the warping moment, M_ω, Eqs.

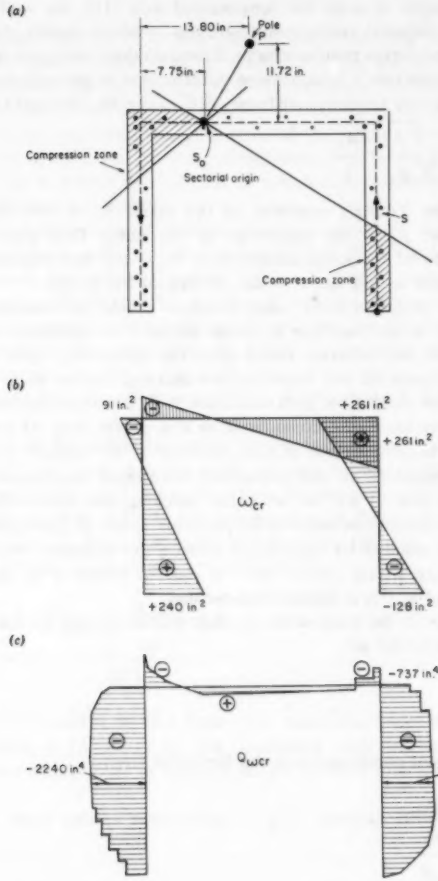

FIG. 7.—Cross-Sectional Properties—Cracked Section: (*a*) Cracked Cross Section; (*b*) Principle Sectorial Co-Ordinates; (*c*) Sectorial Static Moment of Cut-Off Portion

3 and 12. In addition, the warping torsion will cause shear stresses which depend only on the magnitude of T_ω and, therefore, are not influenced by M_ω, Eq. 16. For the sake of simplicity it will be assumed that in the cracked state the response of the beam to M_ω does not depend on the value of T_ω and

that the response of the beam to T_ω does not depend on the value of M_ω. This approximation is analogous to that traditionally used in determining the flexural response of reinforced concrete beams where the influence of co-existing shear forces is ignored.

In determining the response of the cracked cross section to warping moment the concrete in tension is ignored while the individual steel bars are transformed into equivalent areas of concrete by multiplying their areas by the modular ratio E_s / E_c. To arrive at the effective cracked cross section an iterative procedure can be used in which successively more accurate estimates of what concrete is in tension are made. For the section considered in this paper the effective cracked cross-sectional properties when under a positive warping moment are described in Fig. 7.

It can be seen from Fig. 7 that when the concrete cracks the principal sectorial coordinates for the section change (compare Figs. 5(*a*) and 7). The ω values associated with compression zones become smaller in magnitude while those associated with tensile zones become larger. The position of the pole P (often called the shear center) for this section moves up and to the left. Whereas in the uncracked state the ω value was independent of the sign of the warping moment, in the cracked state each point on the section will have two values of ω, one for positive warping moment and one for negative warping moment. Under a negative warping moment the pole will move up and to the right and hence the ω values for the left and the right bottom edges will become +128 in.^{2} ($+82.6 \times 10^{-3}$ m^2) and −240 in.^{2} (-154.8×10^3 m^2), respectively. This movement of the shear center at cracking is analogous to the movement of the neutral axis at cracking for beams in flexure.

From the ω values and the effective areas the cracked sectorial moment of inertia, $I_{\omega\omega cr}$, for this section is found to be 1.29×10^6 in.^{6} (346×10^{-6} m^6) which is about one half of the uncracked value. Substituting the cracked value into Eq. 19 gives $\theta(L/2) = 13.0 \times 10^{-6}\, T$ rad, in which T is, in kip-inches ($115 \times 10^6\, T$ rad if T is, in kilonewton-meters). The ω values, Fig. 7(*b*), indicate that the highest tensile strains will occur in the top right corner of the section. The value of M_ω required to yield the longitudinal steel in this location will be 42,500 kip-in.^{2} (122 kN·m^2) which if all the applied torsion is resisted by warping torsion, Fig. 4(*a*), corresponds to an applied torque of 1,350 kip-in. (153 kN·m).

In the cracked state the shear flows caused by the warping torsion can be found from Eq. 16 provided that the cracked values of the sectorial static moments are used, $Q_{\omega cr}$, Fig. 7(*c*). These shear flows will be resisted by diagonal compressive stresses in the concrete (inclined at an angle α to the longitudinal axis) and tensile stresses in the transverse and longitudinal steel (4). The tensile stress in the transverse steel, f_h, can be found from

$$f_h = \frac{qs}{A_v} \tan \alpha \quad \ldots \ldots \ldots \ldots \ldots \ldots \ldots \ldots \ldots \ldots \ldots \ldots \ldots \ldots \quad (29)$$

in which A_v = the total area of transverse steel in the wall within the spacing s (area of two legs in our case). The value of tan α can be found from Eq. 28 except that t_d should be replaced by the wall thickness t, p_0 by the length of the contour around the wall center line p, and A_h should be replaced by A_v.

For the section considered α will again be 38°. Knowing α, Eq. 29 and Eq. 16 can be used to find the value of T_ω required to yield the transverse steel. Thus, if the applied midspan torque T was all resisted by warping torsion the value of applied torque required to yield the transverse steel would be 2,580 kip-in. (292 kN·m).

Mixed Torsion.—Due to cracking the values of both $EI_{\omega\omega}$ and GK decrease but GK decreases much more than $EI_{\omega\omega}$, therefore, the characteristic length of the section, a, Eq. 24 will increase. For the section considered, the cracked value of a will be 160 in. (4,100 mm). The larger value of a means that after cracking even less of the applied torsion will be resisted by circulatory torsion. The distribution of torsions will again look like that shown in Fig. 6, but now the maximum value of circulatory torsion will be only 0.037 T.

Because the circulatory torsion is so small the predicted midspan rotation will not be greatly changed. It will now equal 12.3×10^{-6} T rad (109×10^{-6} T rad if T is, in kilonewton-meters). There will also only be a small effect on the torque required to yield the longitudinal steel which will increase to 1,420 kip-in. (160 kilonewton-meters). While small, the circulatory torsion will cause substantial strains in the hoop steel, Eq. 27. For the outside legs of the hoops the effects of the shear due to circulatory torsion will add to the effects of the shear due to warping torsion reducing to 2,080 kip-in. (235 kilonewton-meters) the applied torque required to yield the transverse steel.

Contribution of Shear Strains.—The additional twists which arise because of the shear strains due to the warping torsion can be calculated for the cracked state by using an effective shear modulus, G_{cr} for the cracked concrete (4). When substituted into Eq. 25 this effective shear modulus can be expressed as

$$(GK_\gamma)_{cr} = \frac{0.5E_c t I^2_{\omega\omega\,cr}}{\left[1 + \sqrt{\left(1 + \frac{E_c tp}{E_s A_l}\right)\left(1 + \frac{E_c ts}{E_s A_v}\right)}\right] \int_s Q^2_{\omega\,cr}(s)\, ds} \quad \ldots\ldots (30)$$

For the section being considered Eq. 30 will predict that $(GK_\gamma)_{cr} = 7{,}500 \times 10^3$ kip-in.^{2} (2,160 kN·m^2). If the twists due to these shear strains are included in the analysis then the predicted rotation at midspan becomes 20.2×10^{-6} T rad, in which T is, in kip-inches (179×10^{-6} T rad if T is, in kN·m^2). It is worthy of note that the shear strains cause the rotation to increase by more than 60%.

Inelastic Response

For the beam under consideration the circulatory torsion will be very small at this stage and therefore, rather than dealing with the more complex case of mixed torsion it will be assumed that all of the applied torque is resisted by warping torsion. As a further simplification, it will again be assumed that the response of the beam to M_ω does not depend on the value of T_ω.

Response to Warping Moment.—As the magnitude of the warping moment is increased the longitudinal concrete and steel strains will also increase. At higher strain levels the assumption of linear elastic material response will be

inaccurate. The actual material stress-strain curves may resemble those shown in Fig. 8. Such stress-strain relationships can be represented by

$$f_s = E_{\text{secant } s}\epsilon_s\epsilon_s \quad f_c = E_{\text{secant } c}\epsilon_c\epsilon_c \quad \ldots\ldots\ldots\ldots\ldots\ldots\ldots\ldots \quad (31)$$

in which the secant moduli of the steel and the concrete are functions of the strain.

For a section made from materials having such nonlinear stress-strain relationships the response to warping moment can be calculated by an iterative procedure. The cross section can be subdivided into small steps along the s coordinate.

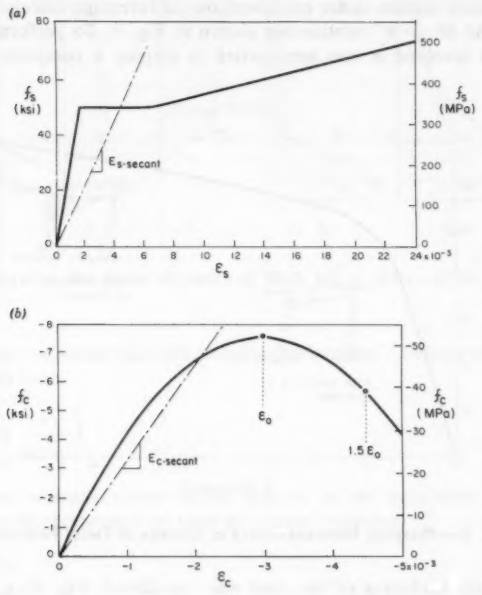

FIG. 8.—Stress-Strain Curves for Steel and Concrete: (*a*) Steel-Tension or Compression; (*b*) Concrete—Compression Only

For a particular value of M_ω the distribution of longitudinal strains over the cross section can be represented as:

$$\epsilon_s = \epsilon_c = \frac{M_\omega}{E_{c\text{ACI}} I_{\omega\omega\text{ inel}}}\omega_{\text{inel}} \quad \ldots\ldots\ldots\ldots\ldots\ldots\ldots\ldots\ldots\ldots \quad (32)$$

in which $E_{c\text{ACI}}$ = the elastic modulus of the concrete given by the ACI expression and $I_{\omega\omega\text{ inel}}$ and ω_{inel} are the inelastic cross sectional properties for the particular value of M_ω. As an initial estimate the cracked elastic values of $I_{\omega\omega}$ and ω can be used. From the calculated strains, Eq. 32 and the stress-strain relationships (e.g., Fig. 8) the secant modulus for each concrete step and each reinforcing

bar can be evaluated. Using the secant modulus values the concrete steps and steel bars can be transformed into equivalent areas of concrete with a modulus of E_{cACI}. From the transformed cross section the new estimates of $I_{\omega\omega\ inel}$ and ω_{inel} can be calculated, Eqs. 11 and 13, and the whole process repeated. When convergence has been obtained, the rate of change of twist, θ'', corresponding to the value of M_ω can be found from

$$\theta'' = \frac{d^2\theta}{dz^2} = -\frac{M_\omega}{E_{cACI} I_{\omega\omega\ inel}} \quad \ldots\ldots\ldots\

of the section to simultaneously resist a warping moment of 69,300 kip-in.^{2} (199 kN·m^2) and a warping torsion of 1,100 kip-in. (124 kN·m) must be investigated. As it has been assumed that the longitudinal strains, ϵ_l, only depend on M_ω, the values determined in the warping moment analysis can be used, Fig. 9 and Fig. 10(*a*). Furthermore, the cross-sectional properties determined for this value of M_ω can be used to find the magnitudes of the shear flows from Eq. 16. Fig. 10(*b*) shows these values for the most highly strained wall.

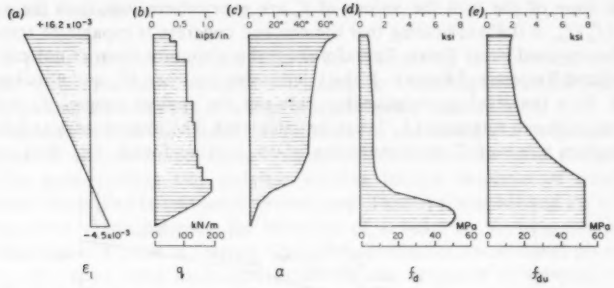

FIG. 10.—Investigating the Shear Capacity of Wall: (*a*) ϵ_l; (*b*) q; (*c*) α; (*d*) f_d; (*e*) f_{du}

The shear flows will cause diagonal compressive stresses, f_d, whose magnitudes can be found (4) from

$$f_d = \frac{q}{t}\left(\tan\alpha + \frac{1}{\tan\alpha}\right) \quad \ldots\ldots\ldots\ldots\ldots\ldots\ldots\ldots\ldots\ldots\ldots\ldots\ldots\ldots \quad (34)$$

The shear flows will also cause tensile stresses in the transverse steel, Eq. 29. Angle α can be determined (4) from geometric condition

$$\tan^2\alpha = \frac{\epsilon_d + \epsilon_h}{\epsilon_d + \epsilon_l} \quad \ldots\ldots\ldots\ldots\ldots\ldots\ldots\ldots\ldots\ldots\ldots\ldots\ldots\ldots \quad (35)$$

in which ϵ_d = the compressive strain associated with f_d; and ϵ_h = the tensile strain associated with f_h. For the longitudinal strains shown in Fig. 10(*a*) and the shear flows in Fig. 10(*b*), Eqs. 29 and 34, the stress-strain curves of Fig. 8 and Eq. 35 can be used to arrive at the predicted angles of diagonal compression shown in Fig. 10(*c*) and the predicted values of diagonal compressive stress shown in Fig. 10(*d*).

The ability of the cracked concrete to resist the diagonal compressive stresses will be reduced by large deformations of the concrete. A suggested value (4) of the ultimate value of this diagonal compressive stress, f_{du}, is

$$f_{du} = \frac{3.6 f'_c}{1 + 2\dfrac{\gamma_m}{\epsilon_0}} \le f'_c \quad \ldots\ldots\ldots\ldots\ldots\ldots\ldots\ldots\ldots\ldots\ldots\ldots\ldots\ldots \quad (36)$$

in which γ_m = the maximum shear strain in the concrete, which is found from

$$\gamma_m = \epsilon_h + \epsilon_l + 2\epsilon_d \quad \ldots \ldots \ldots \ldots \ldots \ldots \ldots \ldots \ldots \ldots \ldots \ldots \ldots \quad (37)$$

For the wall section being studied the strain values at this load level result in the values of f_{du} plotted in Fig. 10(*e*).

Because the wall section is at the ultimate value of M_ω, in the compression zone of the wall the value of f_d (which is here essentially longitudinal) reaches f_{du} (which is here equal to f'_c). This does not indicate a shear failure. In the tensile zone of the wall the values of f_d are everywhere less than the values of f_{du} ($f_d/f_{du} \leq 0.48$) indicating that the cracked concrete is capable of transmitting the required shear flows. Therefore, for this structure shear is not critical.

Predicted Response of Beam.—If the relationship between M_ω and θ'' is known, Fig. 9, then the resulting relationship between the applied torque, T, and the resulting midspan rotation $\theta(L/2)$ can be calculated. The procedure is as follows. For a given value of T the distribution of M_ω can be found, Fig. 4(*a*), which

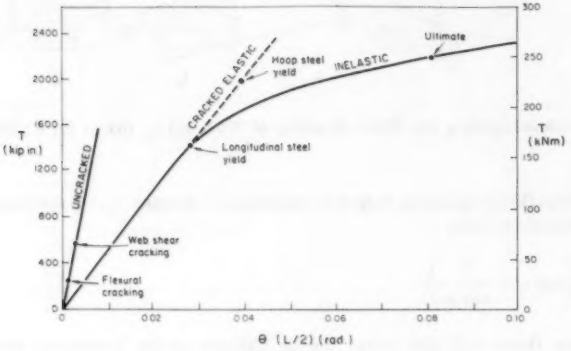

FIG. 11.—Predicted Response of Beam

in turn can be used to find the distribution of θ''. The well known procedures by which deflections are found from curvature distributions (e.g., moment-area or double integration) can then be used to find $\theta(L/2)$ from the distribution of θ''.

It has been shown that the shear strains due to T_ω result in an appreciable increase in the value of $\theta(L/2)$. While an analysis similar to that used in preparing Fig. 10 could be used to find the shear strains at each point on each cross section along the beam, such an analysis would be unnecessarily complex. As a simplification, a constant value of GK_v equal to the cracked value previously calculated will be used to calculate the additional rotation.

The final predictions for the response of the beam are summarized in Fig. 11. It is predicted that flexural type cracks will begin to form at the ends and at midspan when only about 12% of the ultimate load has been applied. At this stage the load-deformation response will begin to deviate from the uncracked elastic response. At about 26% of the ultimate load diagonal web-shear

type cracks should have formed along the length of the beam causing a further loss of stiffness. By about 65% of ultimate the longitudinal steel at the ends and at midspan should begin to yield while at about 95% of ultimate the hoop steel along the length of the beam should be yielding. This yielding of the steel will cause a very marked loss of stiffness. The final failure should occur due to flexural crushing of the concrete at the ends and at midspan at a torque of 2,200 kip-in. (249 kN·m).

Concluding Remarks

This paper has presented procedures for calculating the torsional response of thin-walled open reinforced concrete members. The procedures were illustrated by calculating the response of a reinforced concrete channel beam.

It was shown that the traditional theories for predicting the warping torsion response of elastic, homogeneous beams could be modified and extended so that the post-cracking and inelastic warping torsion response of reinforced concrete thin-walled beams could be predicted. The paper emphasized the intrinsic analogy that exists between the behavior of a beam in warping torsion and the behavior of a beam in flexure. Once the sectorial cross-sectional properties, ω, $I_{\omega\omega}$, Q_ω have been calculated predicting the response to warping torsion is no more difficult than predicting the response to flexure. While not as well known, the calculation procedures for determining ω, $I_{\omega\omega}$, and Q_ω are mathematically comparable to those used in determining y, I_{yy}, and Q_y (6).

It is suggested that for important reinforced concrete structures of the type shown in Fig. 2, it would be appropriate to perform a torsional analysis similar to that described in this paper. Such an analysis would help the engineer to predict the behavior of the structure at all load levels up to ultimate. In addition it is recommended that the designer use the cracked elastic section properties when analyzing the overall structure rather than the uncracked elastic values. As was shown in the paper, after cracking the stiffness drops substantially, the characteristic length increases, deformations due to shear strains become significant and the portion of the applied torsion carried by circulatory torsion decreases. Use of the cracked stiffness values will lead to a more accurate assessment of the actual force distributions throughout the structure.

In a companion paper (9) the observed behavior of a large thin-walled reinforced concrete channel beam tested in pure torsion is compared with the preceding predictions obtained.

Appendix I.—References

1. "Building Code Requirements for Reinforced Concrete (ACI 318-77)," ACI Committee 318, American Concrete Institute, Detroit, Mich., 1977.
2. "Torsion in Concrete, 1784-1974," *ACI Bibliography No. 12*, ACI Committee 438, American Concrete Institute, Detroit, Mich., 1978, 148 pp.
3. Collins, Michael, P., "The Torque-Twist Characteristics of Reinforced Concrete Beams," *SM Study No. 8*, Inelasticity and Non-Linearity in Structural Concrete, University of Waterloo Press, Waterloo, Ontario, 1972, pp. 211–232.
4. Collins, Michael P., "Towards a Rational Theory for RC Members in Shear," *Journal of the Structural Division*, ASCE, Vol. 104, No. ST4, Proc. Paper 13697, Apr., 1978, pp. 649–666.

5. Grob, Joseph, and Thürlimann, Bruno, "Wölbtorsionsverusche an Stahlbetonbalken mit offenem Querschnitt," *Publication No. 6506-6*, Institut für Baustatik, ETH, Zurich, Switzerland, Dec., 1974.
6. Kollbrunner, C. F., and Basler, K., "Torsion in Structures," *Springer-Verlag*, New York, N.Y., 1969.
7. Krpan, P., "The Behaviour of Open, Thin-Walled, Restrained, Reinforced Concrete Members in Torsion," thesis presented to the University of Toronto, at Toronto, Canada, in 1974, in partial fulfillment of the requirements for the degree of Doctor of Philosophy.
8. Krpan, P., "WARPT1—Computer Program for Warping Torsional Constants," National Technical Information Service, Springfield, Va., 1978.
9. Krpan, P., and Collins, M. P., "Testing Thin-Walled Open RC Structure in Torsion," *Journal of the Structural Division*, ASCE, Vol. 107, No. ST6, Proc. Paper 16332, June, 1981, pp. 1129–1140.
10. Mehlhorn, G., and Rutzel, H., "Wolbkrafttorsion bei dunnwandigen Stahlbetonragern," *Der Bauingenieur*, Berlin, West Germany, 1972, Heft 12.
11. Mitchell, D., and Collins, M. P., "Diagonal Compression Field Theory—A Rational Model for Structural Concrete in Pure Torsion," *American Concrete Institute Journal*, Vol. 71, Aug., 1974, pp. 396–408.
12. Timoshenko, S. P., and Goodier, J. N., *Theory of Elasticity*, McGraw-Hill Book Co., Inc., 1970.
13. Vlasov, V. Z., "Thin-Walled Elastic Beams," 2nd ed., Moscow, U.S.S.R., 1959, Published for the National Science Foundation by the Israel Program for Scientific Translations, 493 pp.
14. Zhirohowski-Koscia, K. F., "Stress Analysis of Cracked Reinforced and Prestressed Concrete Thin-Walled Beams and Shells," *Magazine of Concrete Research*, London, England, V. 20, No. 65, Dec., 1968, pp. 213–220.

Appendix II.—Notation

The following symbols are used in this paper:

A_h = cross-sectional area of one leg of closed hoop;
A_l = cross-sectional area of longitudinal steel;
A_0 = area enclosed by shear flow;
A_v = total area of transverse steel in wall within spacing, s;
a = characteristic length of cross section, Eq. 26;
E_c = modulus of elasticity;
E_{secant} = secant modulus of elasticity;
f'_c = crushing strength of concrete as determined from cylinder;
f_d = diagonal compressive stress;
f_{du} = value of f_d which will cause failure;
G = shear modulus;
I_{yy} = $\int_A y^2\,dA$ = moment of inertia;
$I_{\omega\omega}$ = $\int_A \omega^2\,dA$ = sectorial moment of inertia;
K = St. Venant's torsion constant;
K_γ = equivalent torsion constant for twist due to shear strains;
L = span of beam;
m = distributed torsional moment acting on member;
M_y = bending moment in vertical plane;
M_ω = warping moment;
p_0 = perimeter of area enclosed by shear flow;
p = length of contour around wall center line;
Q_y = $\int_0^u y\,t\,ds$ = static moment of cut-off portion;

Q_ω = $\int_0^s \omega t\,ds$ = sectorial static moment of cut-off portion;
q = shear flow;
s = coordinate around center line of cross section;
s = spacing of stirrups;
T = applied torque;
T_c = circulatory torsion;
T_ω = warping torsion;
t = wall thickness;
t_d = $0.75\,A_0/p_0$ = effective wall thickness;
V_y = vertical shear force;
v = displacement in y-direction;
x,y = coordinates in plane of cross-section;
x_i,y_i = smaller and larger dimensions of component rectangles;
z = coordinate along length of member;
α = angle of inclination of diagonal compressive stress;
γ = shearing strain;
γ_m = maximum shear strain;
ϵ = longitudinal strain;
σ = longitudinal normal stress;
τ = shear stress;
θ = rotation of cross-section;
θ' = $d\theta/dz$ = twist;
θ'' = $d\theta^2/dz^2$ = rate of change of twist;
θ_γ = additional rotation due to shear strains;
ω = sectorial coordinate; and
ϕ = d^2v/dz^2 = vertical curvature.

Subscripts

Apart from the subscripts used above, subscripts have the following meanings:

c = concrete;
cr = cracked value;
inel = inelastic value; and
s = steel.

TESTING THIN-WALLED OPEN RC STRUCTURE IN TORSION

By Petar Krpan[1] and Michael P. Collins,[2] M. ASCE

INTRODUCTION

While a very large number of experiments have been conducted to investigate the torsional response of reinforced concrete beams with closed sections (box beams) or with squat, solid sections (3), very few open, thin-walled, reinforced concrete beams have been tested in torsion (4). To obtain detailed information on the actual behavior of such members a large, reinforced concrete, thin-walled, channel beam was loaded in pure torsion. This paper describes the results of this test. A companion paper (6) presents procedures for calculating the torsional response of thin-walled, open, reinforced concrete members. In this paper these predictions are compared with the observed behavior of the test specimen.

TEST SPECIMEN

Fig. 1(*a*) gives the overall dimensions of the test specimen. The desire to use two-legged stirrups dictated the choice of a 3-in. (75-mm) wall thickness. To ensure that the specimen behaved as a thin-walled beam (8) the width and height of the cross section were made to be about ten times the wall thickness, while the length was made to be one hundred times the wall thickness. In addition, large end diaphragms (solid blocks) were provided to restrain the warping of the end cross sections.

The reinforcement, Fig. 1(*b*), was uniform throughout the length of the beam. The main longitudinal reinforcement consisted of 24-#5 bars arranged in the four corners of the beam and anchored in the end diaphragms. To supplement this steel there were 9-#2 longitudinal bars which were intended to control cracking in the middle regions of the sides. Each stirrup was bent from a single 15-ft (4.6-m) piece of #2 undeformed bar which resulted in a single 15-in. (380-mm) lap in the middle of the top face, Fig. 1(*b*). The stress-strain characteristics of the #2 and #5 reinforcing bars are shown in Fig. 2.

[1]Asst. Prof., Ecole d'Architecture, Univ. Laval, Quebec, Canada.
[2]Prof., Dept. of Civ. Engrg., Univ. of Toronto, M5S1A4, Toronto, Canada.

Note.—Discussion open until November 1, 1981. Separate discussions should be submitted for the individual papers in this symposium. To extend the closing date one month, a written request must be filed with the Manager of Technical and Professional Publications, ASCE. Manuscript was submitted for review for possible publication on December 8, 1978. This paper is part of the Journal of the Structural Division, Proceedings of the American Society of Civil Engineers, ©ASCE, Vol. 107, No. ST6, June, 1981. ISSN 0044-8001/81/0006-1129/$01.00.

Because the end diaphragms must resist large torsions, each was reinforced with 8-#5 closed stirrups and 12-#7 bars placed perpendicular to the axis of the beam. These #7 bars acted as the longitudinal bars for the end diaphragms (see Fig. 3).

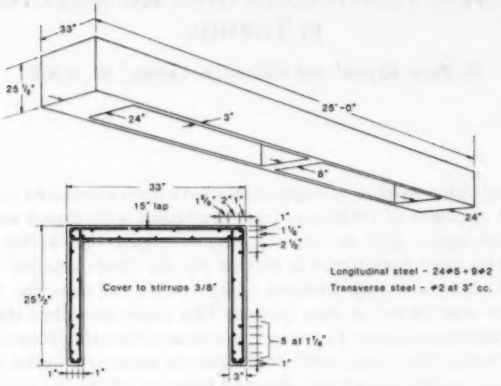

FIG. 1.—Dimensions of Beam Tested: (*a*) Overall Dimensions; (*b*) Cross Section

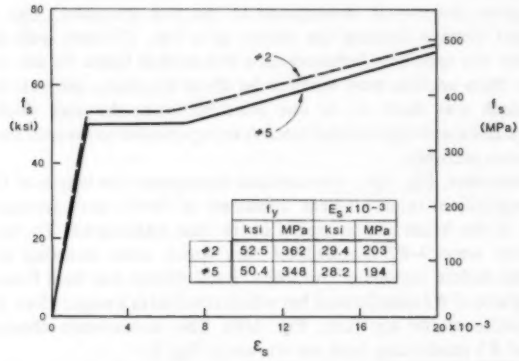

FIG. 2.—Stress-Strain Characteristics of Reinforcing Bars

The normal weight concrete for the specimen was supplied ready-mixed in two batches. Each batch had a slump of 3 in. (75 mm), a maximum aggregate size of 3/8 in. (10 mm), and attained a cylinder strength of 7,500 psi (52 MPa) at the time of testing of the specimen (about 50 days after casting). The measured stress-strain curve of the concrete was essentially parabolic with the peak stress being reached at a strain of about 0.003.

Test Set-up

A schematic diagram of the testing arrangement is shown in Fig. 4. The test rig applied a pure torsional moment to the midspan of the specimen while torsionally restraining the ends of the specimen.

The torsional load at midspan was applied via a "torsional loading frame" clamped to the middle diaphragm. To produce the required torsion, two 20-tom (180-kN) jacks applied equal tensile forces to two vertical rods 92 in. (2,340 mm) apart.

At the ends of the specimen torsional restraint was provided by a "torsional reaction frame" which was tied down to the reaction floor. Rocking plates

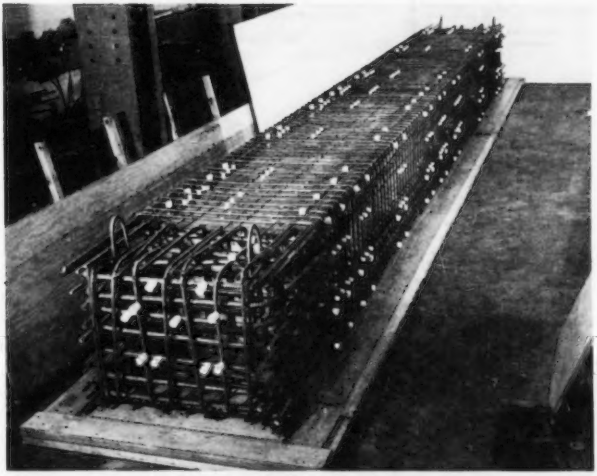

FIG. 3.—Reinforcing Cage Prior to Casting

and Teflon bearings under this end reaction frame ensured that the only significant restraint provided was that against torsional rotation.

During the test the torsion was increased at a very slow rate until a "load stage" was reached at which time the deformation was held constant. At each load stage, a very large number of strain readings (110 readings on longitudinal steel, 168 readings on the stirrups, and 29 readings on the concrete) were taken by means of demountable mechanical strain gages (see Fig. 5). In addition, at each load stage, the applied torque at midspan, the rotation of the middle diaphragm relative to the end diaphragm, the rotation of various sections along the span, the horizontal and vertical deflections of each flange of the beam, and when appropriate crack widths, were all measured.

Because of the large number of readings, the test took nearly 10 days to complete. A listing of the approx 10,000 readings taken during the test can be found in Ref. 5.

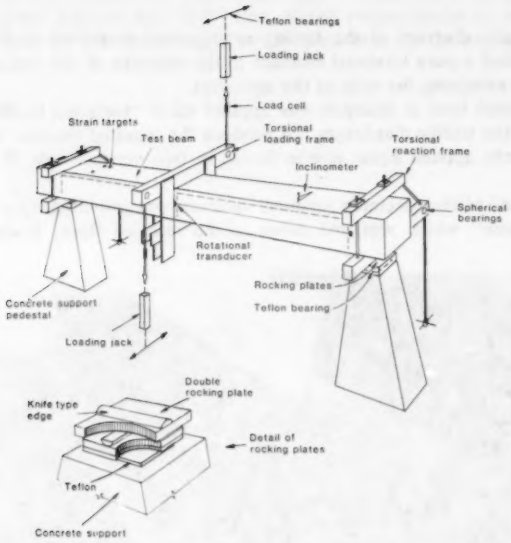

FIG. 4.—Schematic Diagram of Testing Arrangement

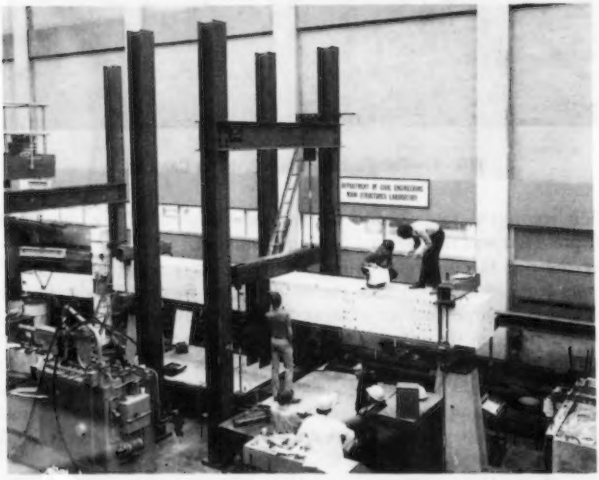

FIG. 5.—Specimen During Test (Load Stage 4)

Behavior of Test Specimen

In describing the observed behavior of the test specimen, it is convenient to refer to Fig. 6, which relates the applied torque to the resulting midspan rotation. The predictions shown on this figure were calculated in a companion paper (6) while the experimental points shown refer to measured torques and measured rotations at various load stages. It should be noted that the procedure for arriving at the predicted response took into account the actual stress-strain relationships of the concrete and the steel. Further the predictions include the deformations resulting from the shear strains which at times account for more than one third of the total deformation.

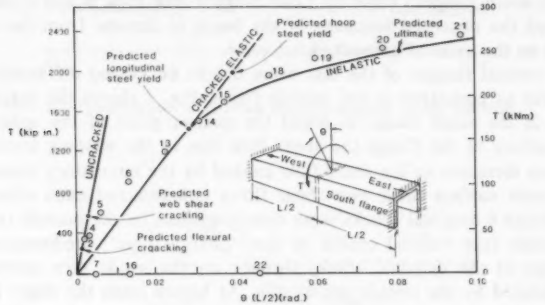

FIG. 6.—Comparison of Predicted and Observed Relationships Between Applied Torque and Resulting Midspan Rotation

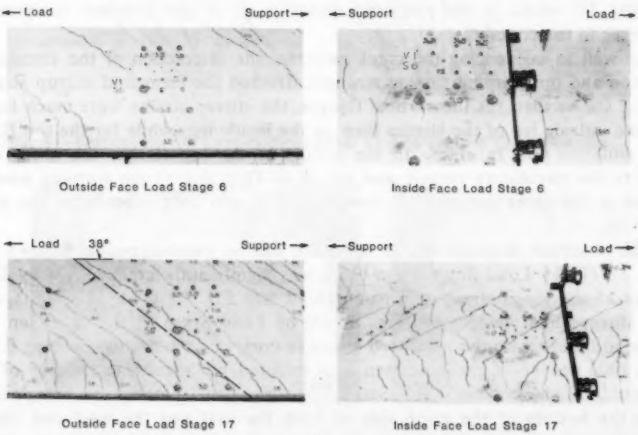

FIG. 7.—Crack Development in South Flange, Midway Between Load and Support, East End of Beam

If the sequence of the load stage numbers shown in Fig. 6 is examined, it will be seen that the load on the specimen was not simply monotonically increased to failure, but rather the specimen was at several stages unloaded and then reloaded. For clarity, some of the load stage points were omitted in Fig. 6. Thus, Load Stages 3, 9, and 11 were at zero torque while Load Stages 8, 10, and 12 were at the same torque as Load Stage 6 and Load Stage 17 was at the same torque as Load Stage 15.

During the test, the first cracks were observed when the applied torque was about 200 kip-in. (23 kN·m). These were vertical "flexural type" cracks, occurring at midspan, at the bottom of the south flange. At about 350 kip-in. (40 kN·m) "web shear type" diagonal cracks opened on the outside surfaces of both the north and south flanges, while by Load Stage 4 (see Figs. 5 and 6) the cracks had caused the observed response of the beam to deviate from the response predicted on the basis of uncracked behavior.

In the vertical flanges of the test beam cracks developed differently on the inside faces as compared to the outside faces. Fig. 7 shows the cracking that occurred in the south flange at about the quarter point of the span. On the outside surface of the flange the shear flow due to the warping torsion acted in the same direction as the shear flow caused by the circulatory torsion while on the inside surface these two shear flows counteracted each other. Thus, at Load Stage 6 diagonal cracks were clearly evident on the outside face while on the inside face vertical cracks of the "flexural type" predominated. The initial slope of the diagonal cracks forming on the inside face corresponded to that dictated by the circulatory torsion. At higher loads the shear flow due to the warping torsion began to dominate and new diagonal cracks inclined in the opposite direction formed on the inside face. It can be seen from Fig. 7 that by Load Stage 17 (this was a reloading load stage at the same torque as Load Stage 15) the diagonal cracks on the outside face were inclined at approx 38° which is the predicted direction (6) of the diagonal compressive stresses in the concrete.

As well as influencing the crack patterns, the interaction of the circulatory torsion and the warping torsion strongly affected the measured stirrup strains. Fig. 8 shows that, for the vertical flanges, the stirrup strains were much higher on the outside leg of the stirrup than on the inside leg, while for the top flange the situation was reversed. In the middle of the top flange, the shear flow due to the circulatory torsion and the shear flow due to the warping torsion, acted in the same direction on the inner face and counteracted on the outer face (6).

The observed response of the specimen can be summarized as follows (see Fig. 6): (1) By Load Stage 4 the beam was significantly cracked; (2) by Load Stage 15 the longitudinal steel had yielded (see Fig. 9); (3) by Load Stage 19 the stirrups had yielded (see Fig. 8); (4) by Load Stage 21 the specimen was close to failure with the measured concrete compressive strains reaching 0.004. The final failure of the specimen was initiated by anchorage failures of the longitudinal steel. After Load Stage 19 longitudinal splitting cracks appeared near the bottom of the north side of both the east and the west end blocks (see Fig. 10). By Load Stage 20 the longitudinal bars in these locations had begun to lose tension (see Fig. 9). After one more attempt to increase the applied torque (Load Stage 24) the test was concluded.

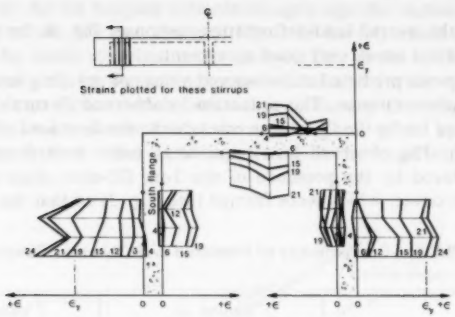

FIG. 8.—Distribution of Stirrup Strains around Cross Section

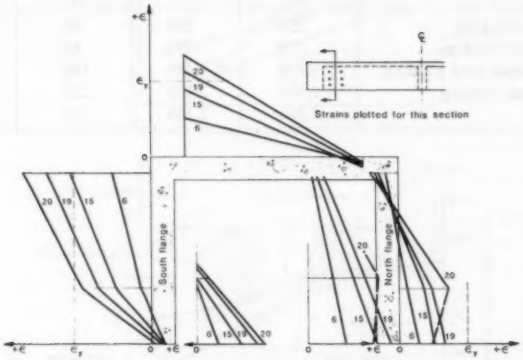

FIG. 9.—Distribution of Longitudinal Steel Strains around Cross Section

FIG. 10.—Anchorage Failure of Longitudinal Steel: (*a*) Overall View of West End at Failure; (*b*) Close-Up of West End Anchorage Failure

Comparisons of Predicted and Observed Behavior

In terms of the overall load-deformation response, Fig. 6, the predicted and observed behaviors are in very good agreement.

Table 1 compares predicted and observed values of cracking torques, yielding torques and failure torques. The reduction in observed flexural cracking load can be accounted for by the flexural stresses due to the dead load of the specimen and the rig (5). The observed load required to cause web shear cracks may have been reduced by the presence of the 1-in. (25-mm) diam circular holes in the concrete cover, which were formed (see Fig. 3) so that the strain targets

TABLE 1.—Comparisons of Predicted and Observed Torques

Variables (1)	Values, in kip-in.		Values, in kilonewton·meter	
	Predicted (2)	Observed (3)	Predicted (4)	Observed (5)
Flexural cracking	257	200	29	23
Web shear cracking	578	350	65	39
Longitudinal steel yielding	1,420	1,690	160	191
Hoop steel yielding	2,080	2,130	235	240
Ultimate	2,200	2,360	249	266

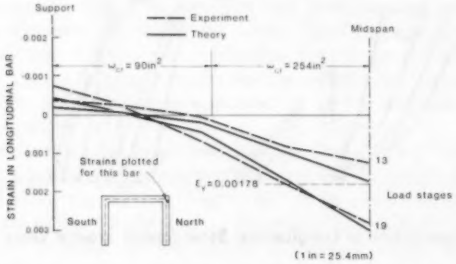

FIG. 11.—Comparison of Predicted and Observed Strains in Longitudinal Bar

on the reinforcing steel could be reached. In comparing the yield load values given in Table 1, it should be realized that the steel strains were measured over a base length of 8 in. (20 mm) and that in the case of the longitudinal steel this base length was not centered upon the most highly strained section (see Fig. 9). Taking these factors into account the predicted and observed values are in good agreement.

As well as predicting overall response the procedures described in Ref. 6 are capable of predicting the pattern of strains throughout the structure. An example of such a detailed prediction is given in Fig. 11 where the predicted and observed distributions of strains along a longitudinal bar are compared. The strain in this bar changes from tension at midspan to compression near

the support because of the change in direction of the warping moment (see Fig. 4 of Ref. 6). As the warping moment changes sign the sectional co-ordinate of the position of the bar also changes (Fig. 7 of Ref. 6) which in turn causes the slope of the strain distribution to change. The strain in the longitudinal bar is caused not only by the warping moment but also by the warping torsion and the circulatory torsion which both cause tension in the longitudinal steel. This additional tension means that at the quarter point of the span, where the warping is zero, there is still a significant tension in the longitudinal steel.

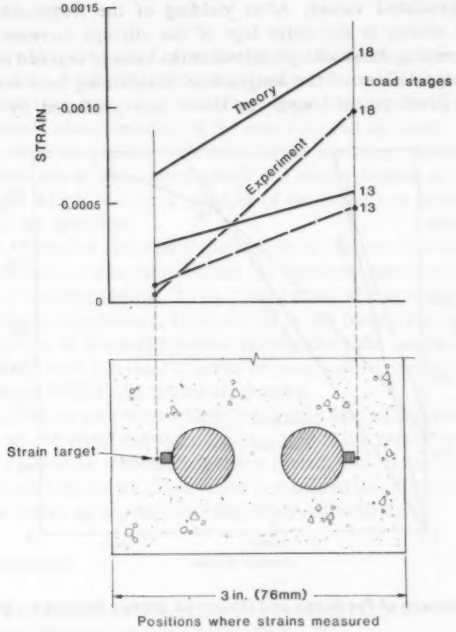

FIG. 12.—Variation of Longitudinal Strains Across Wall Thickness

In the theoretical procedures described in Ref. 6, the cross-section is represented by the centerline of the thin walls and hence it is the longitudinal strains on this centerline which are predicted. As can be seen in Fig. 9 and Fig. 12, there is a considerable change in longitudinal strain across the thickness of the wall. This bending about the centerline of the wall is referred to as secondary warping (7). The predicted distributions of longitudinal strains across the wall thickness were obtained by modifying (5) the equations for elastic secondary warping (7). It can be seen that further refinements of this theoretical model are necessary.

It has already been mentioned that in the vertical flanges of the test beam

the outer legs of the stirrups are subjected to higher strains than the inner legs. Fig. 13 compares the strains measured in these vertical stirrup legs (the strains plotted are the average from the 56 locations where strains were measured on the outer legs and the average from the 56 locations where strains were measured on the inner legs) with the strains predicted on the basis of the cracked elastic model (5,6). The model, since it assumes the beam to be fully cracked, predicts that the stirrup strains will commence to grow as soon as load is applied. In fact, straining of the stirrups does not commence until after diagonal cracks have formed. As cracking develops the magnitudes of the stirrup strains converge towards the predicted values. After yielding of the longitudinal steel (Load Stage 15) the strains in the outer legs of the stirrups increase more rapidly, eventually exceeding the strains predicted on the basis of cracked elastic behavior.

The anchorage failure of the longitudinal reinforcing bars was unexpected. The required development length for these bars predicted by the provisions

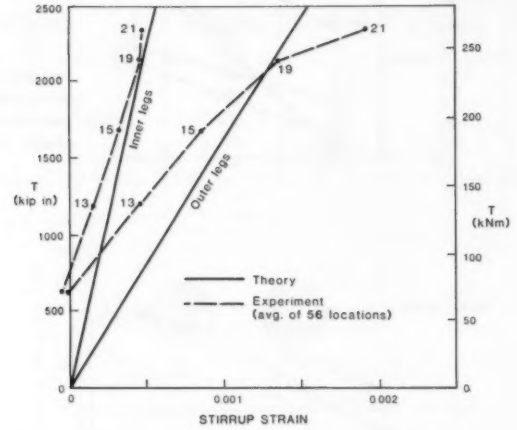

FIG. 13.—Comparison of Predicted and Observed Stirrup Strains on Vertical Flanges

of the American Concrete Institute (ACI) Code (1) is 12.6 in. (320 mm). Even though the bars were anchored into the end blocks for a distance of 23 in. (585 mm) a number of the bars could not develop their yield load. Strains were measured in 14 of the longitudinal bars. At the west end of the specimen 6 of these 14 bars were in compression. Of the 8 bars in tension, 5 were still carrying their yield load at the end of the test. The anchorage of one bar failed at about 60% of the bar's yield load while the anchorage of a second bar failed just at the yield load. The remaining bar was only stressed to about 70% of its yield load. The behavior at the east end of the specimen was very similar to that described for the west end.

In the end blocks the longitudinal bars were not confined by transverse reinforcement (see Fig. 3), were closely spaced, and had very little cover (see Fig. 1). The recent recommendations by the ACI Committee on Bond (2) suggest

that the development length is a function of the concrete cover and the bar spacing. Based on the small cover these recommendations would predict a development length of 21 in. (535 mm) while based on the small spacing they would predict a required development length of 35 in. (890 mm). These predictions are in good agreement with the observed anchorage behavior.

Conclusions

As a result of this work the following conclusions can be stated with respect to the specimen tested:

1. It is possible to predict accurately the load-deformation response of thin-walled, open, reinforced concrete structures loaded in torsion. Such a prediction must take into account deformations due to shear strains and the actual stress-strain characteristics of the concrete and the steel.
2. It is possible to predict with reasonable accuracy the torque at which the concrete will crack, the torque which will cause yielding of the longitudinal steel, the torque which will cause yielding of the transverse steel and the torque which will fail the specimen.
3. In order to predict accurately the strains in the two legs of the transverse steel it is necessary to take into account the interaction between the circulatory torsion and the warping torsion. Even if very small in magnitude the circulatory torsion contributes significantly to the strain in the transverse steel.
4. The variation of longitudinal steel strains along the length of the specimen can be predicted well but the variation of longitudinal strains across the wall thickness is more difficult to accurately predict.
5. The required development length for closely spaced, longitudinal bars with small covers can be significantly underestimated if the provisions of the current ACI Code (1) are used. For the specimen tested, the recent recommendations of the ACI Bond Committee (2) resulted in required development lengths which were in much better agreement with the observed behavior.

Appendix.—References

1. "Building Code Requirements for Reinforced Concrete (ACI 318-77)," ACI Committee 318, American Concrete Institute, Detroit, Mich., 1977.
2. "Suggested Development, Splice, and Standard Hook Provisions for Deformed Bars in Tension," ACI Committee 408, Concrete International, Vol. 1, No. 7, July, 1979, pp. 44–46.
3. "Torsion in Concrete 1784–1974," *ACI Bibliography No. 12*, ACI Committee 438, American Concrete Institute, Detroit, Mich., 1978, 148 pp.
4. Grob, J., and Thürlimann, B., "Wölbtorsionsverusche an Stahlbetonbalken mit offenem Querschnitt," *Publication No. 6506-6*, Institut für Baustatik, ETH, Zurich, Switzerland, Dec., 1974.
5. Krpan, P., "The Behavior of Open, Thin-Walled, Restrained, Reinforced Concrete Members in Torsion," thesis presented to the University of Toronto, at Toronto, Canada, in 1974, in partial fulfillment of the requirements for the degree of Doctor of Philosophy.
6. Krpan, P., and Collins, M. P., "Predicting the Torsional Response of Thin-Walled Open RC Members," *Journal of the Structural Division*, ASCE, Vol. 107, No. ST6, Proc. Paper 16333, June, 1981, pp. 1107–1127.
7. Oden, J. T., "Mechanics of Elastic Structures," McGraw-Hill Book Publishing Co., Inc., New York, N.Y., 1967.

8. Vlasov, V. Z., "Thin-Walled Elastic Beams," Published for the National Science Foundation by the Israel Program for Scientific Translations, Snd ed., Moscow, U.S.S.R., 1959, 493 pp.

DISCUSSION

Note.—This paper is part of the Journal of the Structural Division, Proceedings of the American Society of Civil Engineers, ©ASCE, Vol. 107, No. ST6, June, 1981. ISSN 0044-8001/81/0006-xxxx/$01.00.

Discussions

Discussions may be submitted on any Proceedings paper or technical note published in any *Journal* or on any paper presented at any Specialty Conference or other meeting, the *Proceedings* of which have been published by ASCE. Discussion of a paper/technical note is open to anyone who has significant comments or questions regarding the content of the paper/technical note. Discussions are accepted for a period of 4 months following the date of publication of a paper/technical note and they should be sent to the Manager of Technical and Professional Publications, ASCE, 345 East 47th Street, New York, N.Y. 10017. The discussion period may be extended by a written request from a discusser.

The original and three copies of the Discussion should be submitted on 8-1/2-in. (220-mm) by 11-in. (280-mm) white bond paper, typed double-spaced with wide margins. The length of a Discussion is restricted to two *Journal* pages (about four typewritten double-spaced pages of manuscript including figures and tables); the editors will delete matter extraneous to the subject under discussion. If a Discussion is over two pages long it will be returned for shortening. All Discussions will be reviewed by the editors and the Division's or Council's Publications Committees. In some cases, Discussions will be returned to discussers for rewriting, or they may be encouraged to submit a paper or technical note rather than a Discussion.

Standards for Discussions are the same as those for Proceedings Papers. A Discussion is subject to rejection if it contains matter readily found elsewhere, advocates special interests, is carelessly prepared, controverts established fact, is purely speculative, introduces personalities, or is foreign to the purposes of the Society. All Discussions should be written in the third person, and the discusser should use the term "the writer" when referring to himself. The author of the original paper/technical note is referred to as "the author."

Discussions have a specific format. The title of the original paper/technical note appears at the top of the first page with a superscript that corresponds to a footnote indicating the month, year, author(s), and number of the original paper/technical note. The discusser's full name should be indicated below the title (see Discussions herein as an example) together with his ASCE membership grade (if applicable).

The discusser's title, company affiliation, and business address should appear on the first page of the manuscript, along with the *Proceedings* paper number of the original paper/technical note, the date and name of the *Journal* in which it appeared, and the original author's name.

Note that the discusser's identification footnote should follow consecutively from the original paper/technical note. If the paper/technical note under discussion contained footnote numbers 1 and 2, the first Discussion would begin with footnote 3, and subsequent Discussions would continue in sequence.

Figures supplied by the discusser should be designated by letters, starting with A. This also applies separately to tables and references. In referring to a figure, table, or reference that appeared in the original paper/technical note use the same number used in the original.

It is suggested that potential discussers request a copy of the *ASCE Authors' Guide to the Publications of ASCE* for more detailed information on preparation and submission of manuscripts.

Aerodynamic Response of Long H-Sections[a]

Discussion by Carl H. Gronquist,[3] F. ASCE

This excellent paper constitutes an exceedingly valuable report on the aerodynamic investigations and wind tunnel model testing of the long H-section tension members which were employed on the Commodore Barry Bridge. Application of the findings of these and related investigations to the design of long span bridge members should altogether eliminate the likelihood of the occurrence of fatigue failures of this type in the future.

The Commodore Barry Bridge is the longest span cantilever highway bridge in the United States, with anchor span lengths of 822 ft (250.6 m) and a main span of 1,664 ft (501.2 m).

The members of these trusses are mainly closed box and H-shape sections, welded in the shop and high strength bolted at field connections. Many of the web members are unusually light and slender in general.

There are several known instances in the United States of wind excited vibrations of bridge members which required subsequent corrective measures. Notably there was the tied arch span of the Tacony-Palmyra Bridge over the Delaware River near Philadelphia in 1929, whose H-type hangers vibrated during completion of construction and were immediately stiffened by strutting. Similar cases of wind vibration of bridge members have also occurred in Canada, Europe, and Japan.

Erection of the three-span cantilever trusses was begun in February 1972 and proceeded normally, except for some vibration of the verticals at panel point 14 of both trusses. Wire rope guys were then placed to tie those members to the adjacent rigid midheight panel point 13M. By the middle of March 1973, the erection of the two anchor spans and more than two-thirds of the center span was substantially completed, but from March 17, 1973–March 19, 1973, strong winds averaging 35 mph–45 mph (56 km/h–72 km/h), were recorded, and on March 19th and thereafter a total of seven verticals were found severely fatigue cracked as described in the paper. Temporary splices were placed over the open cracks in uninterrupted day-and-night work within the ensuing 24 h, and the temporary splice plates were replaced with permanent splice material during March and April 1973.

Additional splices were installed where inspection by visual, ultrasonic, or dye penetrant methods indicated active fatigue cracks. Cracks in the initiation state were stopped by a drill hole and bolt at the tip of the crack.

Damping devices in the form of double wire rope guys were installed to tie the centers of 16 critical verticals to adjacent rigid panel points, immediately after March 19, 1973.

---

[a]January, 1980, by Frances J. Maher and Larry E. Wittig (Proc. Paper 15105).

[3]Consultant, Steinman Boynton Gronquist & Birdsall, 50 Broad St., New York, N.Y. 10004.

Bethlehem Steel Corporation on May 1, 1973, retained Steinman Boynton Gronquist & Birdsall to conduct a comprehensive independent investigation of the technical and safety problems which surfaced with the discovery of the cracks in the several verticals on March 19, 1973, including the study of temporary and permanent measures to prevent further damage.

In addition to the installation of the temporary guys described above, wire rope guys at 12 panels arranged to serve as horizontal X-bracing were installed at midheight between the two trusses. A detailed program for the maintenance of the temporary restraining guys, as well as for systematic inspection of critical members for fatigue crack initiation, was instituted by the contractor on the basis of their consultant's recommendations.

Most essential, in connection with this investigation, was the computation of the natural frequency and critical wind velocity, due to vortex shedding, of the H-sections and box sections of the long web members of the trusses at onset of vibration. Approximately 226 web members of the two trusses were determined to be susceptible to vibration in winds below 100 mph (159 km/h) by the method described by Ulstrup (17).

An aerodynamic investigation in connection with the failure of the long H-section truss members of this bridge by Howard, Needles, Tammen & Bergendoff for the Delaware River Port Authority was authorized April 30, 1974. In this investigation the foregoing consultants had the very valuable assistance of Wardlaw, et al. (5,15), and the excellent laboratory facilities of the National Aeronautical Establishment of the National Research Council of Canada, Ottawa, Canada. The results of these investigations were comparable to those reported in this paper, but included the development of vibration dampers as described in this paper.

It is the conclusion of the writer that bridge members must be designed in the future to meet the criterion that the critical wind velocity at onset of vortex shedding vibration should not be less than that for a 50-yr period or 100 mph (159 km/h), and that intermediate struts and transverse bracing should be employed as necessary in order to stiffen the members.

The use of a perforated web in H-sections has proved adequate in many cases in avoiding vortex shedding vibration, but it tends to lower the critical wind velocity for galloping as mentioned in the paper. Box sections, either with or without perforations, are definitely to be preferred over H-sections for bridge members, although nonperforated box sections are susceptible to vortex shedding vibration and galloping. However, the writer knows of no reported vibration of the closed box sections which were used on the Osaka Harbor cantilever bridge completed in 1974 in Japan. This is a double-deck bridge with a main span of 1,673 ft (510 m).

Appendix.—Reference

17. Ulstrup, C. C., "Natural Frequencies of Axially Loaded Tension Members," *Journal of the Structural Division*, ASCE, Vol. 104, No. ST2, Proc. Paper 13512, Feb., 1978, p. 357-364.